2005

Time-resolved analysis of ribosomal RNA dynamics

Scott Patrick Hennelly
The University of Montana

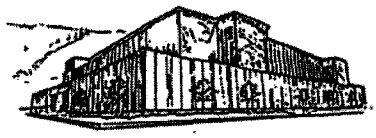

Time-Resolved Analysis of Ribosomal RNA Dynamics

by

Scott Patrick Hennelly

B.S. University of Montana 1998

A dissertation submitted in partial fulfillment of the

requirements for the degree of

Doctor of Philosophy

Division of Biological Sciences

The University of Montana

May 2005

Approved by:

Chairperson

Dean of the Graduate School

6-10-05

Date

Hennelly, Scott P., Ph.D, May 2005 Biochemistry/Microbiology

Time-Resolved Analysis of Ribosomal RNA Dynamics

Chairman: J. Stephen Lodmell

Within the last six years the study of the ribosome has fundamentally shifted. There are now atomic and near atomic resolution models from crystallographic studies of the subunits and the 70S ribosome. There are also many structure/function insights from complexes of ligands and the ribosome from medium resolution cryo-EM models. This wealth of information has provided insight into the existence and relevance of several fine and gross conformational changes on the ribosome as it undertakes particular translational tasks. It is now known for certain that the ribosome is a ribozyme and that RNA actively participates in the act of translation. These data will continue to add mechanistic detail to our understanding, but their most promising application is in the generation of testable hypotheses for other biochemical techniques. There is now a structure upon which researchers can hang their collective hats. And with this, blanks between the static structures as well as their functional relevance can be investigated.

Toward this end we have developed a technique that blends the tried and true power of chemical modification structure probing with quench flow fast mixing techniques to provide time resolution of conformational changes on the ribosome as they occur in response to functional ligands. In doing so, the initial studies have shown that the ribosomal subunits form interactions with each other in a stepwise manner suggesting a conformational intermediate in the process. Other data have also shown that mRNA alters the structure of the 30S subunit toward a structure found in the 70S subunit, eliminating the necessity for a post-association structural change. Finally, there are indications that the association of a natural messenger with the 30S subunit through its Shine-Dalgarno sequence may induce a structure that precludes interaction of the mRNA in the A site of the subunit.

Acknowledgements

I could not have hoped for a better environment to work in for my Ph.D. I could, however, have hoped for a shorter time in that environment, but while life is short its not like anyone ever really has anywhere to be other than here. I have experienced the excitement of learning what no one else knows and trepidation in the face of my great ignorance. Along the way I have had the pleasure of meeting and working with a large cast of very talented and, almost to the person, eccentric individuals. I would like to credit all of them with my success by giving me encouragement, help, council and a hell of a lot of fun. I would like to specially thank Dr. Walter E. Hill who gave me a place in his home for the wayward and the insight required to do research. He is truly an amazing and good person. I would also like to recognize Dr. John Stephen Lodmell for doing the impossible in taking over another lab when he already had his hands full, and herding a rambunctious crew to successful completion. His quiet, gentle style is worthy of universal emulation. Also Dr. Lodmell's Lab; Dr. Jean-Marc Lanchy is a good friend, mentor and surely one of the most capable researchers. I'd also like to thank my wife Kristin and my son Haven for keeping it all in perspective. And finally my lab mom, if I'd been lucky she'd of been the real deal, she keeps the trains one time in all sorts of weather, Martha Rice.

Table of contents

Table of Figures

Chapter 1

Introduction:

Ribosomal RNA can no longer be thought of as a rigid and catalytically inert party to the act of translation. As information concerning the structure and function of the ribosome has increased so has evidence of the dynamic nature of ribosomal RNA (rRNA). However, only some few examples of the conformational rearrangements of which these particles are capable have been discovered by previous research and no full cycle of a particular conformational change has been characterized in molecular detail. This is due in no small part to the technical challenge of these investigations. Up to now there has been no way to monitor the fine structure of the ribosome as it morphs through a particular conformational cycle. The research presented in this dissertation covers the inception and use of a technique suited to this task.

This first chapter will begin with a review of the mechanistic details known of translation. This will outline of the four phases of translation (initiation, elongation, termination and recycling) as well as when, where and how all factors known to promote protein synthesis interact with the ribosome. Emphasis will be given to the details of conformational dynamics that have been so far characterized.

Translation

The ribosome is old. Many who work in RNA catalysis consider it to be a remnant of the RNA world, a time on the threshold of the pre-biotic/biotic divide when

roving sets of increasingly complicated autocatalytic reactions developed a chemical memory and began to reproduce. This was an exciting time to be a molecule in this crazy world, change was in the air, everyone felt it. What remains of the potentially all RNA progenitor of the ribosome in prokaryotes is a 2.5 MDa complex of protein and RNA. Approximately two thirds of the mass is RNA, with the protein contingent represented by more than 50 separate chains denoted as ribosomal proteins (r-proteins). The most basic functional unit of the ribosome is the 70S ribosome. The 70S is in turn composed of a 50S and 30S subunit that associate and dissociate for every round of protein synthesis (Figure 1-1).

The ribosome is, of course, responsible for the conversion of genetic information encoded as linear DNA sequences into a linear polypeptide chain whose amino acid sequence is dictated by the original DNA sequence. The information is presented to the ribosome in the form of messenger RNA (mRNA) transcribed from the genomic DNA. Amino acids are delivered to the ribosome as esters covalently linked through the 3' terminus of other functional RNAs, known as transfer RNA (tRNA). Every tRNA is "charged" with an amino acid that is matched to a three-nucleotide sequence in a loop known as the anticodon. The anticodon can interact with a three-nucleotide codon on the mRNA in a complementary manner. The mRNA is parsed into these codons that are the universal code of life. The code is degenerate, with only 20 common amino acids and 64 possible combinations for three base pair sets. There are also codons that do not correspond to a tRNA, but instead signal a stop for protein synthesis.

The 70S is capable of undertaking translation with only the mRNA and appropriate tRNAs present. However it does so slowly and with some caveats. To aid in

accelerating the innate function of the 70S ribosome, a host of factors are recruited at appropriate points during translation. These factors are segregated into groups representing the phase of translation where they primarily act i.e. initiation, elongation, termination and recycling.

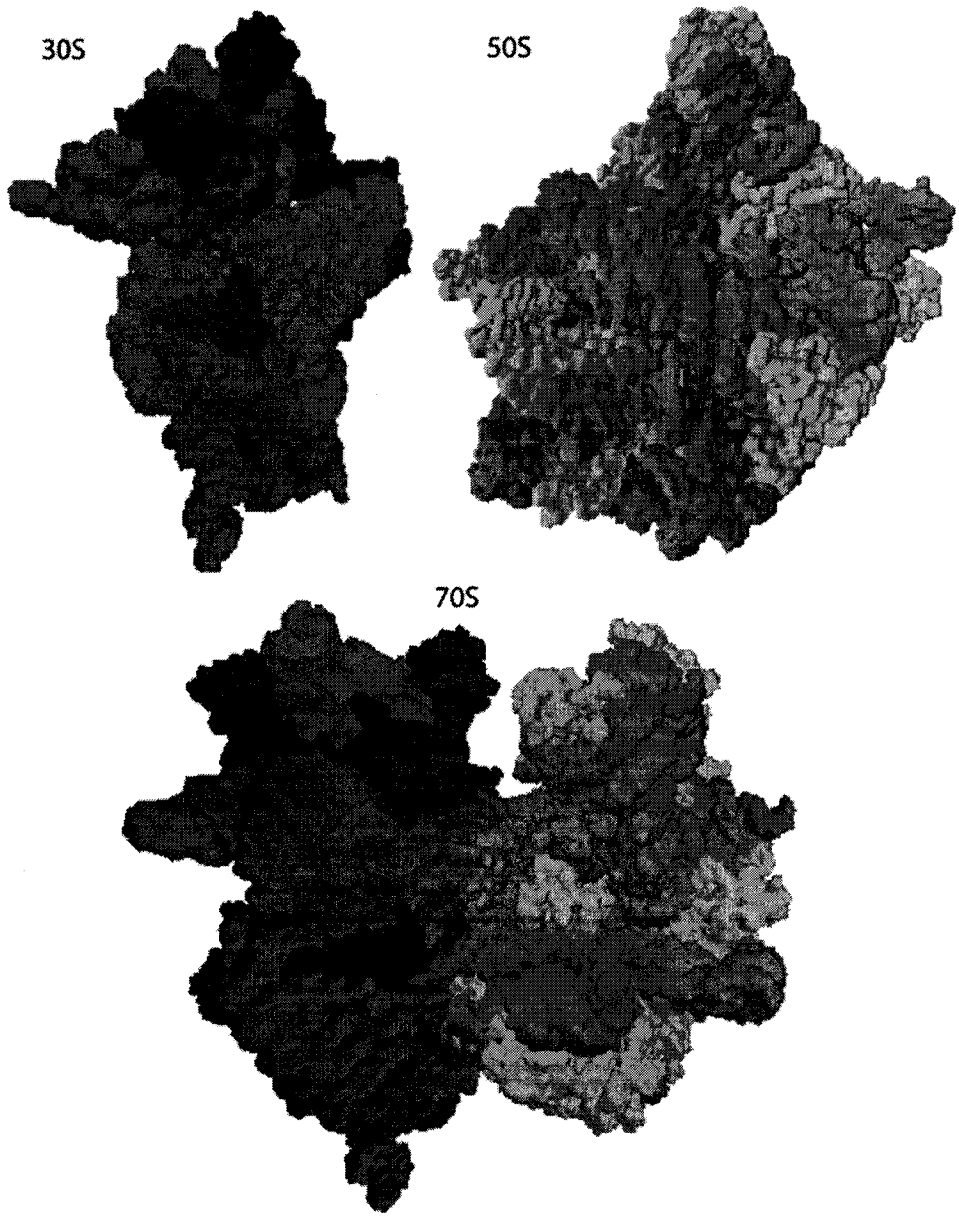

Figure 1-1. Views of the ribosomal subunits; 30S and 50S from the interface side of each. Below, the subunits in the proper orientation as they approach each other to form the 70S ribosome. Ribosomal proteins are in red on the 30S and Italian marble gray on the 50S.

Initiation

Translation in prokaryotes is coupled to transcription. Initiation proceeds even as mRNA is being polymerized off the genomic DNA. This is in stark contrast to initiation in eukaryotic organisms where translation and transcription are separated by time, space and a potentially large amount of post-transcriptional modification. The increased complexity of eukaryotic organisms is due in no small part to an ability to effectively regulate transcription and translation, a direct result of uncoupling transcription and translation. This is reflected in the vast array of factors eukaryotes rally to facilitate translation initiation. In prokaryotes, by contrast, there are only three factors involved in the initiation of protein synthesis.

There are three binding sites for tRNA on the 70S ribosome known as the A (aminoacyl or acceptor), P (peptidyl), and E (exit) sites. During the elongation phase of translation, the tRNA carry the next amino acid to the A site with the concomitant transfer of the peptide chain from the P site to the A site tRNA. Translocation catalyzes the release of a deacylated tRNA from the E site while moving the newly deacylated P site tRNA into its place. As shown in Figure 1-2, the tRNA binding sites span the intersubunit gap. With the division of binding interactions between the subunits there is also a division of activity. The 50S catalyses the transfer of the nascent peptide chain of the growing protein from the ester linked P site tRNA to the amino terminus of the incoming charged A site tRNA. The 50S subunit also triggers the GTPase activity of the GTP binding translation factors via interactions at its GTPase associated center (GAC). The 30S, on the other hand, is responsible for facilitating and monitoring the interactions

between the codon and anticodon. Inherent in this function is mRNA binding, preserving the correct reading frame and fidelity in message decoding.

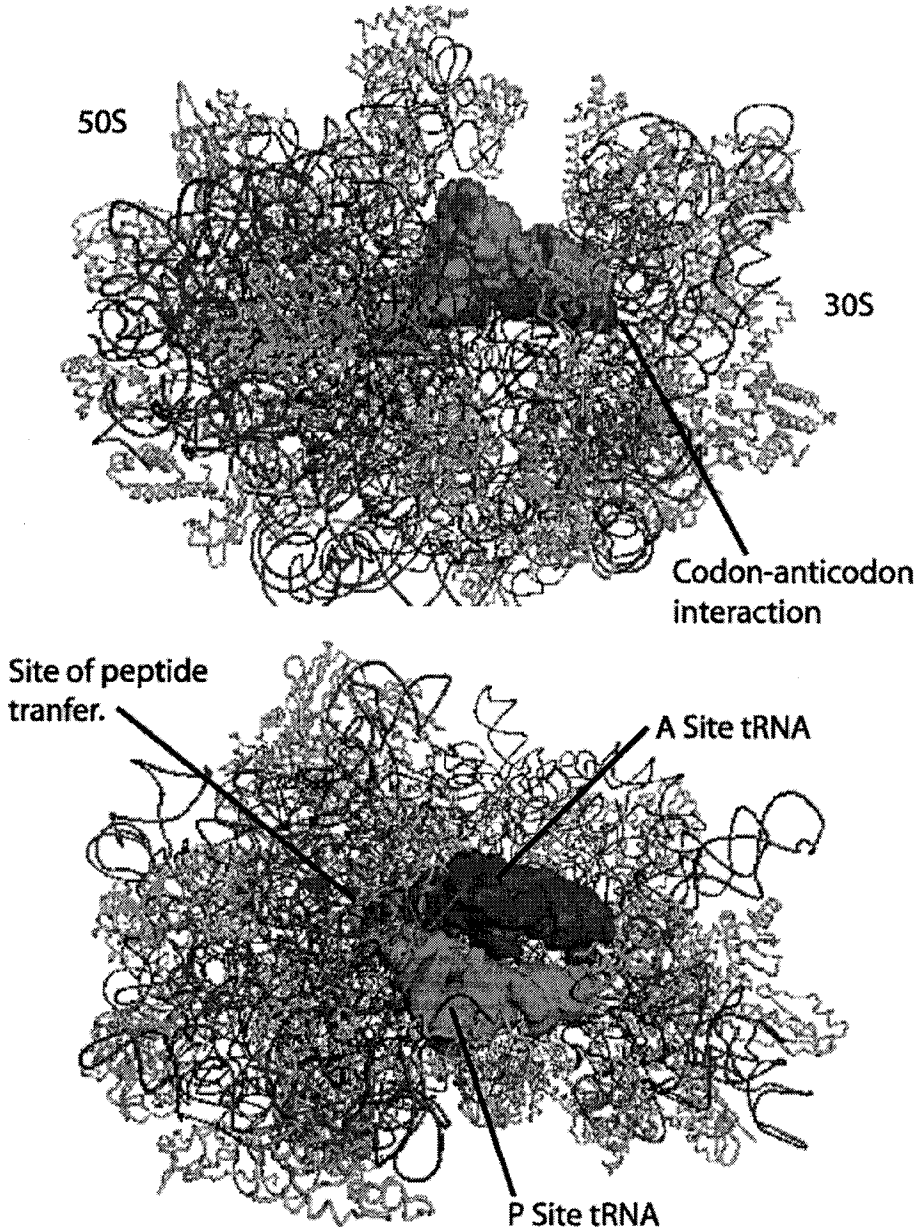

Figure 1-2. tRNA binding to the A site (red) and P site (orange) of the 70S ribosome (1) showing the sites of decodings interaction on the 30S subunit (16S rRNA backbone in red) and interaction of the aminoacyl acceptor ends of tRNA in the peptidyl transferase center (PTC) of the 50S subunit (23S rRNA in blue).

Initiation in prokaryotes simply means placing a charged initiator tRNA (a specialized formyl-methionine carrying tRNA) on the start codon. The start codon is most often an AUG and is usually 5-9 bases from the SD. The SD aids in the accurate selection of the start site. Decoding of the start site is fundamentally different from that of all the subsequent codons in a given mRNA. Not only does it occur prior to the association of the 50S subunit with the 30S, but also the initiator tRNA must be placed in the typically non-decoding P site to afford an empty decoding A site for subsequent elongation of the chain. This is accomplished with the help of protein initiation factors and an innate ability of lone 30S subunits to bind tRNA to a start codon in the context of the mRNA's translation initiation region (TIR). Following the correct placement of the fMet-$tRNA_f^{Met}$, the now 30S initiation complex (30S IC) with mRNA, tRNA, and factors, recruit 50S subunits to form a 70S initiation complex (70S IC). The exact order of addition for the factors and mRNA is unknown and may proceed in a random manner. However, it is known that both IF1 and IF3 also play a role in the recycling of ribosome, IF1 lowers the energy barrier for association and dissociation of subunits while IF3 possesses anti-association activity and as such couple termination to initiation. Therefore under physiological conditions these factors may reside on the 30S subunit prior to recruitment of other initiation complex components. The participants in the formation of the 70S initiation complex will be delineated individually, outlining their known functions, binding sites and mechanisms of action. A schematic overview of the initiation process is provided in Figure 1-3.

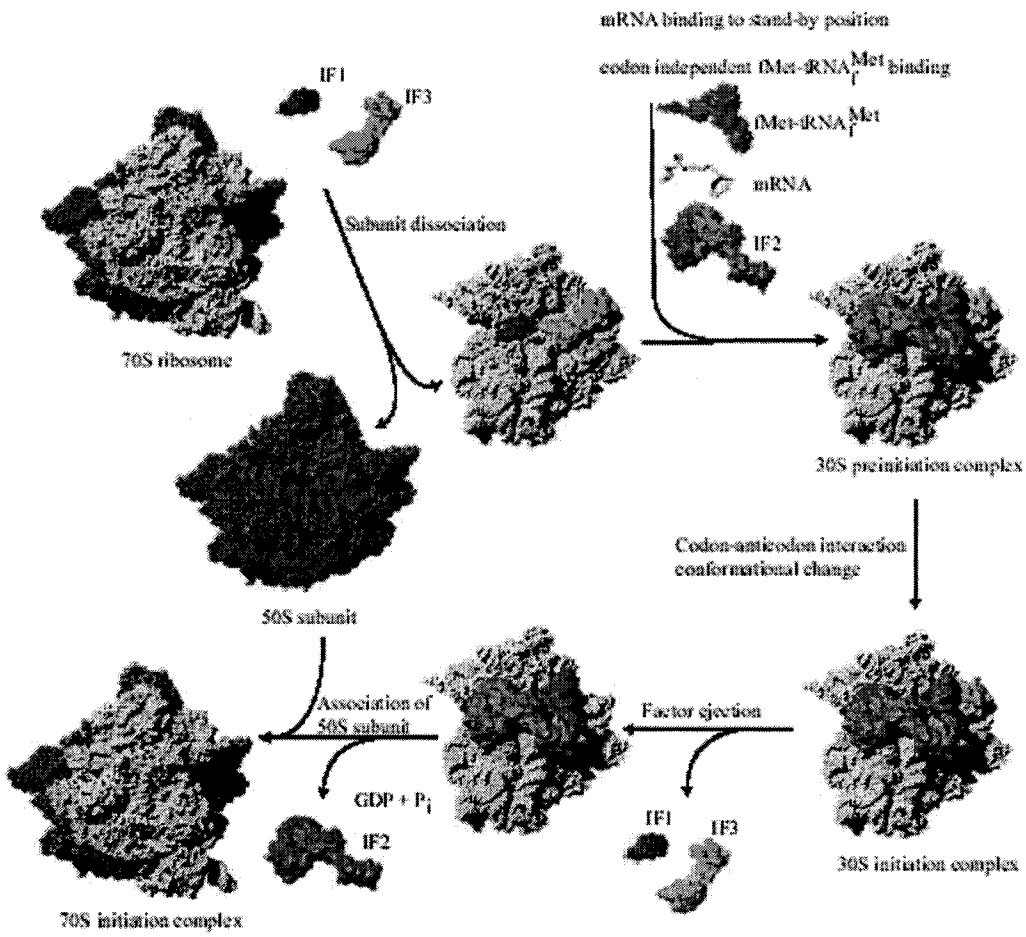

Figure 1-3. Schematic of the initiation process starting with dissociation of the 70S post termination complex and leading to the formation of the 70S IC (initiation complex). Figure taken from (*2*).

mRNA

mRNA in prokaryotes generally bind to the 16S rRNA anti Shine-Dalgarno sequence (ASD) via the a complementary SD sequence in the 5' untranslated region (UTR). This interaction promotes the initial binding of the mRNA in what is known as the standby position (*3*). The degree of complementarity between the ASD and SD has been correlated to the efficiency of translation for a given protein. A strong or maximal length between the elements is more highly translated than those with weak interactions (*4*). However, the ability of the message to proceed to elongation on the 70S can be

compromised by the additional affinity. Ribosomal protein S1 has been shown to aid in the disruption of the ASD:SD interaction and promote translation of messages with strong SDs or secondary structure in the 5' UTR (*5, 6*). S1 was also shown to act in concert with IF3 in discriminating against canonical start codons that are either 5' terminal or proximal (*5, 7, 8*). Considering these functions as well as the fractional occupancy and mRNA binding capacity of r-protein S1 it is tempting to look on it as another initiation factor for mRNA recruitment.

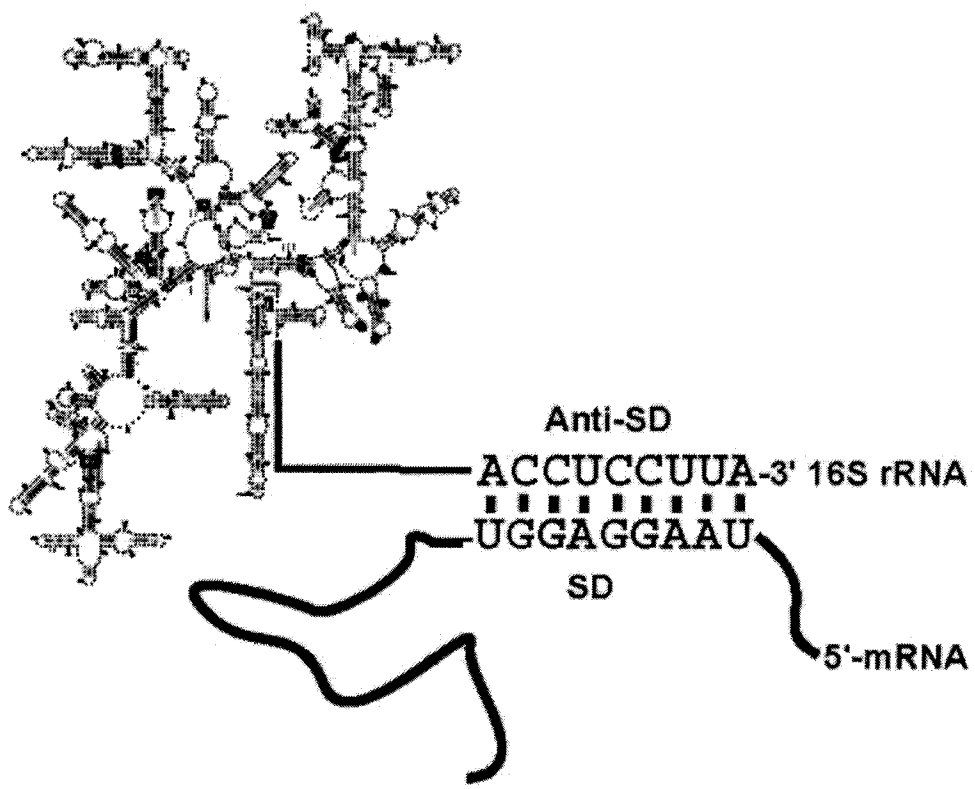

Figure 1-4 Secondary structure map of the 16S rRNA emphasizing the Shine-Dalgarno interaction between mRNA and the 3' end of 16S rRNA. mRNA can contain all or part of the polypurine SD sequence.

The TIR of a given message contains the SD portion of the 5' UTR as well as the start codon. The spacing between the SD and the start codon is optimally 5 bases from

the A of the AUG to the base that would represent the first base pair of a complete 9 bp ASD/SD helix (*9*). The spacing most likely reflects an inherent spatial constraint within the 30S subunit between the ASD in the 3' terminal region of the 16S and the P site where the fMet-$tRNA_f^{Met}$ must interact with the start codon.

The shift of the mRNA from the standby to the P site decoding position is catalyzed primarily by IF1 and IF3 (*3*). However, the full extent of the shift can only be seen in the presence of, and can be catalyzed solely by initiator tRNA. Experiments have also shown that an oligodeoxyribonucleotide complementary with the 30S ASD was capable of competing with mRNA with and without a SD sequence for binding until the IFs were included (*10*). This confirms the existence of two distinct and potentially exclusive binding modes on the ribosome. Initiation factors apparently possess the capacity to stabilize interactions at both positions. This research also shows that the ribosome has an innate ability to capture mRNA and facilitate the decoding of a P site start codon (Figure 1-5).

Inorder for the ribosome to decode a message and maintain tRNA:mRNA base pairing in both the A and P sites, the 30S subunit must act in the unwinding of the message for a minimum of 6 bases. The path of mRNA on the 30S can be described as a channel around the neck of the 30S that almost completely encloses the mRNA at two points, the entrance and the exit (*11*). Within the A and P sites the under-wound mRNA is packed into a groove with multiple phosphate oxygen and sugar contacts. The bases of the A site and the P site are exposed and available for interaction with tRNA (Figure 1-5). There is a kink between the A and P site which may be required to avoid steric interactions between the two site's tRNAs (*12*).

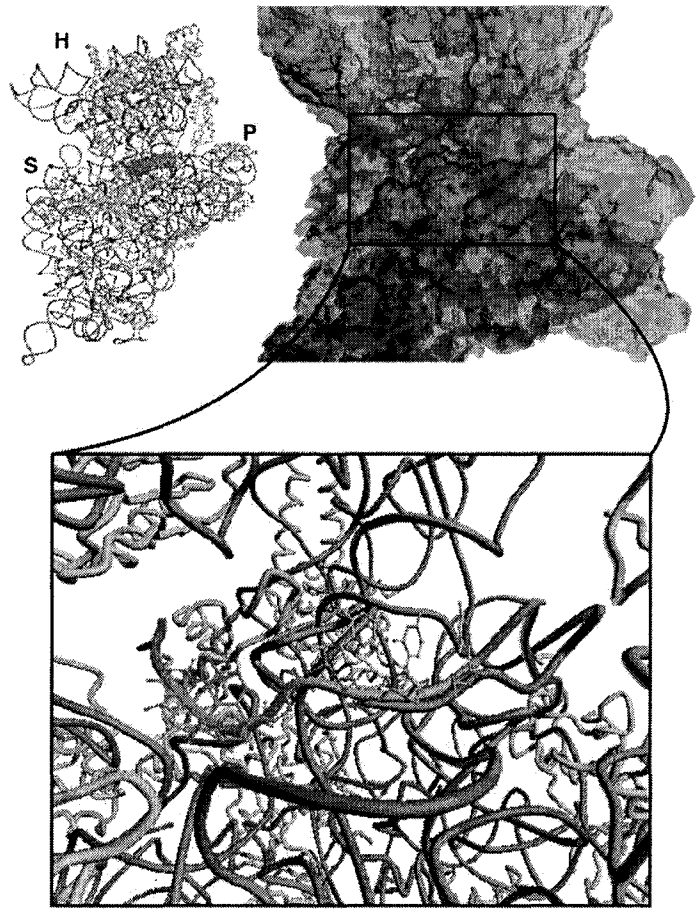

Figure 1-5. The path of mRNA through the ribosome as seen in the crystal structure model of the 70S ribosome (*1*). The 30S subunit (upper left) showing the structural features of the subunit, (H, head; P, platform; S, shoulder) and the path of mRNA around the neck. (upper right) The mRNA is buried in its 30S binding site. The message can be seen in the semitransparent surface rendering of the 30S. The SD interaction occurs in the platform and the message moves from left to right. (bottom) Close-up of the A site (green) and P site (orange) codons. The bases are exposed for engagement with tRNA and there is a kink between the two codons.

IF2/ fMet-tRNA^{fMet}

Initiator $tRNA_f^{Met}$ interacts with the 30S subunit first in a codon independent and then a codon dependent manner (*13*). Codon independent interactions are probably mediated by interactions with IF2 and the dependent binding requires an appropriate P site codon. As such, their may be no preference for the order of addition between

message and the initiator tRNA only a requirement for mRNA before the P site can be occupied by initiator tRNA.

Initiation factor 2 is the largest of the three IFs and is responsible for delivering/stabilizing the interaction of fMet-$tRNA_f^{Met}$ with the P site occupying start codon of the 30S initiation complex (*14*). The structure of IF2 homolog aIF5B has been solved for *Methanobacterium thermoautotrophicum* by X-ray crystallography. An NMR structure model is also available for IF2 from *Bacillus stearothermophilus*. The overall structure can be divided into a nonconserved N-terminal and highly conserved C-terminal domain. The GTP binding G-domain of IF2 is located at the beginning of the extended C terminal domain and is therefore more central in the overall structure. As with RF3, EF-G and EF-Tu, IF-2 interacts with the GTPase activation center (GAC) of the 50S subunit (*15*), which causes the hydrolysis of GTP. The role of GTP hydrolysis in promoting the formation of an elongating 70S ribosome is currently debated. However, while GTP is shown not to be required for the activity of IF2 (*13*) its presence seems to accelerate the formation of the 70S IC and its hydrolysis accelerates the release of the factor (*16*), and in doing so, appears to accelerate the formation of a 70S elongating ribosome.

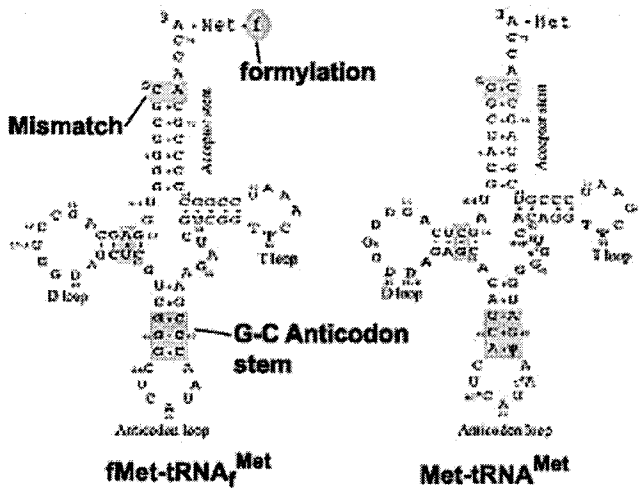

Figure 1-6 Secondary structure map of initiator and elongator methionine bearing tRNAs showing the main variations with functional importance. The original image was modified from (*2*).

IF2 is believed to interact with fMet-tRNA$_f^{Met}$ entirely through a small subdomain in the C terminal domain (*17*). This domain has been shown to interact with N-formyl and N-acyl-amino-tRNA molecules and not with tRNAs bearing free α-amino groups. Bacterial and mitochondrial initiator tRNAs bear a blocked or formylated methionine on fMet-tRNA$_f^{Met}$ which is a dedicated initiator tRNA, and selected for association with IF2 through its acceptor stem. Aside from its formylation, fMet-tRNA$_f^{Met}$ also contains several features that distinguish it from elongator tRNAs (Figure 1-6). Among the differences are a mismatch in the acceptor arm necessary for recognition by IF2 and formyl methionyl transformylase (FMT) (*18*). tRNA$_f^{Met}$ also contains a more rigid G-C base pairing in the anticodon stem loop (ASL) important for selection as an initiator tRNA by IF3 (*19*), and for its structure in association with the 30S in the P site during initiation (*20*). Both elongator and initiator methionine bearing tRNAs are charged by the same synthetase, but after charging and formylation fMet-tRNA$_f^{Met}$ is no longer a

substrate for peptidyl tRNA hydrolase (*21*). This increases the *in vivo* stability of fMet-$tRNA_f^{Met}$ and contributes to a belief that IF2 saturates free 30S subunits and selects from a pool of tRNA for fMet-$tRNA_f^{Met}$ to form the 30S IC (*22*) as opposed to acting as a carrier of initiator tRNA. This scenario is contrasted to that of elongator tRNA that is not found free in an acylated form except after exclusion from the ribosome following proofreading, at which time it is rapidly hydrolyzed and reenters the pool of deacylated tRNA.

The suggestion that initiator tRNA is not carried to the 30S IC is supported by both the weak affinity that IF2 has for fMet-$tRNA_f^{Met}$ *in vitro* and the observation that it can facilitate the template dependent binding of non-initiator tRNAs to the P site presumably without first forming a binary complex with its amino terminus (*23*). This body of work is challenged by others who have created *in vivo* systems for the initiation of translation with initiator tRNAs carrying formylated glutamine and initiating at a glutamine codon (*24*). This work convincingly shows that initiation with this construct is dependent upon the formation of a binary complex between IF2 and the tRNA prior to 30S complex formation. The differences observed in the efficiency of initiation between the modified and unmodified initiator tRNAs was directly proportional to their difference in binding affinity with IF2 and was responsive to changes in the level of IF2 expression. Although much work needs to be done to close this story it appears that IF2 most likely is a carrier for fMet-$tRNA_f^{Met}$ through C-terminal interactions.

The N-terminus of IF2 is a bit of a mystery. First, there are major differences between the size of the N-terminus from different bacterial sources. Many enterobacteria such as *Eschericia coli* express three isoforms of IF2 (IF2-1, IF2-2, and IF2-3) from the

same gene by alternative start site initiation of translation. The two shorter versions (IF2-2 and IF2-3) are nearly the same size, lacking around 157 N-terminal amino acid residues. These shorter isoforms are very similar to those found in other bacteria including the extremophile IF2 whose structure was determined (*25*). Both short and long forms are expressed in approximately equal amounts and are both required for optimal growth, yet the exact function of this region is unknown. Within the 157 aa N-terminus are a very long, basic, unstructured and flexible linker region connecting an N-terminal ~50 aa globular domain. This domain has been studied and a structure determined by NMR (*26*). This region has been shown to bind to the 30S subunit, although the site and specificity are unknown, and both the long and short forms are equally capable of catalyzing the formation of a 30S IC. The full functional implications of multiple isoforms of IF2 are not yet known. However an increase in the ratio of the short to long forms has been reported in response to cold shock adaptation (*27*).

IF2 does not footprint on the 16S rRNA but has been crosslinked to IF1 and multiple small subunit r-proteins (*28*). IF2 from *Bacillus stearothermophilus* has been placed on the ribosome using data from tethered chemical nucleases acting from various positions in its structure (*29*). These data have interesting implications for the overall function of IF2. There may be two separate interaction modes for IF2 in either the 30S or 70S IC. There were no cleavage patterns indicated within the 16S rRNA in the 30S intiation complex. Instead they were present only as a 70S initation complex. Therefore in the 30S IC, the role of IF2 is to stabilize/facilitate a P site interaction of fMet-$tRNA_f^{Met}$ through interactions with the acceptor stem of initiator tRNA and 30S r-proteins and other initiation factors. After joining of the subunits IF2 makes a new set of contacts with

the 30S, some of which are direct contacts with the 16S rRNA. The G-domain is now in a position to engage the GAC of the 50S and activate the hydrolysis of its GTP molecule.

IF2 binding to the 70S has been shown to depend upon the presence of fMet-$tRNA_f^{Met}$ in the P site. A deacylated $tRNA_f^{Met}$ does not permit the binding of an IF2 complex with a nonhydrolysable GTP analog (*30*). Presumably this is because binding of IF2 to the 70S IC (IC) is mediated by direct interactions with the initiator tRNA acceptor stem with the same specificity for a blocked amino acid as when it is free in solution. This interaction would preclude the binding of the acceptor stem with the 50S PTC until the release of fMet-$tRNA_f^{Met}$ by IF2 following GTP hydrolysis. However, IF2's GTPase activity does not require an interaction with the amino terminus of initiator tRNA. IF2 will hydrolyse GTP no matter what tRNA is in the P site as long as it is not an acylated non-initiator tRNA. The sum of these results strongly suggest that GTP hydrolysis with IF2 requires that the P site not be occupied by an aminoacyl or peptidyl tRNA. Found in later sections is that this requirement extends to EF-G as well. The difference is that IF2 has the added ability to bind specifically to the acceptor end of fMet-$tRNA_f^{Met}$ and remove it from the P site, and in doing so allow the 50S subunit's GAC to shift to a structure capable of triggering IF2's GTPase.

IF1

IF1 is the smallest initiation factor (8.2 kDa) and most likely due to this fact, is the only factor to be soaked whole into a crystallized ribosomal subunit for subsequent crystallographic structural analysis (*31*). As such, there is more direct physical information concerning the structural alteration of the 30S subunit by IF1 than any other factor, yet the role of IF1 or even the reason for its existence remains obscure. The

observed activities of IF1 are many. IF1 increases the rate of both association and dissociation of the subunits without affecting the equilibrium point, is synergistic in promoting the activites of IF2 and IF3, aids in the selection of initiator tRNA in the P site and, in a potentially related function, is suggested to be a blocker for A site tRNA interactions (*2*).

IF1 binds to a cleft near the decoding center of the 30S subunit at the top of helix 44. Binding causes a local distortion of helix 44 shifting it towards the platform and flipping out bases in an internal loop where many antibiotics are known to bind. In addition, helix 44 is shifted and rotated, with conformational effects noticeable for a distance of 70 Å. The binding of IF1 to a lesser or greater degree affects most of the bridge interaction sites in the 30S where contact between the subunits are made. It is therefore the only initiation factor that has been shown to cause a global conformational shift in the subunit. While there is no direct evidence for an exact function of IF1, it is tempting to postulate from the data that IF1 alters the conformation of the 30S and in doing so promotes the activities of the other initiation factors while lowering the energy barrier for subunit association/dissociation.

While IF3 has demonstrated anti-association functions, IF1 accelerates the association and dissociation of the subunits. The crystal structure model of IF1 on the ribosome shows the large structural perturbations caused by its binding (Figure 1-7). These are above and beyond the proposed role of A site blocker during initiation and are instead proposed conformational intermediates in the association event (*31*). This activity of IF1 may be related to the activity of mRNA in promoting subunit association. IF1 may open the decoding region and promote the binding of mRNA and subsequent association.

In the absence of IF1 the 30S:mRNA complex retains a conformation with lower energy barrier toward association. In this model, mRNA acts as a doorstop for the conformation catalyzed by IF1.

IF3

IF3 is divided into a C-domain (IF3C) and N domain (IF3N) connected to each other via a short, flexible linker sequence. All of the functions of IF3 can be performed by IF3C (*32*). Since both domains are RNA binding domains it is believed that IF3N is capable of increasing the affinity of IF3C for the 30S subunit. IF3 (i) prevents the association of empty 30S subunits with 50S subunits; (ii) prevents the use of elongator tRNAs or start codons other than AUG, UUG, GUG for formation of 30S ICs, as well as discriminating against fMet-$tRNA_f^{Met}$ for initiation from leaderless mRNAs; (iii) promotes the activity of IF2 in the formation of P site bound fMet-$tRNA_f^{Met}$ on an AUG start codon; (iv) catalyses the shift of mRNA from standby to decoding; (v) and it participates in ribosome recycling by promoting post-termination release of deacylated tRNA and dissociation to subunits (*33*). All of the aforementioned activities can be broken down into two real functions. First, bound IF3 aids in the formation of a 30S P site with a specific affinity for the intiator tRNA codon:anticodon interaction in the context of an mRNA with a 5' UTR (*34, 35*). Second, bound IF3 blocks interactions between the subunits known to be necessary for stability between associated subunits (*36-38*). It is not known if IF3 is bound prior to the dissociation of a terminated 70S ribosome, but it has been shown to be necessary for the recycling of the terminated 30S complex (*39*). This role is accomplished by destabilizing the non-initiator tRNA in the P site of a terminated 30S subunit and in doing so may lead to the dissociation of bound

message. This action preserves the 30S in a free state until the formation of a 30S IC. IF3 has also been shown to increase the rate of formation of the 70S IC by three-fold (*40*). The seemingly opposed activities of preventing association and promoting 70S IC formation can probably be explained by IF3's role in selecting and stabilizing initiator tRNA in the P site.

The structure of IF3 as a whole and the IF3C terminal domain alone, have been determined by NMR (*41*) and X-ray crystallography (*42*) respectively. There have also been several studies concerning placement of IF3 on the 30S subunit (*28, 37, 43-47*). The results include X-ray crystallography of co-crystals with IF3C (*48*). The placement of IF3 between the results is inconsistent, and in light of the recent structure models of the 30S subunit, some placements verge on comical with IF3 bound to impossibly distant regions. Even the results of the co-crystallographic study have been called into question. The model that explains most of the structural and functional data was performed using a tethered chemical nuclease [Fe]-EDTA (*37*). This study utilized the available crystal structure models and 16S rRNA:$tRNA_f^{Met}$ cleavage generated from multiple sites on IF3 to place it upon the 30S IC. The result is a model of IF3 on the 30S with the $tRNA_f^{Met}$ anticodon stem sandwiched between the IF3N and IF3C domains.

RNA dynamics during Initiation

The goal of initiation is to promote the utilization of the correct start site for translation. In order to promote the conversion of a 30S IC to 70S IC, ligands to the 30S must increase the affinity between subunits in order to overcome the anti-associative action of IF3. It has been shown that message alone has the capacity to increase subunit

affinity (*49, 50*). As discussed earlier, one function of IF3 is to promote the shift of mRNA to a decoding conformation in the 30S subunit. Crystal structure models of the 30S have not attributed the binding of mRNA analogs to the decoding site with the formation of a structure more competent in association. There are, however, subtle variations that can be seen between those structures with and without the mRNA analog (*50, 51*). The full effect of these changes is probably only felt during the association process itself. Other ligands, especially initiator tRNA, effect the inter-subunit affinity, but this interactions is likely to have the effect of reducing dissociation since its capacity to stabilize the 70S is through P site interactions on both subunits. Instead, a rational checkpoint preceding association would be interaction with message that affect both the state of the message for decoding as well as changes in the 30S subunit that allow for the progression of the 30S IC to 70S IC. Formation of this structure may be promoted by IF1 and IF3 in shifting the mRNA from standby to P site decoding.

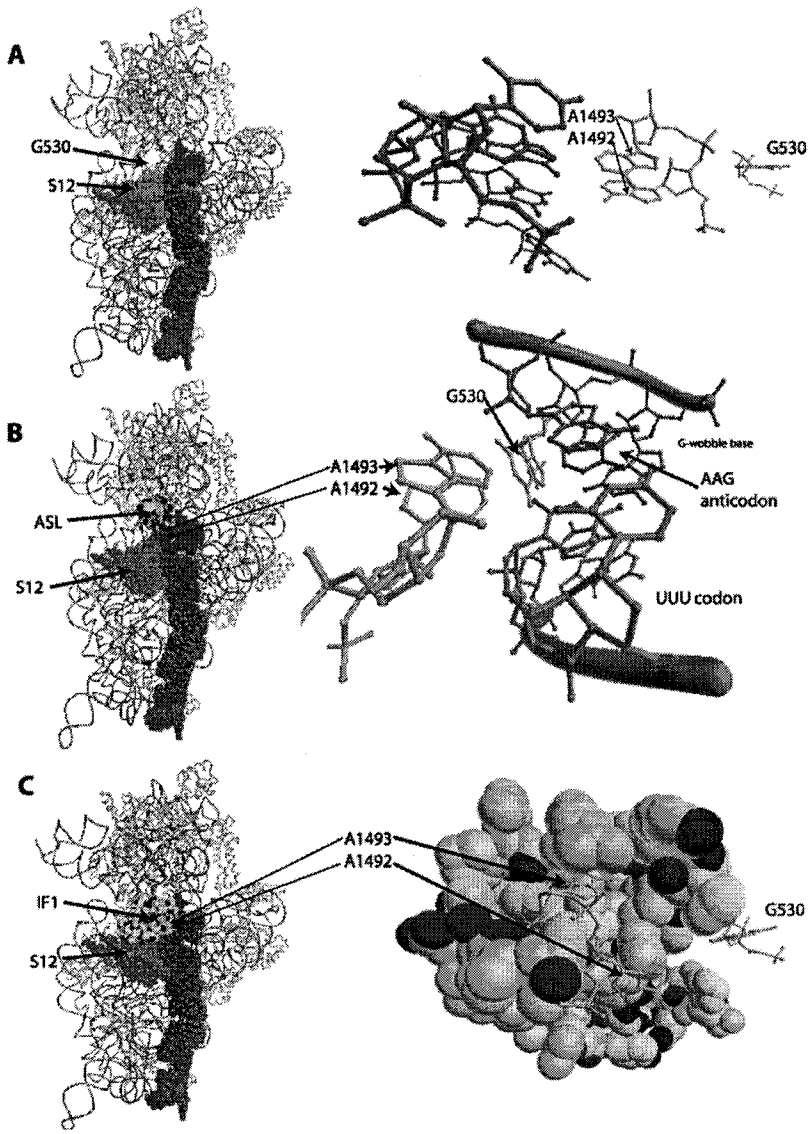

Figure 1-7 Three crystal structure models of the 30S subunit showing changes to the conformation of the decoding region in response to the binding of either an anticodon stem loop analog or IF1. The views on the left are of the complex from helix 44 looking toward S12. (A) Contains no A site ligand note the position of helix 44 in red and to the left a close-up view of nucleotide used in the discrimination of A site tRNA; A1492, A1493 and G530 (orange). A1492 and 1493 are within H44 and cross helix interactions are presented in red (*52*). (B) Model with anticodon stem loop analogs showing A1492 and A1493 flipping out of the helix and interacting directly with the first two bases of the codon anticodon helix. G530 also forms H bonding interactions and helps discriminate at the second position. The wobble G-U base pair does not directly interact with these bases (*53*). (C) The interaction IF1 with the A site is different in many repects from that of tRNA. The distortions to the top of H44 are more dramatic and continue for a 70 Å stretch. Both A1492 and A1493 are flipped out of the helix and interact directly with the factor (*31*).

Presented to this point is a view of the components that come together to form an elongation competent 70S ribosome. The three initiation factors act in unison and synergistically to place an initiator tRNA in the start codon occupied P site of the 30S subunit. Initiation is the rate-limiting step in translation. There is a large energetic cost for the cell of getting initiation wrong. Initiation absolutely must pick not only the correct start site but in doing so preserve reading frame and avoid creating elongation incompetent 70S ribosomes that must be rescued in order to regain function and or produce energetically expensive and possibly toxic noncoded protein product. The linchpin to this activity is the IF2/ fMet-$tRNA_f^{Met}$ interaction. While IF3 and IF1 act in concert to aid in the activity of IF2 to place fMet-$tRNA_f^{Met}$ by themselves their activity results in the 30S subunit remaining dissociated. The placement of initiator tRNA on the 30S increases the affinity between the subunits and allow the 50S subunit to bind and displace IF3 (*16, 54*). The timing of IF1 release is not known exactly, but the hydrolysis of GTP by IF2 decreases IF1's affinity for the ribosome and following its release the ribosome can accept an A site aminoacyl tRNA to begin the elongation phase.

Elongation

The ribosome enters the elongation phase of translation with an initiator tRNA occupying the P site and an empty A site. The next and all subsequent aa-tRNA (aminoacyl-tRNA) are delivered as a ternary complex with EF-Tu:GTP. If the codon:anticodon interaction is sufficiently correct, GTP hydrolysis is triggered via the GAC of the 50S. Following inorganic phosphate (Pi) release, EF-Tu undergoes a conformation change leading to dissociation of aa-tRNA from the factor and the concomitant release of the factor from the ribosome. The acceptance of tRNA into the A

site is preceded by a proofreading step in which aa-tRNA can dissociate from the ribosome. Attendent with full binding to the A site is activation of peptide transfer of the nascent chain to the α-amino group of the incoming aa-tRNA. This completes the formation of the substrate for the second phase of elongation, namely translocation. EF-G catalyses the translocation of the now deacylated P site tRNA and the peptidyl bearing A site tRNA simultaneously. mRNA and tRNA are moved together relative to the ribosome by one codon, at which point the deacylated formerly P site tRNA now occupies the E site. The peptidyl tRNA is in the P site and the empty A site is capable of accepting the next tRNA on the new codon. This completes the cycle of elongation. Now let's look at the players and mechanisms in a little more detail.

Models for the movement of tRNA and the nature of the tRNA binding sites on the ribosome.

Before beginning a discussion of the mechanisms of elongation a description will be provided of the ongoing evolution in understanding of how the subunits come together to create tRNA binding sites and how the interactions of tRNA with the ribosome change to facilitate the various stages of translation.

A classical view of the ribosome having first two tRNA binding sites (A and P) (*55*) then later three with the addition of the E site (*56*) held that tRNA progressed across the interface of the ribosome evenly from one site to the next in a system that is analogous to a conveyor belt. This was modified by the discovery that tRNA under appropriate conditions formed uneven footprints on the two subunits. The footprinting data suggested that there were actually six sites on the ribosome (*55*). In addition to the

classical A, P, and E there were now hybrid sites that seemed to occur naturally at the cusps between the phases of elongation. Mainly, a P/E, A/P and A/T, where the first part of the new site represents the position of the tRNA on the 30S subunit and the second the position on the 50S. The A/P and P/E sites were held to be spontaneous and stable products following the addition of the next aa-tRNA to the A-site. The aa-tRNA would be accepted into A site where reaction with the nascent chain in the P site on the 50S subunit would render the new A site tRNA only A site on the 30S and P site on the 50S and the formerly P site tRNA would occupy a P/E hybrid site. Action by EF-G would resolve the pre-translocation hybrid sites into post-translocation classical sites with an empty A site and the concomitant release of the former E site occupant by the new tenant.

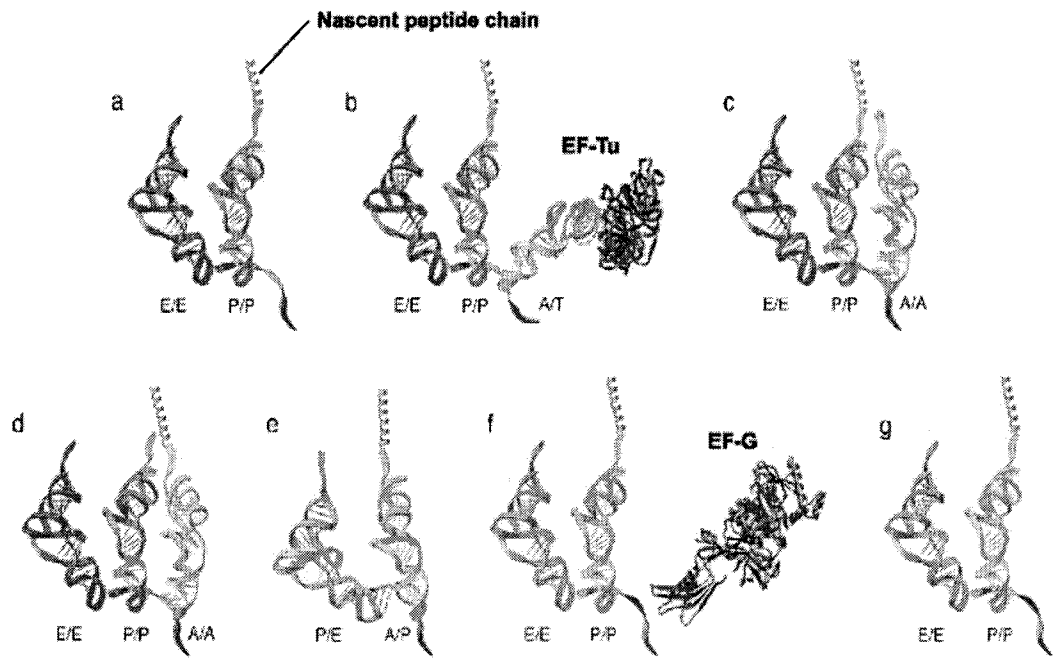

Figure 1-8. Structural representation of the tRNA positions during elongation as proposed in the hybrid sites model. This model suggests that tRNA will spontaneously shift to the hybrid sites following the addition of the next aa-tRNA to the elongating ribosome. Original image from (*57*).

An alternative model for elongation was put forth that maintained only the three sites of tRNA interaction. This model called for an allosteric interaction between the E site and A site interactions of tRNA and a classical view of tRNA translocation between the sites. This was called the α-ε model and relied on findings that aa-tRNA had higher affinity for the A site if the E site was occupied by a deacylated tRNA and vice versa. Both of these models have been modified to fit the increased information, both structural and biochemical, in recent years. The latest versions of the models in their revised forms are reviewed in (*57*) for hybrid sites and (*58*) for the **α-ε** model. Of the two models, most research favors the hybrid sites model, but the nature of the sites is in question. Although hybrid sites were alluded to in some earlier cryo-EM studies (*59, 60*) more recent medium resolution crystallographic (*1, 61*) and cryo-EM (*62, 63*) studies have failed to find the tRNA in a hybrid site spontaneously after peptide transfer. Furthermore, cross-linking of the acceptor end of tRNA has also failed to show its spontaneous movement to hybrid sites. The nature of the experimental conditions used in their discovery, as well as the preponderance of recent structural and biochemical data suggest that the hybrid states exist, but not as the result of peptide transfer. Instead, they are likely translocation intermediates in the massive and concerted effort of the ribosome to move two tRNAs and a mRNA simultaneously and accurately from site to site. This will be discussed in greater length in the next section.

Unlike any other single task a cell must undertake, the substrates of translation are myriad, with 20 different amino acids on dozens of tRNAs, four GTP hydrolyzing factors and a multitude of other associated factors, some of which are likely still waiting to be identified. Yet, the ribosome is both fast (10-20 amino acids per second) and accurate

(error rate of 1 per 3000) (*64*) in translation. While the mechanisms for most aspects of translation remain obscure it is becoming increasing clear that the ribosomes relies upon the identity and state of the tRNA that occupy it for ordering the multiple events of translation. Recent research has shown that the state of acylation of the P site tRNA is particularly important to all phases of translation. When the P site is occupied by a tRNA that is either acylated or bearing a nascent peptide chain the ribosome becomes incapable of stimulating GTP hydrolysis of EF-G and RF3 (release factor 3, responsible for the release of class I peptide release factors RF1 and RF2 in a termination complex), two of the four ribosomal GTP binding proteins (*65*). When the peptide or aa is transferred to the A site the ribosome can then stimulate GTP hydrolysis of EF-G, IF2 and RF3. IF2 is not hindered in GTP hydrolysis by the presence of an aa-tRNA in the P site if it is fMet-$tRNA_f^{Met}$. Furthermore, binding of the factors in the presence of a nonhydrolysable GTP analog was shown to follow the trend with hydrolysis of GTP. No binding of RF3 and EF-G was found in the presence of an aa-tRNA in the P site. IF2 would bind only if fMet-$tRNA_f^{Met}$ occupied the P-site. From this it can be concluded that the ribosome recruits factors only at the appropriate times, not only preventing the wasteful cycling of GTP but also the possibly catastrophic binding of factors to the ribosome that cannot stimulate GTPase on factors that require the hydrolysis of GTP for their release. Both translocation and termination require the P site to be occupied by a deacylated tRNA. In the case of EF-G and RF3 *in vivo,* the nascent chain would have been transferred to the A site tRNA or cleaved from the tRNA by RF1 or RF2 respectively. Studies have also shown that the maintenance of frame for codons is also tied to the presence of either an amino acid or nascent chain on the A site tRNA during translocation (*66*). This suggests

that affinity of the 50S P site for a peptidyl tRNA and its ability to lock the ribosome plays a direct role in correct translocation.

The requirement for GTP hydrolysis in the acceleration of translocation has long been held to signify a kinetic barrier in the process. Spirin described the barrier as the "locking and unlocking" of the ribosome for translocation (*67*). The terminology has gained more significance in recent years. The lock on the ribosome is not merely an energetic barrier to be crossed but instead a physical linkage that involves the interaction of an aa-tRNA in the P site with the 50S subunit. Unlocking the ribosome is concomitant with either the acceptance of an aa or nascent chain by the A site tRNA or the action of peptide release factors. Unlocking has the abovementioned effect of promoting the action of EF-G and RF3. This is apparently the result of allowing the formation of complementary interactions between the ribosome and these factors (*30*). EF-G bound with a nonhydrolysable analog of GTP (GDPNP) cannot form high affinity interactions with a locked ribosome (*30*). No noticeable conformational differences were seen by cryo-EM analysis of ribosomal complexes with or without aa-tRNA in the P site (*68*) only differences in the ability of factors to interact and promote a change. This fact speaks to an induced fit on the part of both the factors and the ribosome, a fit that has been shown for EF-G to allow binding and promote a large conformational changes in the ribosome especially in the orientation of the subunits with respect to each other.

Elongation factor G

EF-G, as previously stated, catalyses the translocation of the peptidyl tRNA from the A site to the P site of the ribosome. The pre- and post-translocations states of the

ribosome appear to be structurally identical as determined by the 10-13 Å resolution of cryo-EM models (*68, 69*). The natural substrate for the interaction of EF-G is a peptide-bearing tRNA in the A site which, as mentioned, is the result of peptide transfer from the P-site. EF-G will act on the ribosome in this state and catalyze a large rotational movement (*68-71*) between the subunits if the subunits are "unlocked" (*68*). If the A site of the 30S is unoccupied and P site tRNA deacylated, EF-G will still catalyze the rotation but will not result in translocation of the P-site tRNA (*62, 72*). However, P site tRNA will be shifted to the P/E hybrid site. This is because an EF-G interaction site on the 30S for translocation appears to involve the A site tRNA in the vicinity of the mRNA:tRNA codon:anticodon interaction (*73*). This is supported by the activity of EF-G truncation mutants that are incapable of catalyzing full translocation of the mRNA:$tRNA_2$ complex but still allow the movement of A site bound peptidyl tRNA to the P site only on the 50S subunit (*74*). Presumably this is because the truncations do not have sufficient length to span the intersubunit distance from the binding site on the 50S subunit to the site of action on the 30S. The resulting product would be tRNAs in hybrid sites of A/P and P/E. Also, EF-G with a non-hydrolysable analog of GTP has been analyzed by cryo-EM and shown to promote the formation of the same hybrid sites (*68*). These stalled intermediates will eventually resolve to post-translocation state via the slow dissociation of EF-G:GDPNP complex, if the A site is occupied by a peptidyl tRNA. This is suggested to be the result of the relocking of the ribosome by the now P site aa-tRNA shifting the subunit to a low affinity for EF-G in complex with GTP. From these data it now seems likely that the hybrid sites are translocation intermediates, but are not spontaneous and require the action of EF-G.

The activity of EF-G on the ribosome seems to proceed from both 30S and 50S ends of tRNA by divergent mechanisms. This can be seen in stopped flow analysis of EF-G catalyzed translocation of fluorescent labeled tRNA on the ribosome (*75*). Initial binding of EF-G to the translocation competent elongation complex is concomitant with a very rapid hydrolysis of GTP (71 per second with a deacylated P site tRNA, and an A site nascent chain peptidyl-tRNA) and a slight decrease in the fluorescence of the tRNA in the A site after which there is a slower increase in the signal accompanying translocation (25 per second). The conclusions taken from these experiments are that binding of EF-G to unlocked ribosomes facilitates the initial shift on the 50S to hybrid sites and triggers GTP hydrolysis, but the acceleration of translocation is the result of the release of Pi from EF-G and/or its subsequent dissociation. Presumably the rapid phase coincides with the ratchet like rotation of the subunits and the slower phase is the resetting of the intermediate, potentially hybrid, ribosomal structure to one exactly like the original except for the coincident pulling of the mRNA:$tRNA_2$ complex to its post translocation state. This scenario is analogous to a motor protein where the action is generated by the conversion of forms following hydrolysis as opposed to the use of the energy of binding to drive a conformational change and GTP hydrolysis is simply for dissociation as in a switch protein. However, the lack of a large structural change between GTP and GDP forms of EF-G, as determined by small angle X-ray scattering (*76*), makes the analogy less convincing. This seemingly small but all important question remains to be answered, " What is the exact role of GTP hydrolysis in EF-G's catalytic mechanism?"

Translocational dynamics of the ribosome.

As discussed, the pre- and post-translocation states of the ribosome are indistinguishable aside from the position of the mRNA:$(tRNA)_2$ complex. During translocation, the intermediate state is the result of a massive rearrangements of the ribosomal structure that was characterized as the "ratchet like movement" by cryo-EM (*68, 69*). The rearrangements include a 10° counterclockwise rotation of the 30S subunit on the interface of the 50S, which opens both the entrance and exit tunnels of the mRNA. Comparison of the entrance and exit tunnels with respect to complexes stalled with EF-G:GDPNP or EF-G:GTP:fusidic acid (fusidic acid allows GTP hydrolysis but not release of P_i or the factor) shows a variation in the timing of the maximum amplitude of the opening between the two complexes. The fusidic acid stalled complex can be considered a partial GDP form of EF-G toward post translocation state. This form has rotation between the subunits but it is diminished by 3°. The opening and closing of the mRNA entrance and exit tunnels, which may act as mRNA clamps, were found to be out of phase and may act on the message in a sort of peristaltic manner.

The most dramatic relative movements between the ribosomal subunits occur within the head of the 30S subunit and its interactions with respect to the 50S subunit. The only bridging interactions found to be altered between the subunits during translocation are within the head (Figure 1-9). These involve conformational rearrangement of the head as well as its movement with respect to the body of the 30S subunit and a large displacement relative to the 50S subunit. These result in both the breaking and movement of interactions between the 50S. The small and large subunit's proteins involved in these bridges make contact with the A and P site tRNAs. These new

arrangements are believed to stimulate the movement of the tRNA on the 50S subunit from the P to E and A to P sites. Alteration of these bridge regions while maintaining the other intersubunit interactions may be the cause for the resulting alterations in 50S and especially 30S conformations. While the majority of the bridges are maintained during translocation, it is unknown how the local structures are deformed as a result. This is of interest when one notes that the center of rotation during translocation is on the axis with a region implicated by a great deal of research as important for rRNA dynamics of the small subunit (*77*).

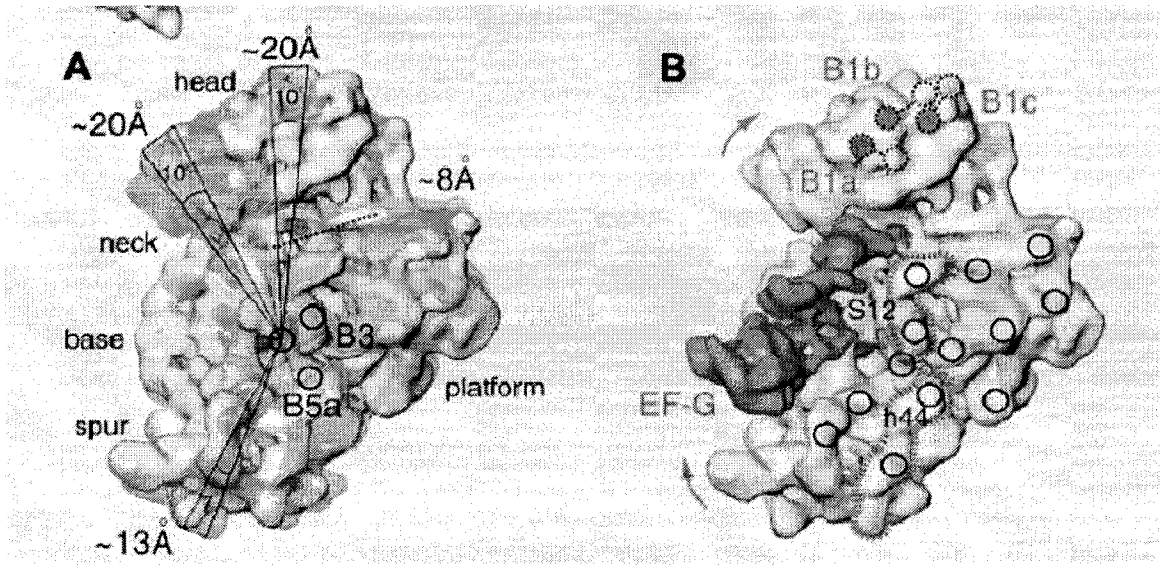

Figure 1-9. The 30S subunit from cryo-EM analysis of the translocation intermediate structure resulting from the binding of EF-G. (A) Overlay of 30S structures with (semitransparent pink) and without (yellow) EF-G bound. The image shows the amount of displacement a certain points as a result of the rotation as well as the center of rotation. (B) Shows the structure with EF-G bound delineating the bridges in the head that must migrate (filled circles) as a result and those that remain bound to their bridge partners in the 50S. Original image from (*68*).

The L1 stalk of the 50S ribosomal subunit in the translocation intermediate appears to rotate toward the intersubunit space by ~20 Å. There are apparently two conformations of the L1 stalk an "open" or "closed" conformation (see Figure 1-10). The

open conformation is seen prior to the action of EF-G on an unlocked ribosome. During the translocation intermediate the stalk closes and interacts with the tRNA now occupying the P/E site. As the intermediate state of translocation resolves to post-translocation, the L1 stalk moves back to the open conformation bringing the P/E site tRNA to the full E site. This would mean that the dissociation of the previous E site occupant precedes the movement of the L1 stalk, and therefore may be the result of the motion.

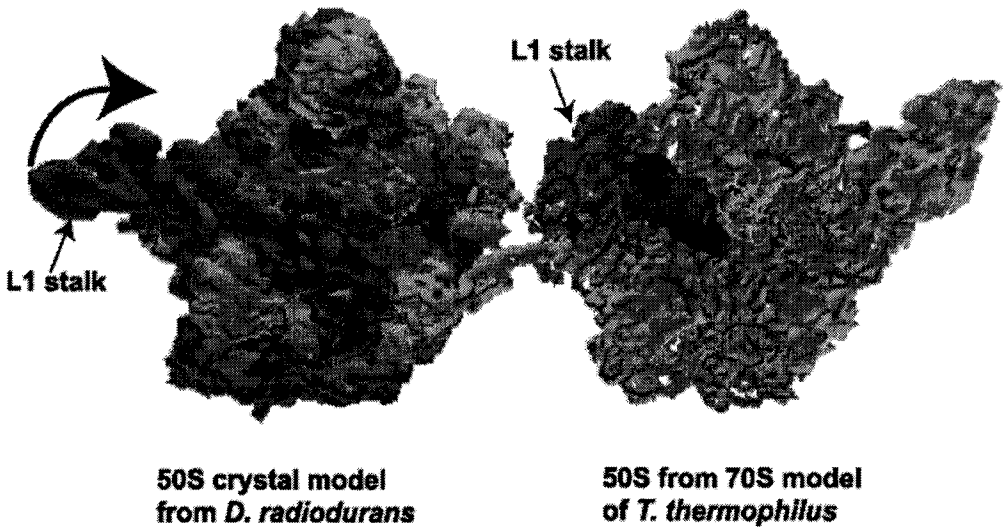

Figure 1-10. Position of the L1 stalk between the crystal structure models of the 50S (*78*) alone (left) and the 50S in a 70S ribosome (1) with tRNA in the A, P, and E site. The L1 stalk in these models appears in similar orientations to those described in the cryo-EM models before and during translocation. The position of the stalk in the 70S crystal model may therefore represent an intermediate intranslocation and an artifact of the 70S crystallization procedure. The E site tRNA (blue) can be seen interacting with the L1 stalk in a closed conformation.

Molecular mimicry on the ribosome

The structure of *Thermus thermophilus* EF-G was solved by two groups using X-ray crystallography in 1994 (*79, 80*), and shortly thereafter the structure of *Thermus aquaticus* EF-Tu as a ternary complex with GTP analog and Phe-tRNA^{Phe} was solved (*81*). There was an immediate realization that the structure of EF-G appeared to be a mimic for that of the ternary complex (*81, 82*). The structures of EF-G:GDP and the ternary complex were almost completely superimposable with domain IV of EF-G forming a rod like structure very similar to the anticodon arm of tRNA. The main exception for structural similarity is a region on the ternary complex that interacts with its guanine nucleotide exchange factor EF-Ts. This was followed by other examples of ribosomal factors whose structures appear to mimic those of tRNA. Included are RRF (*83-85*) which unsurprisingly interacts with the ribosome by occupying the A site during recycling, as well as RF2 (*86*) and eRF1 (*87*) which decode stop codons (Figure 1-11). These discoveries reinforce the belief in the ultimate evolutionary roots of nucleic acid catalysis and also highlight the conserved role that tRNA-like structures play in ribosomal interactions. However, while these structures by themselves have shapes and, in some cases, functions that are very tRNA-like none have been co-crystallized on the ribosome and as such it is unknown whether their mode of interaction is exactly analogous to that of tRNA.

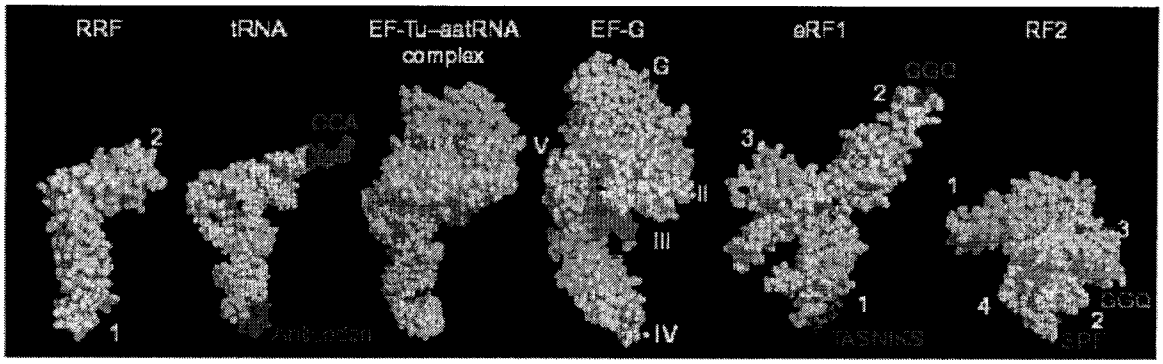

Figure 1-11 Structure of factors that interact with the A site of the ribosome and appear to mimic tRNA. The original image is from (*88*).

All of the GTP binding translation factors interact with the GTPase domain or GAC (GTPase acssociated center) of the 50S subunit. This domain consists of a structure known as the L7/L12 stalk, and together with L10, L11 and the L11 rRNA binding region form the GAC. Another element important for GTPase is the SRL (sarcin-ricin loop) that contains the longest stretch of universally conserved nucleotides (11 nts) in the ribosome. EF-G and EF-Tu ternary complex interact with the ribosome in similar ways as would be expected from their superimposable structures. Both interact with the SRL directly via their G domains as visualized by cryo-EM (*63, 89*). They also interact with the 30S in the region of S4 and S12 via their domain II. The portion of their common structure, which is tRNA in the ternary complex and tRNA protein mimic in EF-G, extends into the A site on the 30S. For the ternary complex this is obviously for the deposition of the new A site tRNA and for EF-G it is presumably the means by which the 30S portion of the translocational feat is motivated to proceed, or at least to proceed in the correct direction.

Elonation factor Tu

Free aa-tRNA is not found inside living organisms, with the possible exception of fMet-tRNA^{fMet}. Instead, free EF-Tu:GDP forms a complex with EF-Ts that catalyses the exchange of GDP for GTP and restores its high affinity for aa-tRNA. All aa-tRNA are found as a ternary complex with EF-Tu:GTP before delivery to the ribosome.

Fidelity on the ribosome can have two meanings. One meaning, as discussed, is maintenance of correct mRNA reading frame. The other is the correct amino acid choice for the codon presented in the A-site. The expected error rate, if selection of the next aa-tRNA were based solely on the difference in stability between the correct tRNA and all of its competitors, would be very large unless the process was extremely slow. This is not the case. The ribosome translates at a high rate and with high fidelity. Fidelity in decoding is the result of cooperative interactions of the ribosome:mRNA and EF-Tu:aa-tRNA:GTP ternary complexes. The individual components interact and allow two main steps in the process to be undertaken with different levels of stringency and velocity. These steps are separated by the irreversible hydrolysis of GTP. The result is not truly proofreading inasmuch as no tRNA is every accepted completely and then rejected. The mechanism can be described in the following terms. Initial interaction of the ternary complex allows the fast interaction of tRNA with the 30S A site where a reasonable codon:anticodon fit will trigger GTPase and the tRNA will be released from EF-Tu. The release of tRNA from the ribosome is now selected on its ability to remain associated by only its interactions in the 30S A site. When released from EF-Tu the tRNA is not oriented in the full A site and must traverse an arc to place the aminoacyl end in the 50S

A site. These steps have been thoroughly described kinetically and rates assigned (see Figure 1-12) (*90-92*).

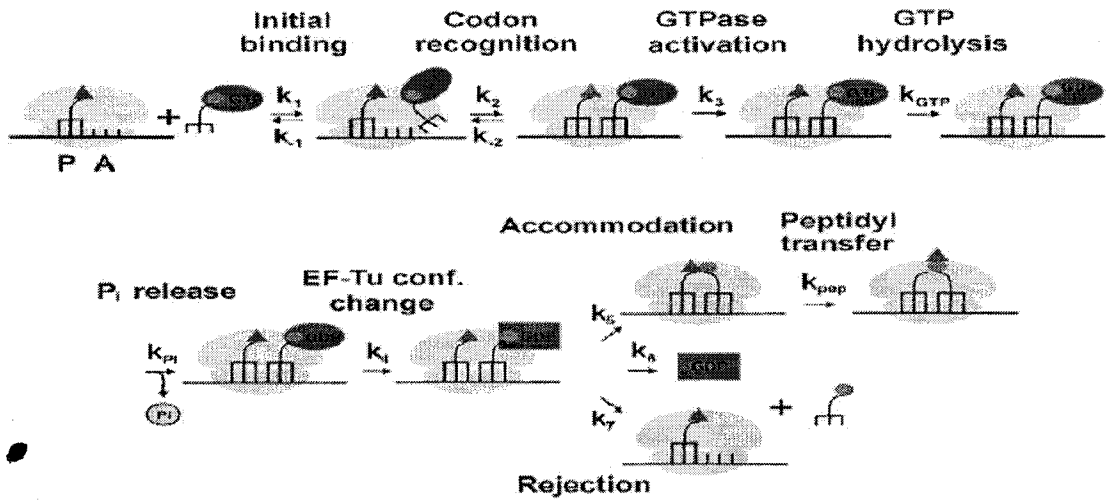

Step		Rate constant (s^{-1}) Cognate	Near-cognate	Noncognate
Initial binding	k_1	110[c]	110[c]	60[c]
	k_{-1}	25	25	25
Codon recognition	k_2	100	100	
	k_{-2}	0.2	17	
GTPase activation and GTP hydrolysis[d]	k_3	500	50	0.005
GTP-GDP conf. change of EF-Tu	k_4	60	70	
Accommodation of aa-tRNA and formation of peptide bond[d]	k_5	7	0.1	
Dissociation of EF-Tu	k_6	3	2	
Rejection of aa-tRNA	k_7	<0.3	6	

Figure 1-12 Schematic of discernable decoding steps and their associated rate constants for cognate, near-cognate and noncognate tRNA. Original image and rate constants are from (*93*) and (*94*) respectively.

The first step is the binding of the ternary complex to the ribosome. Binding of the ternary complex presents the tRNA to the ribosome at a site previously defined biochemically as the A/T hybrid site (*95*). The complex is not particularly picky about the state of the ribosome to which it binds. It will bind to 70S ribosomes in almost any state tested (*91*). Unlike the restrictions discussed for the other ribosomal GTPases and GTP hydrolysis, the state of aminoacylation or identity of the P-site tRNA is not a factor (*30*). Binding of the ternary complex confers a conformational change in and between the

tRNA, ribosome and EF-Tu. The changes have been analyzed via cryo-EM (*63*) of an antibiotic (kirromycin) stalled ternary complex on the ribosome with a cognate tRNA. However the changes in structure have also been demonstrated with variations in fluorescence intensity during stopped-flow experiments with ternary complexes containing near and non-cognate tRNA (*91*). This study also showed the rate for initial binding to be nearly the same between cognate and noncognate. One effect of the conformational change is apparently to utilize the native flexibility of the tRNA to form a codon:anticodon interaction in the A site despite the fact that the A/T site is rotated significantly with respect to full A site interactions (*62*). If the interaction between the codon and anticodon are robust enough, the second step, GTP hydrolysis, occurs. A correct interaction is a cognate tRNA on the codon, but a nearly cognate tRNA or no A site codon can also activate GTPase. However, dissociation without hydrolysis is nearly 100 times faster for the near cognate versus the cognate tRNA and GTP hydrolysis is nearly 10 times slower (*96*). Noncognate tRNA containing ternary complexes dissociate prior to GTP hydrolysis and can therefore be assumed to be in some way incapable of manifesting a structure competent for triggering hydrolysis and as such this represents a first round of selection.

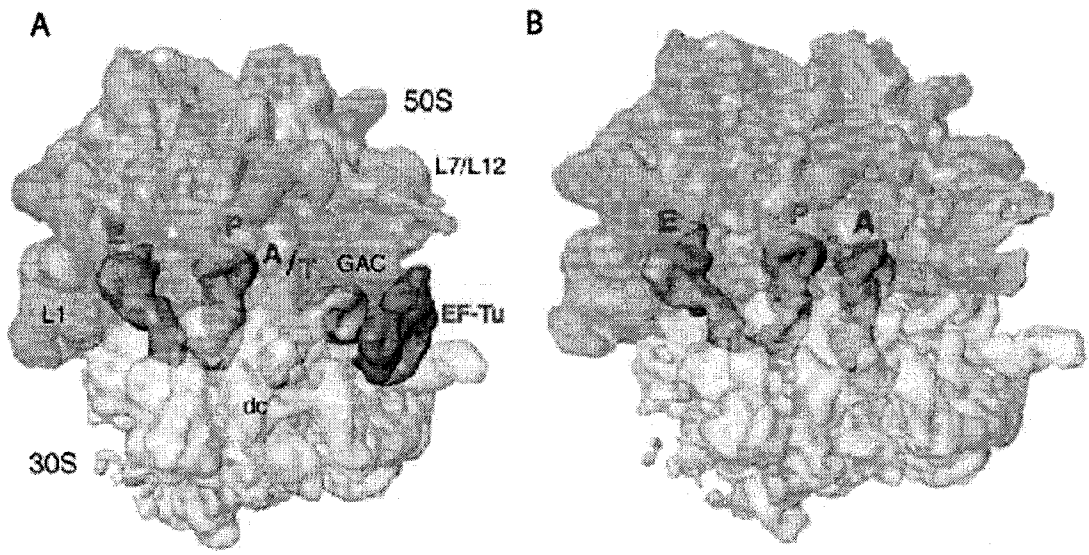

Figure 1-13 (A) The ribosome with EF-Tu ternary complex stalled in the A/T site by the antibiotic kirromycin as visualized by cryo-EM. (B) After GTP hydrolysis and release from EF-Tu proofreading occurs and the tRNA is accepted into the full A site of the ribosome where peptide transfer happens.

At this time it is not known how the correctness of the codon:anticodon interaction signals for the immediate hydrolysis of GTP, although it has been proposed that the necessity of a complete, unfragmented tRNA in the process (*97*) implicates tRNA itself as the conduit for the signal. It can be imagined that a simple mechanism where the constellation of interactions between the tRNA and ribosome constrain the ternary complex precisely enough to prevent the fine interaction of the catalytic atoms in EF-Tu with bound GTP when the codon:anticodon is not perfect. An alternative mechanism could operate through a more indirect signaling pathway that involves the active recognition of the correct codon:anticodon geometry by the decoding center of the 30S subunit. Crystallographic studies of 30S subunits with an A site codon triplet and an anticodon stem loop (ASL) oligomer have shown a structural change in the subunit conformation in response to interactions in the A site (*53*). The change has been characterized as the closing of the 30S subunit around the decoding center. This involves

small shifts in many distant regions of the subunit. The "closing" of structure is promoted poorly by near cognate tRNA alone and well by near cognate in the presence of the error-causing antibiotic paromomycin (*98*). Near-cognate tRNA interactions without paromomycin yield poorly defined structures in which the ASL becomes too random to resolve. The "closing" of the 30S subunit is shown to result from close interactions with the codon:anticodon helix sensing a proper geometry at the first two bases in the helix. The effect is to stabilize a correct anticodon and not necessarily destabilize an incorrect anticodon via a mechanism best described as an induced fit. While the conformational rearrangement has the potential to stimulate GTPase through indirect signalling it undoubtedly plays a role in the acceleration of next step of aa-tRNA selection.

The next selection event follows the release of aa-tRNA from EF-Tu following GTP hydrolysis and is generally referred to as the proofreading step. Unlike EF-G, the hydrolysis of GTP has a great effect on the structure of EF-Tu (*99*). Hydrolysis results in a rotation of 40° between domain I and domains II and III with a maximal displacement of 40 Å. GTP hydrolysis is the fastest step in the decoding process for cognate tRNA (*96*). The conformational changes are rapid but nearly 10 times slower than the hydrolysis. Following the conformational change EF-Tu is released from the ribosome at one half the rate of cognate aa-tRNA accommodation into the A site. Therefore release of aa-tRNA from EF-Tu occurs prior to EF-Tu's dissociation from the ribosome. Accommodation into the A site is the rate-limiting step but is at least 70 times faster for cognate versus near cognate and conversely the rate of dissociation for near cognate is nearly 20 times faster. This proofreading step physically involves the rotation of the aa-tRNA, from the A/T hybrid site occupied when associated with EF-Tu, to the A site.

During this motion, ribosomal binding would be limited to the energy of the three base pair codon:anticodon helix unless stabilized in the "closed" 30S conformation. This is supported by results on the rates of accommodation of various mismatches at different positions in the codon:anticodon helix (*93*). Both cognate and near cognate tRNAs are stabilized by the ribosome, while noncognate tRNA are not. The proofreading step in this scenario becomes an acceleration of correct aa-tRNA rather than an ejector of the incorrect. The rotation of aa-tRNA is itself rather impressive with the acceptor arm of tRNA rotating towards the PTC (peptidyl transferase center) while simultaneously bringing the anticodon arm back into alignment from its nontraditional flexed conformation, a proposed molecular spring (see next section) (*63, 100*).

After full accommodation, peptide transfer occurs spontaneously and the ribosome becomes the substrate for the action of EF-G. Peptide transfer is catalysed in the PTC on the 50S subunit. Here the CCA ends of both tRNAs are brought together and transfer is catalysed by an as yet unknown, but much discussed mechanism. What is known is that the catalysis, whether acid-base, transition state stabilization, proximity or a mix of the above, is carried out by rRNA alone. This revelation that the ribosome is a ribozyme was the first real mechanistic result provided by high resolution crystal structures (*101, 102*) of the ribosome. While the mechanism of peptide transfer is unknown, comparison of the rate constant of aminolysis of a model ester substrate by a primary amine with that catalysed by the ribosome shows a 10^6 fold rate increase (*103*). It has been demonstrated that peptide transfer is sensitive to pH, and a charge relay system was proposed including a base in the 23S rRNA with a modified pK_a (*104*). However, mutational analysis and low conservation of this base and others in the relay system did

not support the proposed mechanism (*105, 106*). At this point it is unknown if the pH dependence is the result of changes in the protonation of groups potentially involved in catalysis or a pH dependent structural change.

Conformational dynamics during aa-tRNA binding to the ribosome

Cryo-EM analysis of EF-Tu:tRNA:GTP binding to the ribosome has reached the 9 Å resolution range. Combined with available high resolution X-ray structures of subunits, 70S ribosome and ternary complex, structural alterations during aa-tRNA acceptance are becoming apparent (*63*). The first observation concerns the flexibility of the EF-Tu associated tRNA as it enters the A site. The junction of the D loop and the anticodon loop of tRNA has long been thought to be a molecular hinge (*107*). The function of the hinge is to allow the codon:anticodon helix to form in both the A/T and A sites as well as the span of arc between the two during proofreading (Figure 1-14). Formation of the flexed form is thought to precede formation of the codon:anticodon interaction because it is required for the helix to form.

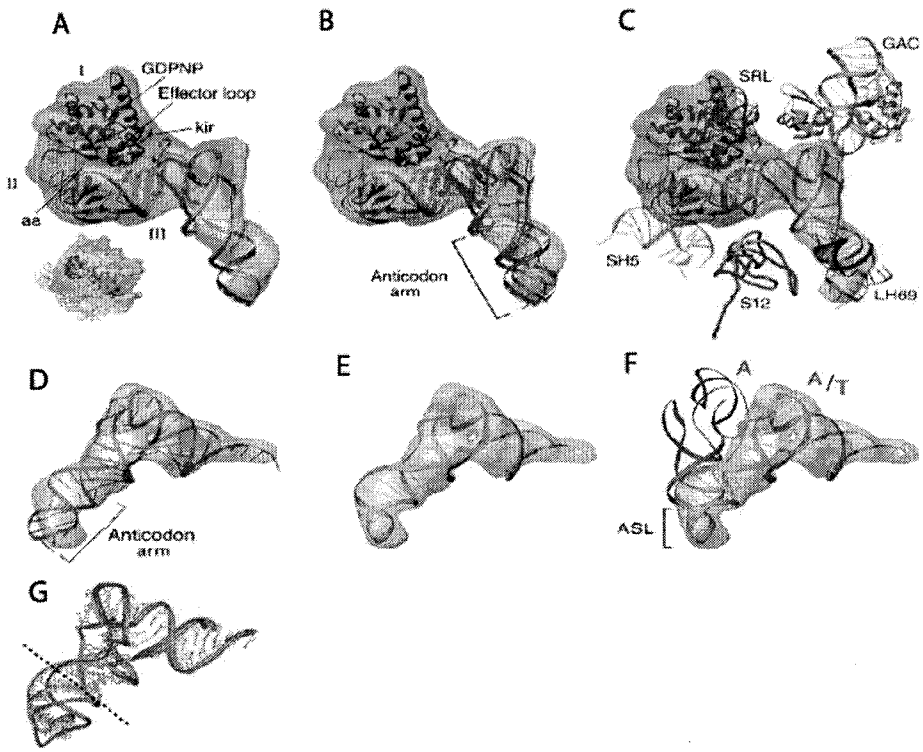

Figure 1-14 The EF-Tu ternary complex crystallographic structure does not fit the density determined by cryo-EM of the ribosome with the complex stalled at A/T site by antibiotic kirromycin. (A) The crystal structure as ribbon fit into the EM determined density of ternary complex on the ribosome (semitransparent gray and red). (B) After moving the structure of the tRNA into the density it still does not fit correctly. (C) Shows the interactions between the complex and the 70S, note that the G domain of EF-Tu does not interact directly with the GAC, instead the interaction is with the SRL. Also 23S Helix 69 (LH69) interacts with the tRNA near the hinge in the the A/T position and therefore follows the tRNA into the A site. (D)The high resolution structure of tRNA in ribbons showing the poor fit with EM density. (E) After modeling the tRNA structure to fit into the cryo-EM density. (F) The A site position and structure of tRNA from the high resolution 70S with tRNA overlaid with the modeled structure. Note that the anticodon conformation is very similar between the two. Movement from the A/T to the A Site accompanies proofreading. (G) Displays the difference between the modeled and ternary complex structures. Original images from (*63*).

The flexing of tRNA may be aided by the interaction of a mobile arm on the 50S subunit that has been shown to interact with the A site and P site as well as the 30S subunit in the crystal structure model of the 70S ribosome (*1*). This helix (H69) is undefined in the 50S crystal model from *Haloarcula marismortui* (*108*). The *Deinococcus radiodurans* 50S structure resolves H69 in a position drastically different than that seen in the 70S structure. In the 50S structure it appears tucked up against the

50S body as opposed to reaching away from the interface (*78*). In the 70S structure H69 makes contact with the tRNA in the A/T site near the hinge and apparently follows the tRNA into the A site. H69 also makes contact with bases in the decoding center of H44 on the 30S subunit where it makes 30S contacts on either side of A1492 and A1493 that have been shown to flip out of H44 and stabilize cognate tRNA. H69 has also been shown to be important for many aspects of translation, from ribosome stability to frame maintenance to decoding. The fact that it contacts the tRNA and the decoding center during and following decoding makes this unsurprising. The flexible nature of H69 and its position between the A and P site tRNAs make it a prime candidate for involvement in signaling between the subunits as well as translocation, and termination.

Opening and closing of the 30S subunit

The closing of the 30S subunit around the decoding center in response to a canonical tRNA:mRNA interactions results in a global change in the conformation of the subunit. The closing is the result of minor groove H-bond interactions between the first two bases of the codon:anticodon helix and three conserved bases in the 16S rRNA (see Figure 1-7). Differences between canonical and noncanonical base pairs lead to unsatisfied H-bonds or steric clashes (*98*). The three base pairs basically sense the geometry of the helix. Since the closed structure allows for more contacts between the helix and the 30S subunit, closing results in a net increase in the stability of the complex. This induced fit is caused by the relatively minute movement of three bases in the decoding center and results in a new global conformation of the 30S subunit.

Termination of translation and ribosome recycling

When a stop codon enters the A site following the last round of elongation it must be decoded as a stop. Class I release factors RF1 and RF2 accomplish decoding in eubacteria and a single eRF1 in eukaryotes, mtRF1 in mitochondria and aRF1 in archaea. RF1 recognizes UAA and UAG while RF2 is specific for UAA and UGA. eRF1, aRF1 and mtRF1 are capable of decoding all three stop codons. Class I release factors also catalyze the second step in termination which is the release of the nascent chain from the P site tRNA. The subsequent release of the class I release factors is then accomplished by the G protein class II release factor, RF3 in eubacteria, eRF3 in eukaryotes. Class II release factors interact with class I release factors as well as with the 50S subunit in the GAC. GTP hydrolysis triggers the release of the class I and class II factors. Following this, ribosome recycling is facilitated by the binding of RRF (in eubacteria, ribosome recycling factor) to the A site. The ribosome is then a substrate for the action of EF-G. GTP hydolysis leads to the dissociation of the subunits.

Class I release factors

The obvious first question with regard to class I factors is, "How does a protein factor interact with the ribosome in a codon dependent manner?" The short answer is that this is not yet known. Early crosslinking experiments confirmed, by a zero length crosslink from the stop codon, that RF2 was indeed in contact with the A site codon (*109, 110*). However, the position(s) in RF2 that were crosslinked was not determined. More recent work has attempted to delineate the region(s) of the RFs that confer specificity

(*111*). By swapping domains between RF1 and RF2 in *E. coli*, it was demonstrated that a minimal tripeptide in the central domain was capable of transferring the stop codon specificity from RF1 to RF2 and vice versa. The two interchangeable tripeptide motifs were SPF and PAT. Also, selective mutation of individual amino acids in the tripeptides allowed the factors to decode all stop codons. Similar results were found in eukaryotic eRF1 by analyzing the compensating mutations in response to reassigning stop codons to amino acids in organisms whose genetic code has slipped (*112, 113*). The central motif had a conserved NIKS amino acid sequence in organisms that used the universal stop codons. The fact that short motifs were in some way responsible for specificity reinforced the belief that decoding would be found to be the result of a protein anticodon.

High resolution structures for both human eRF1 and *E. coli* RF2 have not supported the use of these discriminator motifs as an anticodon (*86, 87*), since these structures are dissimilar in most aspects. The structure of eRF1 does maintain the arrangement of regions associated with ribosomal binding, peptide release, and decoding in a plausible conformation for simultaneous interaction of all, however, the distance between the site of the NIKS motif is 100 Å from a universally conserved sequence (GGQ) necessary for activity in peptide release (*114*). A distance closer to 72 Å was expected if the mechanism of action is requires the protein to span the distance from codon to PTC as a tRNA does.

The situation became more confusing with the publication of a structure for *E. coli* RF2. RF2's SPF tripeptide discriminator sequence was found to be only 23 Å from the GGQ sequence and not in the region suspected of mimicking the anticodon arm of

tRNA. Also, the factor overall had an insufficient maximal span of 64 Å. Furthermore, attempts to dock the RF2 structure in the A site of the 70S model using the SPF in a direct interaction with the stop codon were confounded by clash with rRNA regions. It simply did not fit (*86*).

There are several possible explanations for these observations. Either (*i*) the crystal structure does not represent the active bound form, (*ii*) the GGQ peptidyl release motif does not interact directly with the nascent chain-tRNA in the PTC, (*iii*) the discrimination sequence interacts indirectly with the stop codon. It is known that the GGQ motif, which contains a functionally important post-translational N^5-methylation (*115*) on the glutamine residue, is at least very close to the peptidyl-tRNA in the PTC based on cleavage from a tethered [Fe]-EDTA (*116*). Also, modeling the structure of RF2 as a tRNA mimic on the structure of the 70S without assuming the SPF motif makes direct contact with the stop codon did produce a reasonable A site fit, as well as contacts within the PTC of the 50S subunit (*86*). In this model the domain I tRNA anticodon arm mimic was situated in the gap between H44 and S12 in a manner similar to IF1 and tRNA. The SPF motif made contact with H44 near an internal loop that is universally conserved and functionally important in decoding. This loop contains the binding sites for aminoglycoside antibiotics and is the site of many second site suppressor mutations for RFs (reviewed in (*64*)). Currently the exact mechanism of stop codon recognition is not known, but it can be assumed that the importance of the conserved discriminator sequence, at least in eubacteria, is not as a protein anticodon but more likely an indirect sensor of the codon interaction with the 30S decoding site perhaps through a mechanism like the opening and closing of the subunit via cognate codon interactions.

The mechanism by which RFs catalyze the hydrolysis of the ester link between nascent chain and P site tRNA is not yet known. Despite the universal conservation of the GGQ motif, early indications are that mutations to the tripeptide do not fully abolish activity (*86*). The motif is located in a β hairpin loop of domain III and is disordered in the crystal suggesting a certain inherent flexibility. The site is susceptible to protease cleavage that disrupts its activity in catalyzing hydrolysis without affecting codon-dependent binding (*117*). While the exact mechanism is unclear, one aspect of the catalytic activity can be assumed. In some way, RFs must bring or allow a water molecule to interact with the ester linkage of the nascent chain in the PTC, which by necessity is a hydrophobic pocket on the ribosome. At this point the RF can either catalyze the hydrolysis or allow the PTC to perform the function for which it has evolved with water as the nucleophile as opposed to the A site α-amino group.

Class II release factors

Class II release factors (RF3 in eubacteria) are not required for the activity of class I RFs. RF3 does not accelerate the activity of RF1 or RF2 instead through the binding of GTP class I RFs are ejected from the ribosome following ester bond hydrolysis (*118*). RF3 has been shown to bind to but not act on class-I-RF:ribosome complexes until after the ribosome has been unlocked by the cleavage of the nascent chain (*30*). This is similar to EF-G's binding requirement except that RF3 binds the ribosome in its GDP form (*119*). A direct interaction between the class I and class II RF stimulates the release of GDP and a stable complex is formed. In this way the ribosome:class-I-RF complex acts as a guanine nucleotide exchange factor for RF3. Following cleavage of the ester linkage RF3 binds GTP and changes conformation (*119,*

120). The shift in conformation displaces RF1 or RF2 via the formation of a stable complex with the ribosome. Subsequent hydrolysis leads to a low affinity state and the dissociation of RF3 from the ribosome. The recent work showing EF-G and RF3 share common preferences for high affinity interactions with the ribosome support earlier suggestions that the two are structurally and evolutionarily related.

Although there is no high-resolution structure available for RF3, it does share a similar sequences to EF-G. Similarity between N-terminal domains I, II and IV from EF-G and RF3 led Nakamura *et. al.* to suggest that class I RFs may be related to the C-terminal region (*111*). This idea motivated him to compare class I RFs from different organisms with other translation factors and delineate conserved structural domains that were used in domain swapping experiments to derive the conserved discriminator peptide sequence. This leads to a proposition that the mechanism for the expulsion of class I RFs may be via a conformational change on the ribosome similar to that shown in response to the high affinity EF-G:GTP binding (*68*).

RRF (ribosome recycling factor)

RRF is the most tRNA like molecule of all the proposed tRNA mimics (Figure 1-11). High resolution structures of RRF from *Thermus thermophilus, E. coli,* and *Thermotoga maritima* were solved independently (*83-85*). These structures are composed of two domains, strangely called domains I and II. The three structures superimpose almost perfectly upon one another and with the L-shaped structure of $tRNA^{phe}$, except for lacking the 3'-aa aceptor end of tRNA (*121*). Domain I is an almost perfect rendering in

protein of the anticodon arm of a tRNA while domain II is a truncated version of the acceptor arm.

There are two models for the mechanism by which RRF disassembles the post-termination complex. At this point in translation, the post-termination complex is composed of a 70S ribosome, occupied by mRNA, with A site stop codon and 2 deacylated tRNAs in the P and E sites. Both models agree that the process begins by the binding of RRF to the A site and is then followed by the action of EF-G:GTP. Kaji *et. al.* propose that the mimicry of RRF be extended to the exact function of tRNA (*84*). In this model RRF bound to the A site in a codon-independent manner and without contact with the PTC, is translocated by EF-G as a tRNA. This places RRF in the P site but without the stabilizing interaction on either the mRNA or PTC at which point the ribosome dissociates to component subunits, tRNA and mRNA. This model does not explain some of the data supporting the other model and is itself reliant on an indirect assay for function (*121*).

The alternative model suggests that RRF acts by occupying the A site. The subsequent action upon RRF by EF-G does not yield translocation but instead yields a dissociated 50S subunit and a 30S complex containing a P site tRNA on mRNA (*122*). Evidence supporting this model includes data showing that IF3 is required to displace deacylated tRNA from the 30S subunit following dissociation if the 30S subunit are to be recycled (*39*). Experiments performed by Nakamura *et al.* using *in vivo* complementation and *in vitro* assays also support a model which does not require the actual translocation of RRF (*123*). The experiments use RRF and EF-G from archaea and eubacteria in complementation experiments as well as domain swapping between the different

organisms' EF-Gs to show that RRF interacts directly with EF-G. Further experiments with EF-G mutants incapable of translocation were also shown to promote subunit dissociation. It was also shown that EF-G in its GTP conformation was not compatible with RRF in ribosome binding. These results demonstrate convincingly that the role of RRF, despite its structural identitiy as a tRNA mimic, does not involve translocation to the P site and displacement of tRNA. Furthermore, experiments from another group have also demonstrated by plasmon resonance studies of immobilized RRF that the factor preferentially binds to the 50S subunit (*124*). Taken together with recent results concerning the effect on the conformation of the ribosome by EF-G:GTP (*30, 62, 68*) a mechanism of RRF can be proposed. The action of EF-G:GTP on the ribosome forces the ribosome into its translocation intermediate state where RRF can interact preferentially with regions of the 50S subunit necessary for 70S ribosome stability. This forces dissociation of the subunits prior to the hydrolysis of GTP.

Conclusion

In the last decade great strides have been made in our understanding of the molecular mechanisms of translation. The release of high and medium resolution crystallographic and cryo-EM models in various states peptide synthesis have aided immensely in this endeavor. They have refined and in some instances redefined certain aspects of our understanding, but mainly they have allowed researchers to place their results in an atomic framework. This has allowed many groups to design experiments and interpret results on the same scale as the original modeling work. In this way, the traditional "hammer and tongs" approach to mechanistic and structural analysis is proceeding to unlock the molecular mechanisms of ribosome function. In the future, the

biochemical techniques will aid in dissecting these static images and find the routes by which ribosomes change conformation in order to accomplish a given task. Within the last five years, direct structural analysis has described several instances of ribosomal dynamics, *i.e.* during codon:anticodon interaction on the 30S and translocation, with the former at atomic resolution and the latter at medium to low resolution. Even the atomic resolution models of structural changes await investigation to determine their full implications on function.

To develop a better understanding of rRNA dynamics, we have developed a technique for the discovery and characterization of conformational dynamics within the rRNA of the ribosome. The research presented in this dissertation describes the creation and use of a technique known as *rapid non-equilibrium probing* or RNP.

The second chapter presented is a published manuscript describing a time-resolved study of ribosomal subunit association using RNP. The first section includes experiments providing a proof of concept and defines all the vital parameters for the fast probing of nucleic acids using a fast-mixing quench flow apparatus. The results show RNP can be performed with resolution in the sub-ten millisecond range using dimethyl sulfate (DMS) as the chemical modifier.

The manuscript then describes experiments showing how the rate at which the reactivity of bases to DMS in different regions of the 30S subunit vary as a result of association with the 50S subunit. We discovered that the reactivity of bases associated with different inter-subunit bridging regions change with a minimum of two different rates. Also, some regions contain bases whose reactivity change in a manner indicating that the region's environment is rapidly rearranged in a complex manner.

These data are placed in a structural context by comparing available crystallographic models of the 30S subunit. 30S models are available from crystals of the 70S ribosome with mRNA and tRNA in the A, P, and E site as well as from 30S subunits alone and with tRNA and mRNA analogs. From the differences within these structures clues can be found as to alterations in the 30S structure that must occur for association to proceed.

The third chapter concerns the use of RNP to study the contribution of mRNA to the structure of the 30S subunit and to the 30S's ability to associate with the 50S subunit. The results suggest that mRNA binding to the A site alters the 30S subunit forming a complex that is rapidly converted by interactions to a 30S subunit in the 70S ribosome. We also show that the presence of a Shine-Dalgarno (SD) sequence limits the ability of a message to interact with the A site and catalyses formation of a unique structure on the ribosome. This is justified as a possible allostery between A site and P site decoding that is mediated by the SD sequence interacting with the anti-SD sequence on the 3' terminus of the 16S rRNA.

Chapter four concludes and summarizes the research presented and proposes future research using this technique.

Chapter 2

A Time-Resolved Investigation of Ribosomal Subunit Association.

Scott P. Hennelly[1,2], Ayman Antoun[3], Måns Ehrenberg[3], Claudio O. Gualerzi[2], William Knight[1], J. Stephen Lodmell[1], Walter E. Hill[1,*].

1 Division of Biological Sciences, The University of Montana, Missoula, MT 59812.

2 Laboratory of Genetics, Department of Biology MCA, University of Camerino, 62032Camerino (MC) Italy)

3 Department of Cell and Molecular Biology, BMC, Uppsala University, Box 596, S-75 124 Uppsala, Sweden.

Modified from the manuscript published in, The Journal of Molecular Biology, March 11, 2005

This manuscript represents work by the author of this dissertation with the exception of the light scattering data, which was the contribution of the collaborators, Ayman Antoun and Måns Ehrenberg.

Introduction

Active ribosomes, ubiquitous in all living systems, are composed of two subunits of unequal size that associate and dissociate from one another with each cycle of mRNA translation. Although these processes are facilitated by protein cofactors, the essential recognition elements are intrinsic to the ribosomal subunits. The connections between the subunits serve a vital role, since, in addition to holding the ribosome together, they are likely conduits for signal transmission between the 30S decoding subunit and the 50S catalytic subunit.

The structural aspects of the association of ribosomal subunits have been the subject of many different studies using a variety of techniques. Early studies by Noller's group (*125, 126*) used footprinting methods to identify sites on rRNAs that were protected upon subunit association. Later footprinting studies giving greater detail identified a number of rRNA sites that participate in subunit association (*127, 128*). Crosslinking was also used to show interactions between the 23S and 16S rRNA after association (*129*).

Intersubunit bridges were initially visualized using cryo-electron microscopy (*60, 130, 131*). X-ray crystallography of 70S ribosomes by Noller's group showed details of 12 inter-subunit bridges, most of which were composed of rRNA (*1, 132*). These bridges were then confirmed to be present in solution with cryo-electron microscopy in prokaryotic (*133, 134*) and eukaryotic ribosomes (*135*). By using a chemical modification interference approach, Maivali and Remme (*38*) have identified those bridging residues

in the 50S subunit that play a role in subunit association. These studies, taken as a whole, lead to a picture of the two subunits being associated through a number of tentacle-like interactions of rRNA and rRNA/protein bridges, some having a more central role than others.

The kinetic aspects of the association process have also been under scrutiny for some time. As early as the mid 1970s, Grunberg-Manago and co-workers looked at the effects of Mg^{++} on the kinetics of subunit association, (*136, 137*) and Noll and co-workers reported on various kinds of ribosomes, defining some as tight couples and loose couples, depending upon their propensity to dissociate at moderate levels of Mg^{++} (*138*). Recent studies by Nierhaus and co-workers have shown that the association process follows first-order kinetics and have identified a large activation energy needed for the 30S subunit to participate in association (*49*). The kinetics of the association process has recently also been studied by Ehrenberg's group using stopped-flow and Rayleigh light scattering (*139*). These results indicate that the association process is quite rapid and very complex, with numerous contacts being made between the subunits as association takes place.

Additionally, there is considerable evidence that the ribosome is a dynamic particle, with substantial movement of various domains not only during the association process, but also during the translational process itself (*68, 71, 77, 133, 140-145*). While kinetic studies can indicate the dynamics of these processes, and crystal structures as well as cryo-EM models can provide snapshots at certain times, the details of functional conformational changes that occur as the ribosome is assembled, the subunits associate, or translation takes place remain unknown to a large degree.

In this study we use a novel approach, *rapid non-equilibrium probing*, to monitor the chemical reactivity of nucleotide bases in 16S rRNA in real time as the 30S and 50S ribosomal subunits are associated. This technique couples rapid-mixing in a quench-flow apparatus with the power of chemical footprinting to characterize time-resolved reactivity of specific nucleotides. Thus, during subunit association, the reactive rRNA bases involved can be monitored at discrete, short time intervals as association of the subunits occurs. These time-resolved data allowed us to construct a model wherein some regions of the rRNA bind initially and generate structural changes that allow the remaining contacts to be made for complete association of the two subunits. The results clearly show that some regions of the rRNA interact almost instantly, while other regions react at a later time. The results also suggest that these initial interactions trigger other structural changes that may be required for the transition of independent active 30S ribosomal subunits into the 30S subunits of the 70S ribosome.

Results

Validation of the method:

Initially, it was essential to determine the limits of the non-equilibrium probing approach with respect to modification and quench reaction times. The design was to use a standard quench-flow apparatus containing four syringes and two variable delay lines to allow the necessary components to be added. The first two syringes contained the components to be mixed, the third contained the chemical modification reagent (DMS in this study), and the fourth a quench solution to stop the modification reaction. A diagram of the apparatus is found in Figure 2-1. The design of the apparatus allowed the

sequential rapid mixing of reactants in millisecond to second times by changing the delay lines and flow parameters. The initial question was the rapidity of the DMS reaction and quench. Ultimately, the lower limit of time of reaction of two components would be the sum of the delay time (incubation of the reactants), modification time and quench time.

Figure 1.

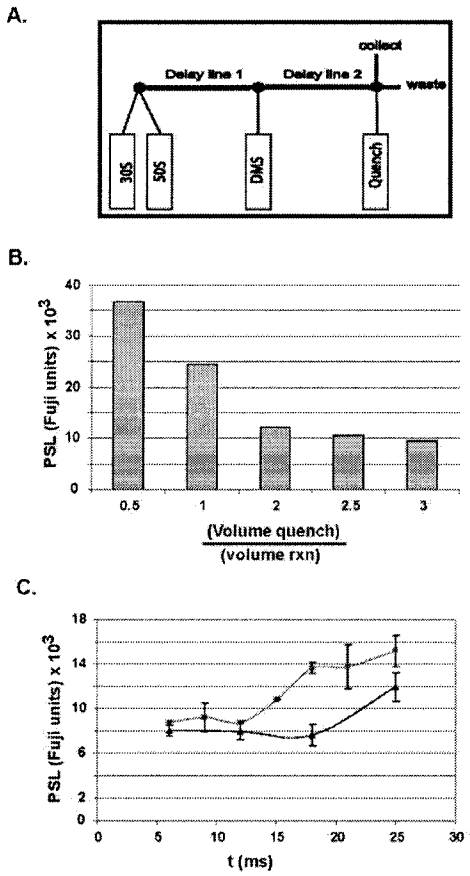

Figure 2-1. The parameters for the rapid modification of the rRNA with DMS were defined by titrating the amount of DMS quench and the time of DMS modification. Modification of A702 in the 16S rRNA of 30S subunits was used as a model for establishing the parameters. (a) A diagram of the flow path for the Bio-logic SFM-400 four syringe quench flow apparatus used in these experiments. (b) The volume quench solution used in the experiments was titrated using a 12 ms DMS modification. The results are expressed as the absolute intensity (units of the Fuji phosphorimager) the primer extension stop at A702 versus the ratio of quench solution over the volume of probing reaction. The amount of solution required for efficient stop is represented by a lack of decrease in the modification of A702. (c) The reaction times of DMS were titrated at A702. The fast phase of the reaction occurs much earlier than the earliest time point taken. At a final concentration of DMS of 4% (v/v) (Squares), the titration shows no increase in modification before 15 ms after which a second phase of modification is observed that is probably the result of the over-modification of the rRNA. At 3% (v/v) DMS (triangles) the early phase is extended before a second phase is observed. The background of bases in unmodified control reactions is typically less than 5% of the modified value. All modifications are performed at a 3% (v/v) final concentration of DMS.

It was necessary to identify a stop solution which was sufficiently reactive to quench the DMS yet not be deleterious toward the rRNA. A 1:1 solution of EtOH:β-mercaptoethanol proved to be satisfactory for this purpose. Early titrations of DMS concentration showed that at final concentrations of DMS less than 2% (v/v) resulted in titrations of modification for DMS reaction times over 6 to 12 ms (data not shown). When a final DMS solution of 3% (v/v) is used and the amount of quench solution titrated, it was possible to find the amount of quench necessary to stop the DMS reaction in times of less than 10 ms. Figure 1b shows the titration of quench in a 12 ms DMS reaction by monitoring the modification of A702 in the 16S rRNA, that has been shown to become protected by association (*128*). The difference in modification between quench volumes starts to approach zero after 2 volumes of stop solution. The amount of modification at 2.5 volumes of quench is ~90% that of 2 volumes.

A requirement for a time resolved assay of base accessibility via a chemical modifier is that the modification reaction be much faster (> 10 fold) than the reaction studied. At a 3% (v/v) concentration of DMS (~300 mM) the fast phase of modification is complete before the shortest delay time (6 ms) physically available. This time is defined by the necessity to deliver a large volume of quench relative to that of the other components while not exceeding a maximum flow rate. Figure 2-1c shows a titration of DMS reaction time from 6 ms to 25 ms using 3% (v/v) and 4% (v/v) final concentrations of DMS. A stable level of modification is seen for the earliest time points after which a second phase of modification appears that is likely due to an alteration in RNA structure caused by DMS. This leads to over-modification that can be seen in the primer extensions as a general increase (data not shown) in background as the modification is allowed to

proceed beyond 15-20 ms. All experiments performed in this study use a 3% (v/v) DMS concentration.

The results of these studies show that fast modification can be achieved and differences resolved using modification times less than 6 ms. However, it is also apparent that differences in modification time for different experiments must have independent controls. All experiments performed for this study use modification times between 12 and 25 ms and separate controls were carried out for each modification time.

Subunit association at equilibrium:

It was imperative that we use some independent method to assure that, under the conditions of this study, subunit association was occurring and 70S ribosomes were being formed. We used an analytical ultracentrifuge to run sedimentation patterns on ribosomal subunits at various magnesium concentrations, with and without poly U present and compared the results with fast modification of the same complexes at equilibrium. The analytical ultracentrifuge results (Figure 2-2a) indicated that under the buffer conditions of this study (10mM Mg^{++} - the concentration used in this study) more than 50% of the 30S particles were associated after a 10 min incubation at 37°C. These results agreed with the 12 ms probing data (Figure 2-2b). Preformed 70S ribosomes were modified for 12 ms at the various Mg^{++} concentrations. The level of modification remains the same as, or slightly greater than that of 30S controls until 10 mM Mg^{++} concentration is reached. Also, whereas subunits alone at 6 mM Mg^{++} produced only a small proportion of 70S subunits, with poly U present, over 50% of 30S subunits associated at 6 mM Mg^{++}, with the presence of polysomes evident (Figure 2-2c). The stabilizing influence on subunit association of poly U and, to a lesser extent natural mRNA, is also apparent from fast

probing of the complexes (Figure 2-2d). This information, coupled with the fact that replicate 30S and 70S controls for every time point were run, provided assurance that the time-dependent changes we observed are a product of subunit association. As an example, the primer extension results of various time points from probing the association process at base A702 are provided (Figure 2-3). The time points ranging from 25 ms to 650 ms show the time course of increasing protection at A702 as association proceeds. Three separate modification times are used for the various points and relevant controls are provided. Normalization of these points coupled with replicate runs provide the data shown in Figure 2-6g.

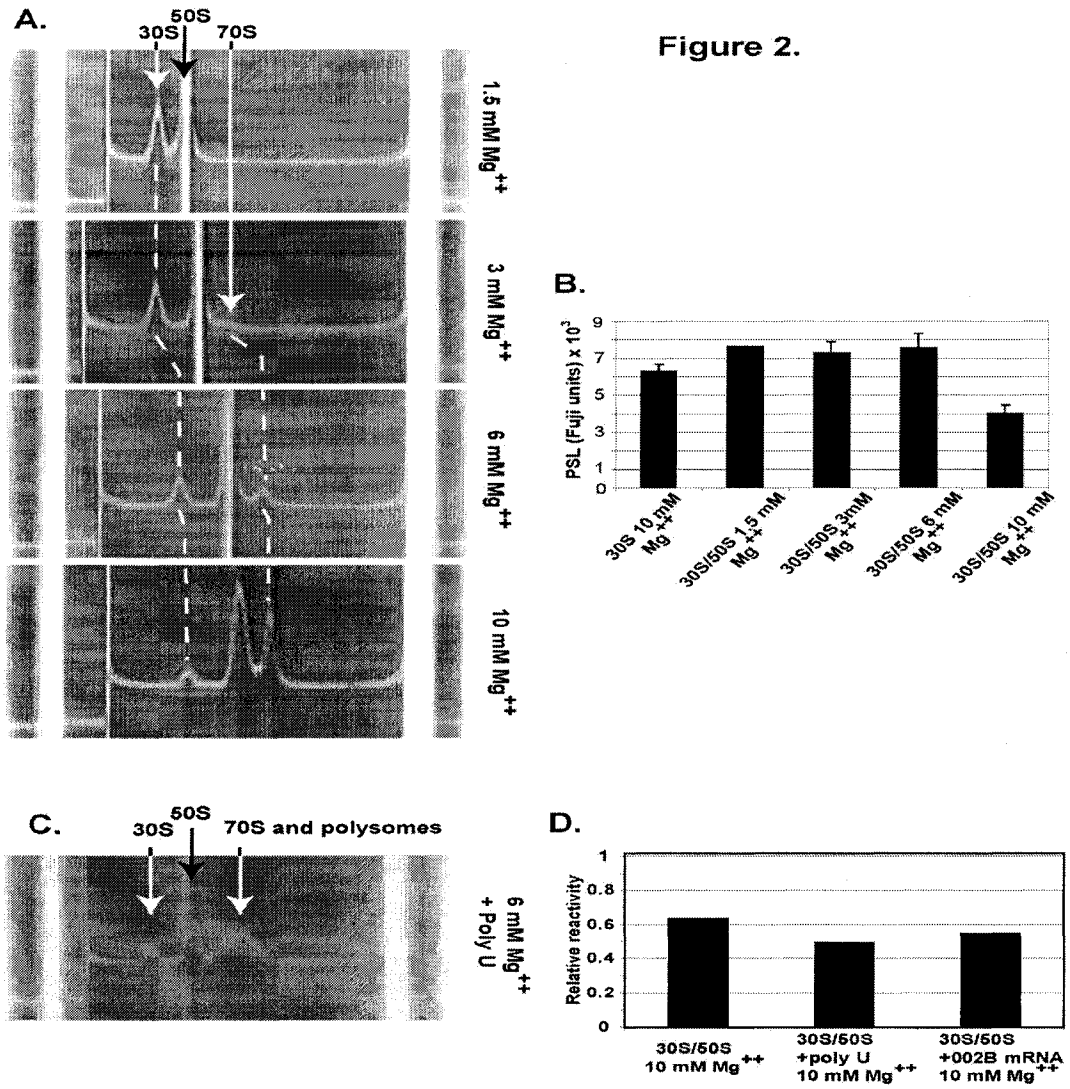

Figure 2.

Figure 2-2. The level of subunit association at equilibrium was determined by analytical ultracentrifugation and compared with results from DMS modification protection at 16S rRNA base A702, which is known to be protected by association. (a) Schlieren images from a Beckman Model E analytical ultracentrifuge showing the increase in association of ribosomal subunits (30S-2 μM, 50S-4uM) as the level of Mg^{++} increases. There are no apparent 70S ribosomes at 1.5 mM Mg^{++} and between 60% and 70 % of the 30S subunits can be seen to become associated in 70S ribosomes at 10 mM Mg^{++}. (b) The same result can be seen in the protection of A702 due to subunit association (30S-1 μM, 50S-2uM). These ribosomes were formed and then probed for 12 ms with DMS and analysed by primer extension. The results are expressed in PSL units from a Fuji FLA-3000G phosphorimager. At levels of Mg^{++} lower than 10 mM modification of A702 is slightly greater than that of 30S subunits alone. (c) The effect of poly U on the equilibrium position of subunit association is apparent in this schlieren image. At 6 mM Mg^{++} with poly U the level of 70S ribosome formation is equivalent to or slightly greater than that of subunits alone at 10 mM Mg^{++}. (d) DMS probing at A702 of associated subunits shows greater protection in the presence of poly U or natural mRNA at 10 mM Mg^{++}. These results are expressed as reactivity relative to A702 in 30S subunits with poly U and no 50S subunits as determined by phosphorimager analysis of the primer extension gels.

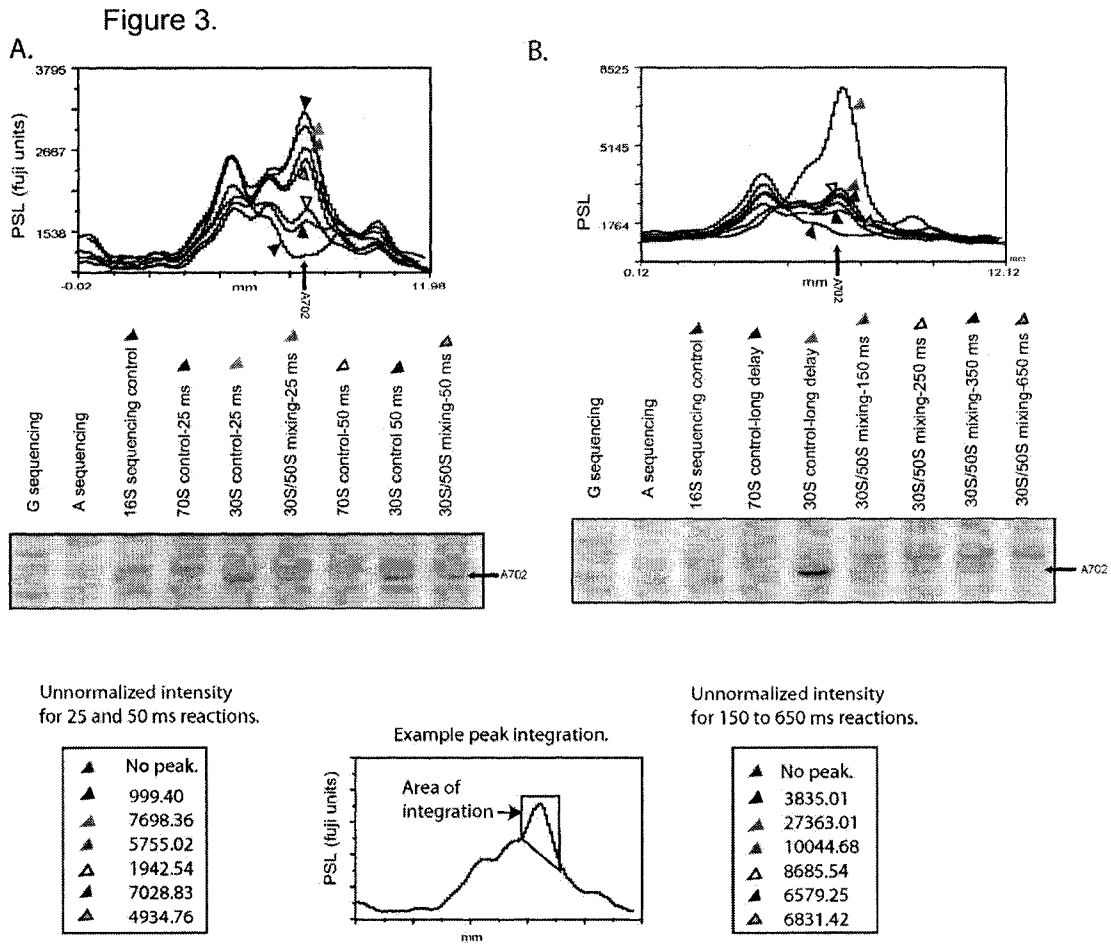

Figure 2-3. Examples of the data used to determine the time-resolved differences in reactivity at various positions in rRNA. Images show primer extension reactions of 16S rRNA from individual time points. These include control; preformed 70S and 30S as well as 30S/50S fast mixing experiments at different pre-quench delays. Above each image is an example phosphorimager intensity trace down the lanes around A702. These traces show the intensity at A702 from the 16S controls through the experiments. Colored markers are used to identify the trace from each lane. Under the Images are the results from the integration of the peaks at A702 and the unnormalized value of the integration. Also shown is an example of how the areas integration are assigned. (**a**) Experiments done at 30S/50S pre-quench delay times of 25 ms and 50 ms with the intensity trace beneath. The 25 and 50 ms experiments use different DMS modification delays of 12 and 25 ms respectively (see experimental methods). (**b**) Experiments done at 30S/50S delay times 150 ms to 650 ms. These experiments use the same DMS modification delay time of 17 ms.

Determination of the association rate constant k_a for ribosomal subunits

To verify the validity of the results of the rapid non-equilibrium probing technique a rate constant for association was determined in the buffer conditions used for

these experiments. The rate was determined by light scattering in a fast mixing stopped flow instrument. It is well known that the concentration of magnesium ions, ionic strength and composition of the buffer have a profound effect on the rate and accuracy of protein synthesis (*146*). It has also been demonstrated that the association rate constant of 'empty' ribosomal subunits increases by almost an order of magnitude when the Mg^{2+} concentration in the buffer increases from 4 to 8 mM (*137*). Figure 2-4 shows that the rate constant of subunit association is 14 $\mu M^{-1}s^{-1}$. The light scattering results verify that association of subunits occurs in the same time scale as the rapid probing results we report here. Determination of an exact association rate constant is challenging with the rapid probing technique. This is due, for the most part, to the fact that the individual bases involved in the process are observed rather than the global association product. Thus, portions of the 30S interact with the 50S subunit at varying rates, as observed by changes in the reactivity of local bases. As will be discussed, the formation of ribosomes from subunits is seen to proceed by steps with a minimum of two rates. Furthermore, the extent of association in these light scattering experiments is estimated at 52% of the 30S subunits (data not shown). This is similar to the amount of relative protection we found between 30S and 70S with poly U in our equilibrium probing results shown in Figure 2-2.

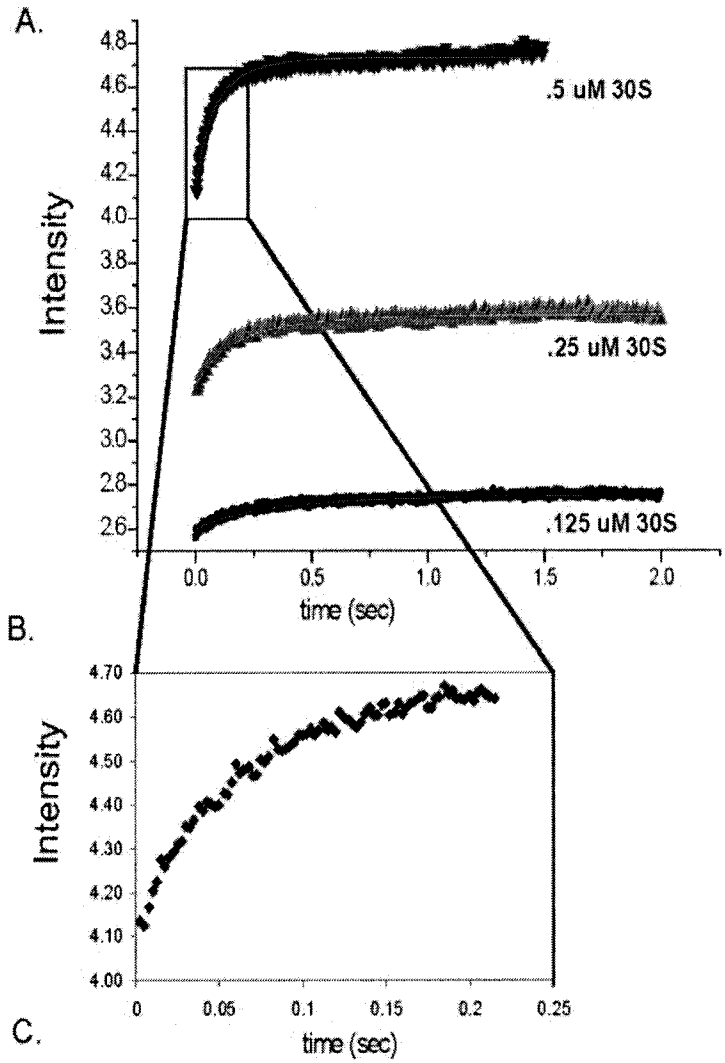

Equation: A*(1-exp(-ka*c*t))/(1-D*exp(-ka*c*t))+B		
[30S] uM	Amplitude	ka association rate constant
0.125	0.154 ±0.003	13.9 ±0.2
0.25	0.314 ±0.004	
0.5	0.583 ±0.005	

Figure 4

Figure 2-4 The association rate constant of 30S ribosomal subunits with 50S subunits (**a**) The extent of 70S formation was monitored as a function of time by light scattering after rapid mixing of different concentrations of 30S subunits with 50S subunits in a stopped flow instrument. The final concentrations of 30S and 50S are: (i) 0.125 μM 30S and 0.25 μM 50S, (ii) 0.25 μM 30S and 0.5 μM 50S or (iii) 0.5 μM 30S and 1 μM 50S. (**b**) Shows the intensity vs. time of the scattering experiment with subunit concentrations of 0.5 uM 30S and 1 uM 50S from 0 to 200 ms.(**c**) The rate equation describing the association of subunits and the rate determined from the experiments in (a). A = amplitude , D = [30S]/[50S], c = concentration of 30S subunits, ka is the rate constant and B= scattering intensity at t=0.

Design of the study:

We studied three different regions of 16S rRNA in the 30S ribosomal subunit that are involved in intersubunit bridges: helix 23 (the 700 region), helix 27 (the 900 region), and helix 44 (the 1400 region) (Figure 2-5). These regions represent 16S nucleotides participating in four separate bridges (B2a, B2c, B5 and B7a, Figure 2-5) that form between the subunits. (*1*) Activated 30S and 50S subunits with poly U as mRNA were used in this study. After mixing the 30S subunits containing poly U with 50S subunits, the samples were delayed for time intervals varying from 25 ms to 5s (these times include the time of modification, which varied from 12 ms to 25 ms) and then quenched. The 16S rRNA was then extracted, sequenced using primer extension, and the resulting time-dependent reactivity of various bases monitored.

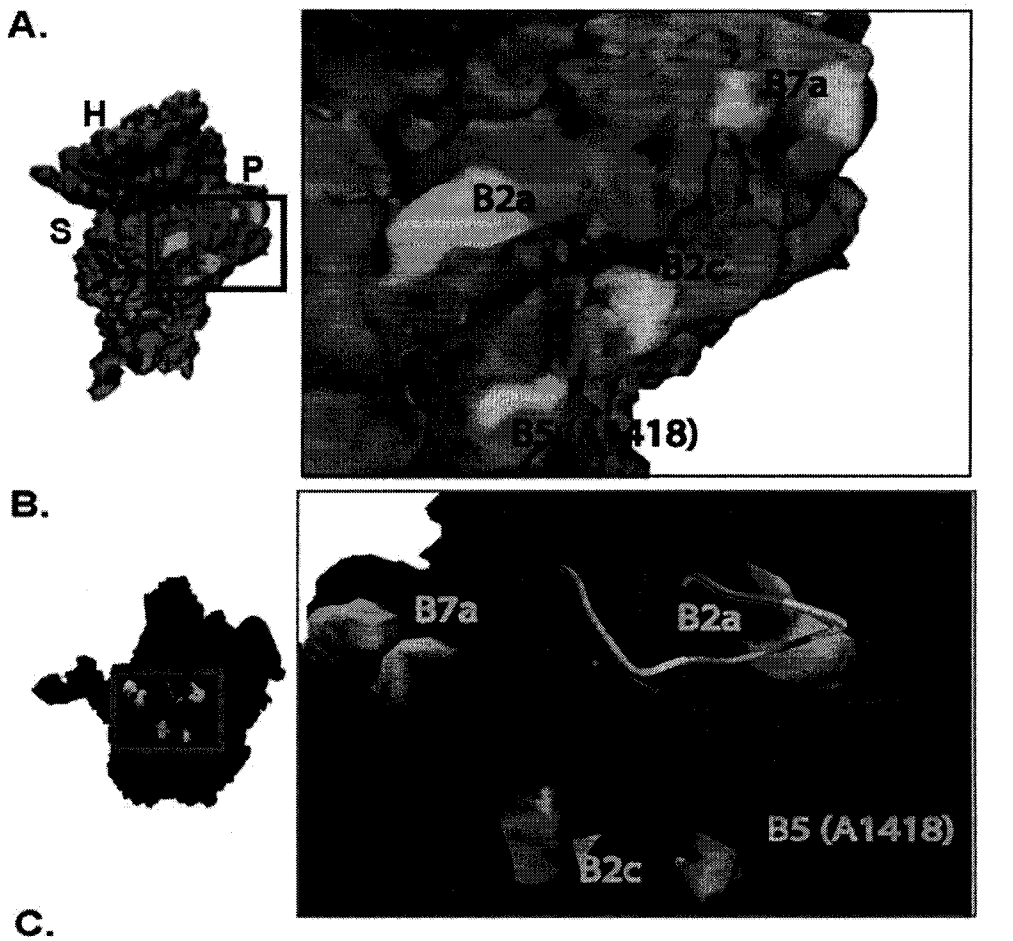

Figure 5.

Figure 2-5 Bridge regions of the 70S ribosome. (**a**) Surface rendering of the crystal structure of the 30S (*52*) subunit showing the head (H) shoulder (S) and platform (P) regions. Nucleotides from intersubunit bridges studied in this report are colored cyan. (**b**) Surface rendering of the 50S (*78*) subunit showing the location of the bridges in orange and the backbone positions of the flexible helix 69 from the 70S crystal model (*1*) shown in magenta and residues involved in bridge B2a in cyan. (**c**) Also included is a schematic of the 16S rRNA from *E. coli* showing the regions investigated and their associated bridges, original image from the Comparative RNA website (http://www.RNA.icmb.utexas.edu).

50S protections of H44.

The penultimate stem-loop (helix 44; bases 1399-1504) of 16S rRNA is situated almost vertically across the body of the 30S ribosomal subunit on the interface side in an ideal position to mediate subunit association (Figure 2-5). Previous footprinting studies reported several bases that were protected from DMS modification upon association of subunits. (*126-128, 147*) These bases included A1413, A1418, A1441 and A1394. We found that bases A1408, A1413, A1418 and A1441 were protected by association with the 50S subunit in a time-dependent manner. A1394 was poorly reactive using this technique, but baseline-level protection (lowest stable level of modification) at A1408, A1413 and A1418 was rapid (less than 100ms) upon the addition of the 50S subunit. However, the behavior of A1408 was somewhat different, with reactivity diminished at the earliest time point measured (25 ms), followed by a rapid decrease to baseline-level protection (Figure 2-6a, 2-6b and 2-6c). On the other hand, A1413 and A1418 exhibited biphasic behavior with slower initial decrease in reactivity followed by a rapid decline.

50S protections of H27.

The earliest changes we observed were in helix 27. This helix lies directly behind and in contact with the 1413 region of H44 (Figure 2-7). Helix 27 (nucleotides 885-912) has been the focus of much attention concerning its possible role in 30S subunit dynamics, although the details of how and when H27 moves are still unknown (*148-154*).

We found the reactivity of bases in H27 to be both protected and enhanced very rapidly in a manner suggesting a rearrangement of the local structure. To an even greater extent than with A1408, there is a very rapid influence of the 50S subunit, independent of and prior to, A1413 and A1418 protections. For instance, the level of modification at base A908 is substantially reduced at even the earliest time point (25 ms) (Figure 2-6d), suggesting a protective influence from association before the earliest time point taken. At the other extreme, base A892, which is stacked upon A908, was found to be more reactive to DMS at the earliest time points (Figure 2-6e), following which it returns to a reactivity equivalent to that of 30S subunits alone. The activity of A909 is attenuated at the earliest time points, similar to the pattern found with A1408, and is diminished thereafter (Figure 2-6f).

A late step in the association process

At a much slower rate, subunit association protects A702 in helix 23 (bases 693-717) and A1441 in H44. H23 is located on the extended portion of the platform in the interface region of the 30S ribosomal subunit (Figure 2-4). Base A702 is available for modification in the 30S ribosomal subunit, and has been shown to become protected after association takes place (*128*). In the present study, this base was increasingly protected as the reaction time was extended. At 25 ms, there was little protection, but as time was extended to 5 sec, the protection progressed slowly to that of the control 70S ribosomes (Figure 2-6g). A similar result was found at A1441 with protection proceeding at an apparently slower rate (Figure 2-6h). The slower protection of A702 and A1441 stand in contrast to the rapid protection of other bases in H44 and immediate changes in H27.

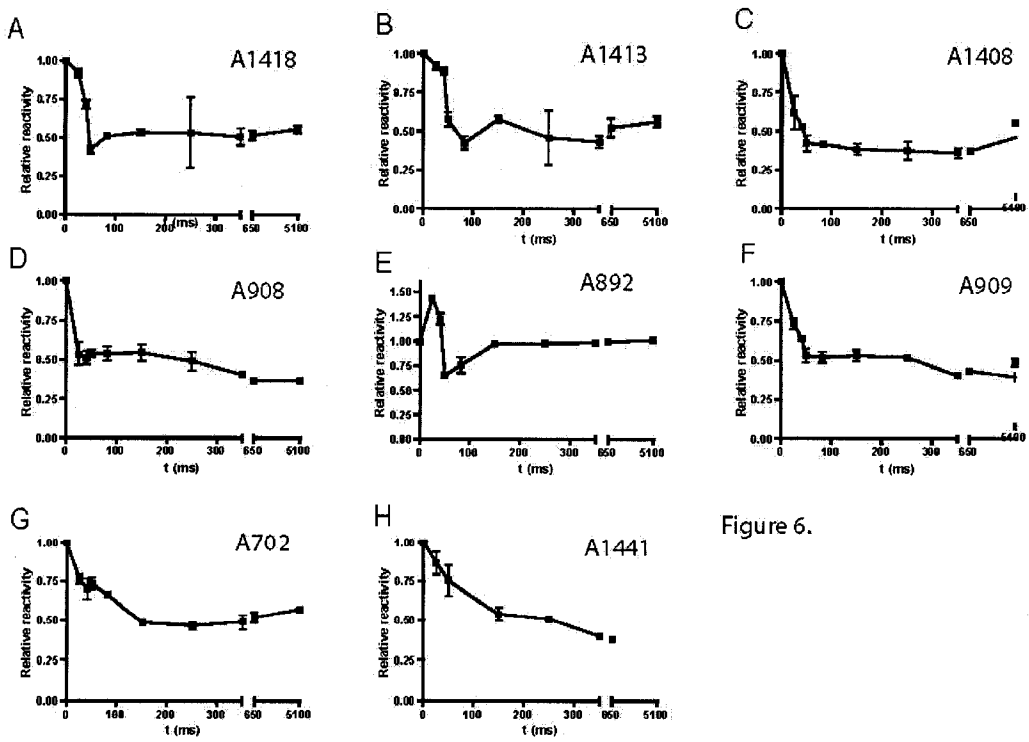

Figure 6.

Figure 2-6. Time resolved DMS reactivity at different bases in the 16S in response to association with the 50S subunit. Reactivity at all bases is determined in reference to that of 30S controls mixing with buffer. Delay times for the mixing of subunits were 25 ms, 41 ms, 50 ms, 83 ms, 150 ms, 250 ms, 350 ms, 650 ms and 5100. (**a**, **b** and **c**) Reactivity changes in the 1400 region of Helix 44 with bases from bridge B5; A1418, an interaction with Helix 27; A1413 and bridge B2a; A1408. (**d, e** and **f**) Bases in helix 27 that displayed varying reactivity. A908 was diminished at the first time point. A892 was hyper-reactive at the first time point but quickly returned to background 30S reactivity. A909 that makes a base triplet interaction with A1413-G1487 was moderately protected at the earliest time point and proceeded quickly to a background level of protection. (**g** and **h**) The reactivity of bases A702 and A1441 show a slow but constant decrease in reactivity (A1441 is shown with only 6 time points from 25 ms to 650 ms).

Computer Modeling.

To more fully understand the sequential association process, we overlayed the structures of three published independent *T. thermophilus* 30S crystallographic models that are available using the Ribosome Builder program (Ribosome builder is available for download at http://www.rbuilder.sourceforge.net). These models provide insight into the relationship between the structures of the 30S independent of or in association with the

50S, tRNA and message. The path of the backbone from the 30S subunit in the 70S model containing a full complement of tRNA and mRNA was overlayed onto the two high-resolution 30S models (Protein Data Bank no. **1GIX**)(*1*)(see Figure 2-7). One of the models contains a P-site tRNA and P- and E-site mRNA mimics (Protein Data Bank no. **1J5E**) (*155*) and the other is an activated subunit only (Protein Data Bank no. **1FKA**) (*156*). The process of overlaying the backbone positions yielded excellent overall agreement in the placement of all helices in the 30S structures. While the axis of helix 44 remains consistent in the 30S and 70S models, from the model of the 30S subunit alone to that in a 70S ribosome, portions of the structure are rotated with an associated small displacement toward contacts within the 50S subunit (Figure 2-7a and 2-7b). There is also an associated unwinding at the top of H44 in the decoding center proximal to bridge B2a (Figure 2-7c).

Our results suggest the formation of this bridge (B2a) to occur earlier than the bridges around A1418 (e.g. bridge B5), whose position between the models remains mostly stationary. Taken together with our other results (e.g. helix 27), this suggests, that the most rapid protections occur in regions that must be rearranged to accommodate proper bridging. It appears that the conformational rearrangement of the upper part of H44 may be part of concerted forces between H27 and H44. But, unlike H44, H27 contacts in bridge B2c require a displacement of the 900 tetraloop to avoid steric clashes with the 23S rRNA in the structure of the 30S subunit alone (Protein Data Bank no. **1FKA**) (Figure 2-7d). The early changes seen in H27 can be seen in the crystallographic models as resulting in a rotation of the helix, with bases A909 and A908 moving toward H44, and the backbone of H44 being locally translated toward the 50S (Figure 2-7e).

Figure 7

Figure 2-7. Backbone posititions of crystallographic models from high resolution 50S(*78*) and 30S(*52, 156*) subunits were overlayed onto the medium resolution 70S ribosome by aligning all possible pairs of defined axis orientations for all helices for best fit. (**a**) Surface rendering of 50S subunit from *D. radiodurans* aligned with the backbone coordinates from *T. thermophilus* 70S ribosome and the backbone of H44 from the three *T. thermophilus* 30S subunit models; containing tRNA and mRNA mimics (red), activated 30S subunit (green) and backbone positions of the 30S subunit from the 70S model (yellow). The flexible backbone positions of 23S rRNA H69 as it occurs in the 70S model is shown in magenta with bridge B2a residues (cyan). (**b**) Bridge B2a positions of 16S-H44 and 23S-H69 showing the rotation/displacement of A1408 and A1410 from the activated 30S subunit to 30S with P-site tRNA mimic to 30S subunit in 70S ribosome. (**c**) From the opposite view point the backbone deviation that occurs around the decoding site in an associated 30S subunit as the helix is locally rotated. (**d**) Bridge B2c interactions between the 50S (orange) and 30S (cyan) require a displacement of the tetraloop from the activated 30S subunit to the 30S subunit in a 70S ribosome, but the residues from the 30S subunit containing a P-site tRNA mimic would not interfere with association. There is also an apparent rotation of H27 from the activated 30S to the 30S in the 70S model. (**e**) The rotation is apparent in the backbone positions of A909 from the activated 30S to the 30S in the 70S model. Positions of A909 and A1413 are shown in orange in the backbone rendering of the 30S subunit from the 70S model.

Discussion

The results of this time-dependent study of ribosomal subunit association show changes in reactivity proceeding more rapidly at positions known to be involved in decoding as well as those involved in ribosome stability. Mainly, changes in helix 27 precede those in helix 44, with the exception of A1408, which changes at the same rate as some residues in H27. These results support a model of association in which the initial contacts include the bridges B2c and B2a of the 30S subunit. Following this, protective interactions proceed rapidly in bridge B5 and an interaction in H44 with H27 (A1413). Finally, sites more removed from the decoding center, bridge B7a and a residue near the loop of H44, base A1441, becomes fully protected. Furthermore, the time-resolved reactivity of bases in H27 point to a conformational change within or including this helix.

In helix 44, base A1408 had not been identified previously as protected from chemical modification after subunit association, although it was reported as protected from cleavage by RNAse V1 upon association, (*157*) and was weakly protected against chemical modification by an A-site bound tRNA. (*95, 158*) The uppermost bridge in

helix 44, B2a, is formed between the loop of helix 69 in the 23S rRNA and contacting bases 1408-1410 in H44, as well as making contact with P-site and A-site tRNA in the crystal structure. (*1*) H69 was found to be disordered in the crystal structure of the 50S subunit from *H. marismortui* suggesting that contacts with 30S and tRNA are required to constrain this helix. (*159*) The universally conserved and potential cross helix interaction for A1408, namely A1493 and its neighbor A1492, were also found to be less than absolutely constrained in the crystal structure of the 30S subunit alone and are believed to rearrange in response to an A-site tRNA binding. (*1, 98, 155*) Just as with A1408, bases A1492 and A1493 were also found to be protected by A-site-bound tRNA (*95*) and by the binding of IF1(*160*), but not by subunit association. (*128*) Thus, the rapid protection at A1408 may be the result of a time-dependent positioning of H69 and organization of the decoding center in preparation for tRNA binding in the A site. This organization takes place before the other bridge contact we studied in H44 (A1418, bridge B5a) is formed. Repositioning of H44 and disruption of a cross-helix interaction at A1408 appear to simultaneously prepare for intersubunit contacts with H69, as well as allow A1493 and A1492 to rotate out into the decoding center. These rearrangements may be critical for the progression of association, since modification of A1912 or A1918 in H69, a portion of the 23S rRNA contribution to bridge B2a, was found to greatly inhibit 70S formation. (*38*)

Since the reactivity changes seen in H27 precede the A1413 and A1418 protections, the former probably result directly from intersubunit contacts within bridge B2c formed between helix 67 in the 50S subunit and H27, instead of being transmitted through H44 (Figure 2-7d). B2c is formed by an interaction between the GNRA tetraloop

capping H27 and its receptor in H24 of the 16S with bases in H67 of the 23S. Recent studies demonstrate the importance of this interaction for the stability and function of the 70S ribosome. (*150, 151*) Mutants in the 900 tetraloop were found to be impaired in association and displayed fidelity phenotypes.

In the 70S crystal structure a direct contact is not found in the portion of H27 containing bases A892, A908, and A909 and the 50S subunit. However, alterations in the conformation of H27, which is located directly behind H44 (Figure 2-7), driven by interactions in B2c, have the potential to reposition H44 and then promote interactions between H44 and the 50S subunit. This may be suggested by the reactivity of A909, which at the earliest time points is attenuated and diminishes rapidly (Figure 2-6f), similar to that of A1408. The protection of A909, as well as protection of the bases in the noncanonically paired A1413-G1487 with which A909 makes a base triplet interaction, (*52*) are class III protections. (*161*) Class III protections are those found in 30S subunits in response to neomycin class antibiotics, tRNA or 50S subunit binding. (*1, 95, 161*) Also, base A892 has been previously identified as having enhanced reactivity in response to A site tRNA binding. (*95*) Thus, it appears that this conformational change, resulting in protections or enhancements previously attributed to tRNA binding (mainly A1408 and A892), occurs very early in the process of subunit association and represents a functional conformer of the 30S ribosome.

There is a large body of experimental data showing the importance of correct functional interactions within and surrounding H27. (*148, 150, 151, 162, 163*) We have added here a view of H27 not simply becoming protected, but instead that the environment of the helix changes in response to factor free subunit association in a

complex manner, early in the association process. Some of the rearrangements appear to be transmitted immediately to H44. Other interactions may drive H27 to move independently of H44. This can be seen in the later time points at A908 and A909, where protection increases even after all other residues monitored have reached a stable level of reactivity (Figure 2-6d and 2-6f). This provides new insight for discussion of the mechanisms at the heart of translation.

In the slowest step of those studied, A702 and A1441 are gradually protected. In x-ray crystallographic models A702 appears to participate in an "A-minor" interaction with the minor groove of H68 in the 23S rRNA. (*1*) Given the solvent exposure of A702 in the 30S crystal structures, it is apparently available for modification until the B7a contacts are made with the 23S rRNA. It is also likely that it is available for interaction with the 50S subunit unless precluded by an incorrect geometry within the 30S subunit during initial contact between the subunits. The interactions that result in protection of A702 by its bridge partner in the 50S subunit may facilitate or be a signal of the completion of a conformational change in the 30S subunit. This also seems likely for the protection of A1441. A1441 does not participate in a direct interaction with the 50S subunit. Like A702, A1441 is relatively far from the decoding center in the 30S subunit near the loop of H44. The protection must be due to a rearrangement of this region as a result of interaction between bridge elements closer to the decoding site.

As discussed earlier, the conformational rearrangement of H27 during association and the subsequent repositioning of H44 may favor association of 30S complexes containing tRNA and/or initiation factors through a conformational rearrangement producing class III protections. The sequence of protection and activation of bases seen in

our association system is suggestive of a mechanism to prevent incorrect association of empty 30S subunits in native conditions. The passage of the 30S subunit in this simple system through conformations previously associated with ligand binding and not association, points to an intermediate in the process that could be stabilized by those ligands. The regions of 16S rRNA containing bridges B2a and B2c undergo conformational rearrangement, in response to the 50S subunit, characteristic of an induced fit between the two subunits.

The 30S structural changes found in this study may be facilitated in native conditions by IF1. The crystal structure of the 30S subunit with IF1 bound (*31*) shows changes around the decoding center relative to the unbound 30S. These include the flipping out of A1492 and A1493, disruption of the A1493-A1408 interaction, and a conformational change over a 70 Å stretch of H44. The distortion in the region of H44 that contacts H27, is most extreme in the region containing the A1413-G1487 base pair. There is also a displacement of the platform moving it towards the decoding center. These regions containing class III protections are rearranged by the action of IF1 distorting the decoding center. Considering this and the stimulatory effect IF1 has on the rate of association (*164*), it becomes possible to propose a role for IF1 in catalyzing the formation of an association-intermediate conformation in the 30S subunit and preparing the A-site for tRNA binding. Further studies using all of the translation initiation factors, with natural mRNA, will be needed to identify such changes.

In addition to the results obtained on subunit association in this study, we have been able to demonstrate the efficacy of a novel approach in the study of rapid conformational changes in rRNA. This study provides evidence of reactivity changes of

specific nucleotides in the 16S rRNA that occur as the ribosomal subunits associate. These protections or activations indicate subtle structural changes occurring in a time-dependent manner as association occurs. The results provide evidence that the association process is multi-phasic, with regions around the decoding center changing structure earlier than outlying regions. There is also evidence that, in the absence of factors or tRNA, the 30S subunit passes through conformers associated with these ligands during the association process. The use of this fast probing approach at various stages of translation will provide a detailed understanding of rRNA structural changes that occur in ribosomes during translation. It is evident that this approach can be applied as well to any dynamic system to observe time-dependent changes in RNA structure. With the development of additional modification reagents, this approach will be applicable to time-dependent alterations in protein structures as well.

Materials and Methods

Ribosomal subunit preparation

Ribosomes were prepared from early mid-log MRE 600 *E. coli* cells. Cells were washed and ground in alumina while frozen, then salt washed in WC buffer (25mM Tris-HCl pH 7.6, 15mM $MgCl_2$ 1M NH_4Cl) to remove factors. After pelleting they were resuspended in 30/50 buffer (25mM Tris-HCl pH 7.6, 1.5 mM $MgCl_2$ 100 mM KCl) and loaded onto a 1200ml 10-40% sucrose gradient in a Beckman Ti-15 zonal rotor and centrifuged for 14 hrs at 30k r.p.m. 30S and 50S fractions were then collected and the subunits pelleted, washed and stored in NB10 (25mM Tris-HCl pH 7.6, 10mM $MgCl_2$ 60mM NH_4Cl) buffer at -80°C prior to use.

Defining experimental parameters.

Fast mixing experiments were performed on a Bio-Logic SFM-400 (Bio-Logic Science Instruments, Grenoble, France) fast mixing apparatus in quench flow mode. The four syringe fast mixing apparatus has separate delay lines for subunit mixing delay and DMS modification delay. Experiments were performed on 30S subunits to identify the rate at which DMS reacted and the rate at which it could be quenched. A titration of quench volume was done on 12 ms DMS modifications of 30S subunits. A 1 μM solution of 30S subunits was pushed from syringe 1 and mixed to 3% (v/v) DMS and quenched with various volumes of quench solution (50% β-mercaptoethanol in EtOH with .2 volumes 5M NH_4oAc pH-7.6). The titration of DMS reaction time was performed from 6 ms to 25 ms using 1 μM 30S subunits and 2 volumes of quench and either a 3% (v/v) or 4% (v/v) final DMS concentration. We used DMS reaction times between 12 and 25ms in our association studies. Reaction times with DMS were kept in this range while extending the delay times for subunit mixing. When DMS reaction times were varied separate controls were used in determining the extent of modification .

Equilibrium association experiments were performed on a Beckman Model E analytical ultracentrifuge. Subunits (30S-2μM, 50S-4μM) were incubated for 10 min. at 37°C in buffers containing 25 mM Tris-HCl, 60 mM NH_4Cl, and either 1.5 mM, 3 mM, 6 mM or 10 mM $MgCl_2$ and with or without 0.2 mg/ml poly U (Sigma-Aldrich). The mixtures were then loaded in an ANH analytical centrifuge rotor and run at 56k r.p.m. Schlieren images were taken every 4 minutes for 20 minutes. Probing experiments on subunits (30S-0.5μM, 50S-1μM) were also performed after incubation buffers for 10 min

at 37°C at the 4 Mg^{++} concentrations. The preformed complexes were probed for 12 ms and quenched with 2 volumes of stop buffer. Results were analysed as described below.

002B mRNA is a derivative of 002 mRNA (*165*) with the amino acid sequence repeated to create 22 codons instead of the original 10. The mRNA was transcribed from a synthetic DNA template using T7 RNA polymerase. Two DNA oligonucleotides were chemically synthesized and ligated together with T4 DNA ligase and a bridging oligonucleotide after which, the product was gel purified, annealed with an oligonuleotide containing the complementary T7 RNAP promoter sequence and transcribed.

Determination of subunit association by Stopped flow combined with Light Scattering.

The association of ribosomal subunits was monitored with light scattering after rapid mixing in a stopped flow instrument (Bio-sequential SX-18MV, Applied Photophysics, Leatherhead, UK) (*16, 139*). To determine the association rate constant of naked subunits, two mixtures, A and B, were prepared. Mixture A contained either 0.25 μM or 0. 5 μM or 1 μM 30S. Mixture B always contained either 0.5 μM or 1 μM or 2 μM 50S. The two mixtures were pre-incubated at 37°C for 10 minutes. To remove dust particles, the mixtures were centrifuged for 3 min at 14000 rpm before they were loaded into the syringes of the stopped-flow instrument thermo stated at 20°C for at least 5 minutes. After rapid mixing of equal volumes of A and B mixtures with the concentration of B particles always twice that of A particles, light scattering at 436 nm at right angle to the incoming light was recorded as a function of time.

Kinetics of macromolecular complex formation analyzed by stopped-flow and light scattering.

In a typical light scattering experiment to monitor a binary complex formation between particles of type A and B, a solution containing particles A is rapidly mixed with a solution containing particles B. Initially, the mixture contains particles A and B in concentrations *a (0)* and *b (0)*, respectively, while the concentration, *c (0)*, of complex C is zero. The scattering intensity, *I (t)*, at a time *t* after the mixing is the sum of the scattering intensities from free A- particles, free B- particles and C-complexes:

$$I(t) = a(t) \cdot I_A + b(t) \cdot I_B + c(t) \cdot I_C \qquad (1)$$

Here, *a(t)*, *b(t)* and *c(t)* are the concentrations of free particles A and B and complex C, respectively. Full details of the light scattering theory are described in (A. Antoun et.al., 2004). Since per every complex C formed, one particle A and one particle B are consumed, *a(t)=a(0)-c(t)* and *b (t)=b(0)-c(t)*, so that Eq. (1) becomes:

$$I(t) = I(0) + c(t) \cdot \Delta I_C$$

ΔI_C is the increase in light scattering intensity when the two particles A and B form a complex C.

The differential equation used in deriving k_a (association rate constant for 70S complex formations) is $dc/dt=k_a*[30S]*[50S]$. The solution is $c(t)= [30S]_T*(1-exp(-Q*t))/(1-([30S]_T/[50S]_T)*exp(-Q*t))+B$, where $[50S]_T$ is the total (or initial) concentration of 50S, $[30S]_T$ is the total (or initial) concentration of 30S and Q = $k_a*([50S]_T-[30S]_T)$.

The scattered light intensity is given by $I(t)= A1*(1-exp(-Q*t))/(1-[30S]_T/[50S]_T *exp(-Q*t))+B1$, with *A1* and *B1* as experimental parameters. In the light scattering experiments

of this study $[50S]_T = 2*[30S]_T$, so that $Q=k_a[30S]_T$ and the amplitude $A1$ of the intensity signal depends linearly on the concentration of subunits.

Fast probing experiments.

Syringes 1 and 2 contained 30S subunits, 50S subunits or 1X NB10 buffer depending on experiment. Subunits were activated by incubation in NB10 buffer at 37°C for 10 min. immediately prior to use. 30S and 50S mixing experiment used 1μM 30S/.2mg/ml poly U versus 2μM 50S and were mixed in a 1:1 ratio by volume. All experiments were made using a 6:100 mixing ratio between 50% DMS in EtOH delivered from syringe 3 and sample pushed from syringes 1 and 2. DMS reaction delay times varied depending upon experimental design between 12 and 25ms. Delay times for the mixing of subunits were 25 ms, 41 ms, 50 ms, 83 ms, 150 ms, 250 ms, 350 ms, 650 ms and 5100 ms. These delays represent the total time from first mixing of subunits to quench. Control experiments for 70S and 30S were mixed 1:1 against buffer with the final concentration the same as the 30S/50S mixing experiments and experiments with the same delay times as the 30S/50S mixing experiments were used. 70S ribosomes for controls were formed by preincubating 30S and 50S subunits in a 1:2 ratio(1μM:2μM) for 10 min. at 37°C in NB10 buffer with poly U (.2mg/ml). DMS reactions were stopped by mixing 2 volumes (2X the volume delivered from syringes 1 and 2) of quench buffer from syringe 4. Delay lines were washed with a minimum of 10 volumes of buffer between experiments. rRNA was extracted (2 times with phenol, 2 times with 1:1 phenol:chloroform and 2 times with chloroform) after precipitation and then re-precipitated.

Analysis of probing experiments.

Samples were sequenced using 5' ^{32}P-labeled DNA oligonucleotides complementary to sites less than 100 bases from the modified base of interest. Extension was done using AMV-RT (Seikagaku America) and loaded onto a 6% poly acrylamide sequencing gel and electrophoresed for an appropriate period of time. The gels were exposed and bands quantified using a Fuji FLA-3000G phosphorimager and Image Gauge software (Fuji Biomedical). Band intensity was normalized using overall lane intensity. Normalization coefficients were applied to all results bands on that gel. Relative reactivity was established by setting normalized band intensity in 30S control experiments of the same DMS reaction time to 1. All controls and experiments were repeated at least three times and standard deviation between the normalized intensity of bands was used to generate error bars.

Alignment of Ribosomal Subunit Models.

Two different PDB models of ribosomal subunits were aligned by the Ribosome Builder program using a helix alignment algorithm. This algorithm uses vectors directed along the helices of the rRNA chains and then searches for the best alignment of the subunits using a pair of helix vectors. The vector of a helix is defined by two points, A and B. Point A is the midpoint between the backbone atoms of residues R5b and R3e, where R5b is the beginning residue of the 5' side of the helix and R3e is the ending residue of the 3' side of the helix. Point B is the midpoint between the backbone atoms of residues R5e and R3b, where R5e is the ending residue of the 5' side of the helix and R3b is the beginning residue of the 3' side of the helix.

Let the two PDB models be called model i and model j, where model j will be aligned to model i. For a given pair of helices H1 and H2 that are defined in both models, let the vectors of H1 and H2 in model i be named vH1i and vH2i and let the vectors of H1 and H2 in model j be named vH1j and vH2j. Model j is aligned to model i in 3 steps. In step 1, model j is translated so that the beginning endpoint of vH1j is aligned with the corresponding endpoint of vH1i (Fig 1). In step 2, model j is rotated about an angle θ so that vH1j is aligned with vH1i (Fig 2). In step 3, model j is rotated about an angle ϕ where ϕ is the angle between vectors vPmi and vPmj, where these vectors are formed by projecting the midpoints of vH2i and vH2j into the plane defined by vH1i (Fig 3). This results in the best possible alignment of the second helix vectors while maintaining the alignment between the first helix vectors.

To find the pair of helices that will produce the best alignment between the two PDB models, each helix in model i is iterated. If the corresponding helix exists in model j, model j is transformed so that the helices are aligned as described in steps 1 and 2 above. Then, starting with model j in this intermediate transformation, each remaining helix in model i is iterated. If the corresponding helix exists in model j, then model j is transformed so that the second helices are optimally aligned as described in step 3 above. After each alignment, the RMS difference is computed between the backbone atoms of all residues in the rRNA chains of the two models. The helix pair that produces the smallest RMSD is then used for the actual alignment of the PDB models.

Chapter 3

Effects of mRNA on ribosomal conformation and subunit association.

Introduction

Lost in the fundamental research on the structure and function of the ribosome are a multitude of basic questions. One of these questions concerns the contribution of mRNA to translation. Of course, mRNA is the template from which the polypeptide chain is constructed but the role of mRNA in changing the ribosome's conformation and promoting the various steps of initiation and elongation remains unknown to a large degree. mRNA has been seemingly relegated to the role of inert participant in this very complex process. In this chapter investigation is carried out on the contribution of mRNA to the structure of the 30S subunit and the role it plays in promoting the formation of the 70S ribosome. The results show that mRNA has a profound effect on the structure of the 30S subunit when it occupies the A site. These changes promote the formation of a structure related to the associated 30S subunit in the 70S ribosome. The mechanism of association with A site bound mRNA is explored in terms of a potential translocation intermediate in the association process. There is also evidence that the binding of message containing a Shine-Dalgarno (SD) sequence to the 30S subunit precludes the occupancy of message in the A site via a mechanism that is potentially allosteric in nature.

There is one clear concept that emerges over and over in the literature concerning the structure and function of the ribosome: the correct and efficient functioning of the ribosome depends greatly on the interactions between the subunits. Not only do elements on either subunit interact with the mRNA and tRNA in the interface to catalyze translation, but the very affinity between the subunits is a determinant in the correct operation of the ribosome. Early in ribosome research came the realization that mono- and divalent ion concentrations were of extreme importance in the isolation and functioning of active ribosomes. Even after four decades the same discussions can be found in the literature and almost every laboratory has defined a particular system for the isolation and use of translating ribosomes. Some are minor permutations on a common buffer while others are complex mixes of organic and inorganic ions.

The reason for the attention to these seemingly simple details is in the complexity of the ribosome itself. The ribosome must reversibly associate not only with a multitude of ligands but also the myriad moving parts must glide along a narrow energetic threshold in order to maintain proper functional flexibility. This includes the all important intersubunit interactions. 70S ribosomes can be assembled from random subunits of any origin by the simple manipulation of Mg^{++} concentration. However, as Mg^{++} concentration increases from physiological concentrations (3-5 mM) the ability of the ribosome to undertake translation decreases until it is inert at concentrations from 15-20 mM. Obviously this is not a biologically relevant state. Instead the high Mg^{++} conformation likely represents the most stable intermediate in the cycle of elongation: that of a 70S ribosome with an amino acyl tRNA occupied P site (a "locked" ribosome). This can be seen in research on the many aspects of ribosome function, structure and

stability. Ribosomes free of factors, mRNA and tRNA (referred to as vacant ribosomes or vacant couples) are stable at physiological concentrations of divalent ions and sediment as 70S ribosomes. If these ribosomes are formed on a mRNA and a deacylated tRNA is bound to the P site, the ribosome becomes a more diffuse 60S structure at isotonic ion levels (*166*). These ribosomes are susceptible to dissociation by the action of EF-G:GTP in a manner reminiscent of termination with ribosome recycling factor (RRF) or can be collapsed into true 70S ribosomes by the addition of acyl tRNA. Also, locked ribosomes whose P site peptidyl tRNA has been deacylated by the action of puromycin also sediment at a decreased S value (*167*). The relationship between the more diffuse and slower sedimenting mRNA-bound ribosomes and a particular function may be alluded to in a class of ribosomes commonly isolated called loose couple ribosomes (LC) (*138*). LC ribosomes are defined as not being stable as associated subunits below 7 to 10 mM Mg^{++}, as opposed to the tight couple vacant ribosomes. LC ribosomes were shown in later research to be potentially trapped intermediates in the translocation process (*168*).

The conformation of loose couples that confers the instability is located on the 50S subunit. LC ribosomes contain different intersubunit contact sites (*169*). This is consistent with our modern cryo-EM derived understanding of a translocation associated intersubunit rotation (*68, 71*). The intermediate appears to involve the mobile L7/L12 stalk on the 50S subunit and, interestingly, can be rescued by incubation of the LC 70S in the presence of poly U and EF-G complexed with GTP:fusidic acid (fusidic acid prevents the release of P_i and as a result the full conformational change in EF-G necessary for its release). Research has now shown that the rotation is catalyzed by the action of EF-G on the 50S subunit and does not require the interaction of EF-G with the 30S subunit. These

results seem to imply that the addition of mRNA and a deacylated tRNA decrease the affinity between the subunits. Instead the collapsed stable 70S vacant ribosome seem to be less capable of undergoing the conformational changes that may be associated with translocation. And while one form of this mobile interaction may be less stable, the ground state is probably more stable.

It should be noted that the existence of stable vacant ribosomes is more physiologically unusual than the less stable partially occupied ribosome (ribosome on message with a deacylated P site tRNA) since this represents a relevant state of the ribosome prior to termination. A stable vacant ribosome is a useful functional state only during the stationary phase when ribosomes run off messages due to tRNA drop off. At this point the action of RMF (ribosome modulating factor) acts upon these vacant structures to create stable 100S ribosome dimers for storage purposes.

The formation of active translating ribosomes, in light of the aforementioned facts, can be seen as the creation of quasi-stable structures. This makes sense when one remembers that the act of translocation requires that the subunits rotate dramatically with respect to one another and facilitate the simultaneous movement of the $tRNA_2$:mRNA complex between sites. The locked form of the ribosome, occupied by messenger and peptidyl tRNA in the P site, is a well defined 70S form as determined by sedimentation assays, as are vacant ribosomes. This implies that the P site peptidyl tRNA on mRNA provides a stabilizing interaction between the subunits. This form is not translocatable and, as mentioned in previous chapters, will not even interact with factor EF-G:GTP presumably because it cannot shift the "locked" structure of the 50S to a form with high affinity for EF-G:GTP (*68*). A ribosome bound on message without tRNA may be

inherently conformationally unstable and prone to oscillation between the conformations associated with the translocation of tRNA. Binding of mRNA to the 30S may be accompanied by a lowering of the energy barrier required for both association and dissociation by lowering the energy barrier of the transition during translocation, implying that the two possess a common intermediate conformation.

This study centers on the contribution of mRNA to the interaction between the subunits and directly upon the structure of the 30S subunit to which it binds. The role that mRNA plays in the conversion of subunits into translationally competent ribosomes is unknown. However, in addition to the aforementioned studies there are recent results indicating that mRNA plays a role facilitating the accommodation of the 30S to a form required in 70S ribosomes. These data indicate that a significant structural alteration is required for the 30S subunit alone with an associated activation energy of 78 kJ/mol (*49*). The research also reveals that the presence of mRNA in the form of polyuridylic acid (poly U) accelerates the association of the subunits. Also, the resulting 70S appear to sediment as a more structurally disorganized molecule that can be collapsed to a sharp 70S peak by the addition of N-ac-phe-tRNA to the P site (*49*).

The process of association between the 50S and 30S:poly U complex was investigated in the previous chapter using Rapid Nonequilibrium Probing (RNP). It was also shown that the addition of poly U alters the equilibrium position of association at physiological Mg^{++} concentrations. In this chapter the association of subunits without mRNA is analyzed and compared to the results obtained from association with poly U. this research also follow the changes in the structure of the 30S as natural mRNA or poly U associates. The results indicate that when no message is present most of the protections

seen in the association with message still occur. However, the very fast rearrangements seen in H27 in the presence of poly U do not occur during the message free association. Instead they are induced by the 50S subunit after association is complete.

Results

Subunit association without mRNA

The previous chapter demonstrated that the association of subunits occurs at differing rates depending upon the region of the subunit being analyzed. This was determined via RNP with resulting protections associated with inter- or intra-subunit interactions. What is immediately apparent from the data presented in chapter 2 is the very rapid influence of the 50S upon helix 27 (Figure 3-1) of the small subunit. Helix 27 (H27) undergoes a rapid change in conformation with multiple bases experiencing alterations in their time-dependent reactivity to chemical modifier. The rearrangement involving H27 causes, or is followed by, the protections arising in the decoding center proximal to the 1400 region at the top of helix 44 (H44). Other regions appear to seat themselves at a slower rate signifying a final relaxation to the 70S form. Provided here is a study of association without mRNA for comparison with the previous results. While the 70S ribosome assembles, some regions respond at different rates. There are significant differences in the reactivity profiles for bases in the decoding center and associated H27. Without mRNA the subunits appear to follow a different path to formation of the ribosome. The differences indicate that both the path to and product of vacant 70S ribosomes are distinct. There is also an indication that the process requires a large degree of adaptation on the part of the 30S subunit.

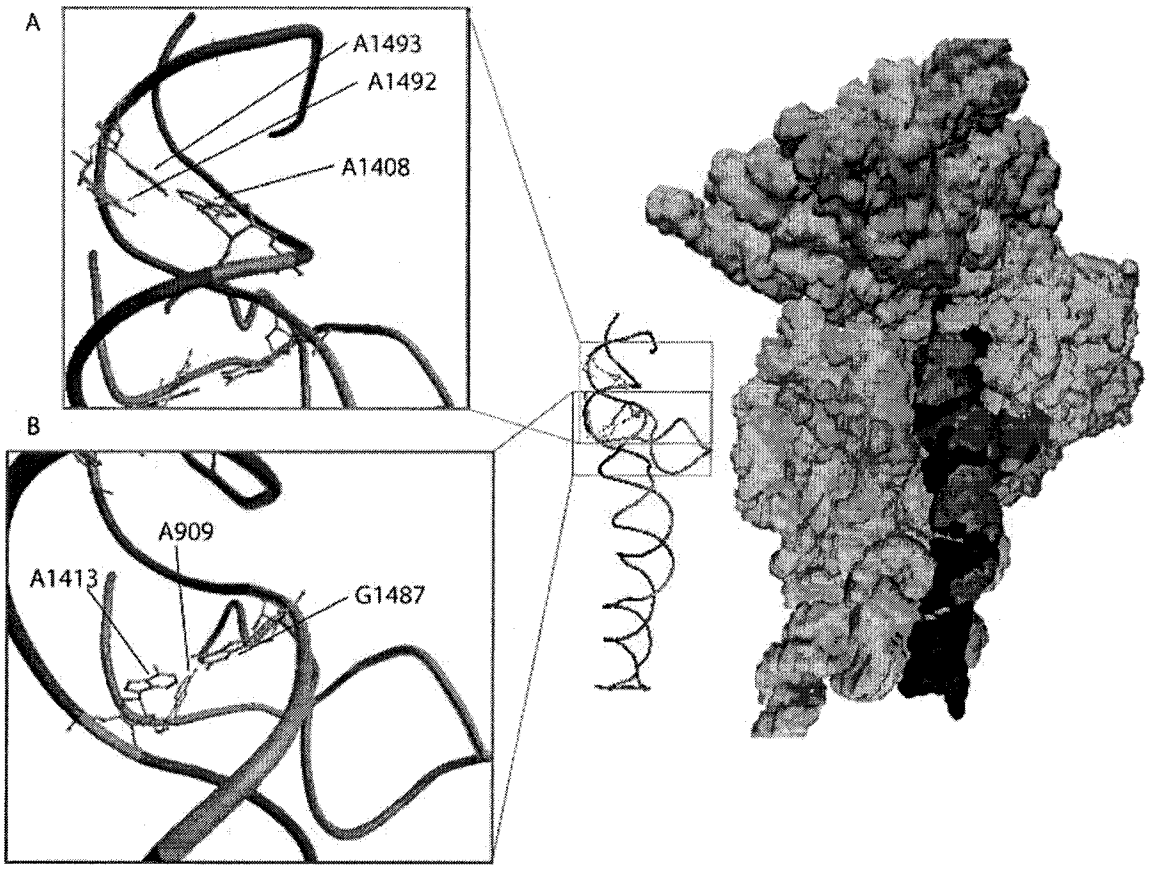

Figure 3-1. (A). The top of helix 44 containing the majority of the contacts that make up the A site. Bases A1492 and A1493 that change conformation in response to A site tRNA binding as well as A1493's cross-helix partner A1408 are shown in purple. Sites of bridging interactions between the subunits are shown in green. (B). The site of interaction between H27 (red) and H44 (blue). Bases A1413, G1487 in H44 and A909 in H27 that are involved in an important base triple interaction between the helices are colored purple. Bridge B3 is formed between the 50S and the 30S bases in H44 are shown as green bases next to G1487. Also shown is the position of the helices on a surface rendering of the 30S subunit. The coordinates are originally from PDB accession # 1J5E (*52*). Helix 27 can be seen to wrap around from behind H44 where its tip contains residues involved in bridge B2c. Positions at the top of H44 involved in the bridge B2a interaction with H69 on the 50S are indicated in the surface rendering in cyan.

Helix 27 and the decoding center

During association with poly U as a mRNA, A1413 in H44 was seen to become rapidly protected (chapter 2). This protection is likely due to a structural alteration in this portion of H44 linked to movement in H27 (*1*). A1413 forms a noncanonical base pair with G1487 across H44 (Figure 3-1). The G:A pair is also involved in a base triple interaction with A909 in H27 (Figure 3-1). The protection of A1413 is rapid but follows

that of A909 during association with poly U (Figure 2-6) . Without poly U the reactivity of A909 and A1413 become uncoupled from the progress of the subunits toward association. A1413 is not protected at short intervals, instead it becomes hyper-reactive simultaneously with an immediate tendency toward protection at A1408 and A1418, after which A1413 levels off at the same reactivity as 30S controls over the remaining period of probing (Figure 3-2). A909 experiences no change in reactivity suggesting the process of association does not immediately influence its environment. However, comparison of the reactivity of A909 and A1413 in preformed 70S controls without poly U shows their equilibrium reactivity is dramatically decreased relative to the short time intervals and equivalent to the association experiments with poly U. Interestingly, bridge B3 (Figure 3-1) makes contact with the bases immediately 5' to G1487. A1483 is involved in this bridge and is undoubtedly protected directly via this interaction. Although A1483 was not monitored in the association study with poly U, without message it follows a path to protection that perfectly parallels that of A1413, G1487's crosshelix partner, suggesting both a common mechanism of protection between these bases as well as a fundamental difference in the process of bridge formation between the two studies.

Figure 2

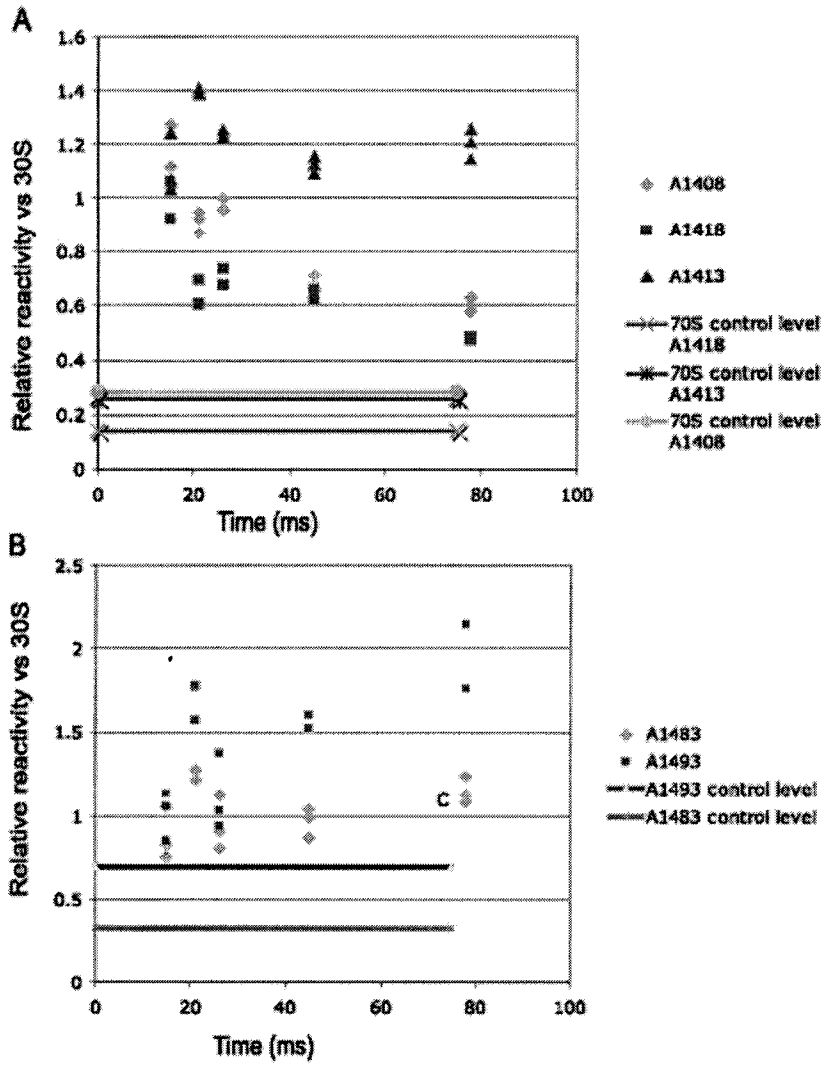

Figure 3-2. Reactivity as a function of the time of incubation between 30S and 50S subunits before probing with DMS in the decoding center at the top of H44. Reactivity was determined by primer extension analysis of stops at a given base using phosphorimager intensity. Each time point is plotted with the reactivity from multiple experiments. A. Reactivity at bases on the 5' portion of helix 44 showing some protections occurring immediately as was the case with poly U. Exceptions include a lack of protection at A1413 as well as the disruption of the protection profile at A1408 and A1418 after 20 ms. B. Protections in the 3' portion of H44. A1493, which is the noncanonical helical interaction with A1408 is becoming hyper-reactive in a mirror image of the protection at A1408. A1483 is a protection previously attributed to association (*128*) and is seen here following a path almost exactly the same as A1413. Level of reactivity of the bases after association as determined by the fast probing of preincubated complexes of 30S and 50S subunits.

The crosshelix interaction for base A1408, namely A1493, becomes hyper-reactive during the time points. The reactivity profile for this base approximates a mirror image of the profile for A1408 suggesting that the process of association increases the

accessibility of A1493 at the same time it is decreasing it for A1408. This would be expected if the bases were reacting to the presence of an A site tRNA binding. The reactivity increase is temporary, however, and in equilibrium controls it is partially protected. This suggests that the protection is due to a secondary rearrangement and/or a slow seating of the 50S at this position. The bridging interaction at this point in the helix is with the curious, mobile H69 of the 50S subunit (see Figure 3-12, Figure 3-1). This helix makes contact on either side of H44 and brackets A1492 and A1493. This helix also makes contact with tRNA in the A site and as discussed, so do the ever important A1492 and A1493 when they are flipped from their interhelical loop in response to a cognate tRNA. The state of these bases is likely to be directly related to the possible conformations of many bases examined in this study, especially those that were shown to be protected via a slower interconversion of structure after association.

Unlike association with poly U, where early effects of association were evident first in H27, protection of A1408 and A1418 tend toward protection more rapidly than those of H27 in the absence of message. Indeed, for the duration of the delay times in this study only A892 and A908 in H27 experience an influence from association on their reactivity; in the equilibrium controls only A909 becomes protected (Figure 3-3). The temporary reactivity changes in A892 and A908 are in opposite directions, suggesting that, just as in the experiments with poly U present, the environment of this region changes in a complex manner during association. Yet the process is much slower and fundamentally different without poly U. H44 appears to be the first and primary mediator of intersubunit interactions in this region in the absence of mRNA. Protections resulting

from interaction between H44 and H27 and within H27 manifest only after an extended incubation or not at all.

Figure 3

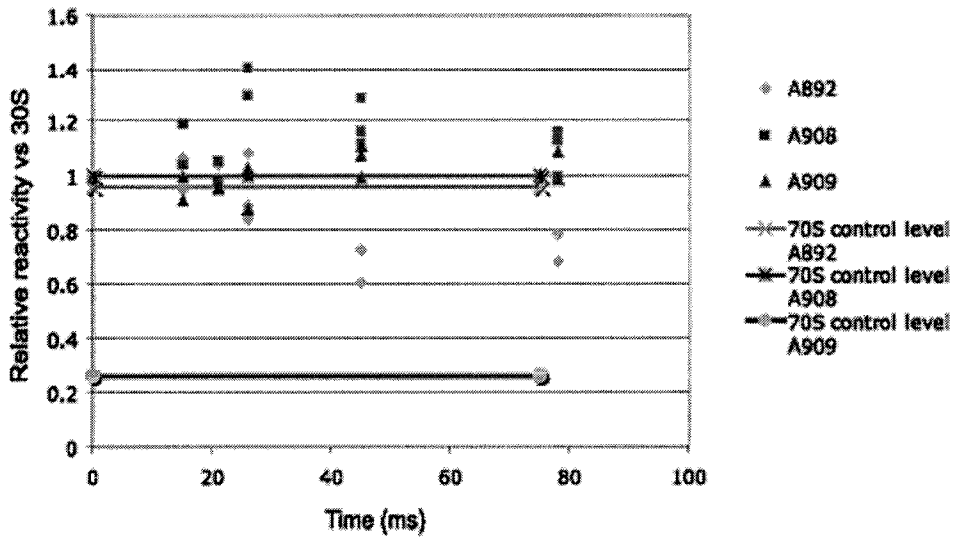

Figure 3-3. Protection time course for bases in H27 in response to the 50S associating and after association as indicated by the solid lines. Only A909 is permanently protected after association and none of the bases is significanlty altered during the process.

The path toward protection is significantly different for the bases in H44 between the two experimental sets. The reactivity trend for the bases in H44 does not follow an expected smooth progression. For A1413 there is an initial sharp spike in reactivity, while A1418 and A1408 are rapidly protected followed by a relief of protection and then a gradual decrease in reactivity (Figure 3-2). A possible explanation for this observation is that without poly U, association requires a transition in the structure within this region that would be normally facilitated by poly U. This may cause the bases in this region to become more reactive or lead to the partial dissociation of the subunits. This hypothesis is supported by the observation that poly U shifts the equilibrium point for association dramatically when association is carried out at 6mM Mg^{++} (see Figure 2-2). Furthermore, this would imply that under normal physiological conditions H27 interactions with H44

and between both H44/H27 and the 50S subunit are linked to the presence of a mRNA in the decoding center. Under physiological conditions initiation factors may produce a similar structure. The rearrangements not only promote early interactions between the subunits but also increase the stability of the 70S by forcing these interactions.

Reactivity changes in other regions in response to association without mRNA

The 790 loop of the 30S subunit has been shown to be important for association and for the binding of IF3 (*170, 171*). This region becomes protected by the binding of tRNA, 50S subunits, or neomycin class antibiotics. As such, it is a member of a group of bases known as class III sites of protection (*172*). Other members of this class that have been mentioned are the A1413:G1487, A909 base triple (Figure 3-1). The class III protections have been suggested to be a functional conformational state of the 30S subunit that results from a tightening of the decoding site (*1*). A very interesting trend in the protection of class III bases during association without message is that all of these bases display the same trend; they only become protected after extended incubation with 50S subunits and are basically unprotected during the fast phase of association. This includes A790, which is unchanged during the delay times but becomes protected in the equilibrium control modification experiments (Figure 3-4). This suggests that the major differences between association with and without mRNA is related directly to the structuring of the decoding site that must be catalyzed slowly by complementary structural interactions with the 50S subunit in the absence of message. And this in turn will likely be related to the final disposition of A1492 and A1493.

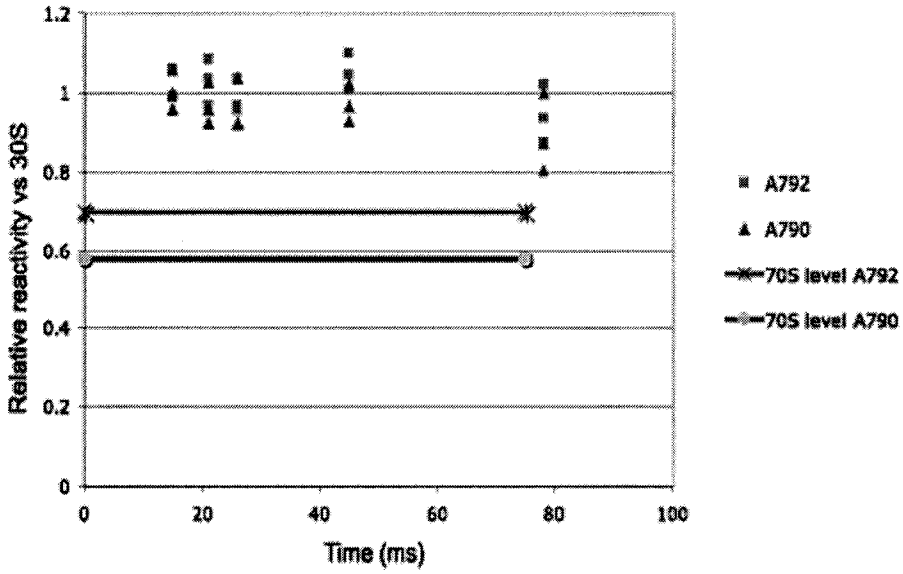

Figure 3-4 Protection of bases in the 790 loop in response to association. A790, another class III site of protection, and to a lesser extent A792 become protected after association is complete.

The 790 loop is proximal to the decoding site on the platform side and interacts directly with the P site tRNA. At the extreme reach of the platform is base A702, which is directly involved in a bridge between the subunits. A702 was found in the association study with poly U to be protected at a rate significantly slower than those closer to the decoding site, but a fast initial phase can be inferred from the reactivity of the earliest time point taken, ~ 75 % at 25 ms. In this study the rate is also slower than that of bases in H44 but this is due to a very different path to protection. The current study concentrates the resolution of delays to 10 through 80 ms. In this time domain the reactivity of A702 is seen to be composed of a very fast phase toward protection that is interrupted by an almost complete relief of the protection (Figure 3-5). This is similar to A1418 and A1408 in H44 except with a delay in its appearance, an increased overall magnitude of deprotection, and slower resumption toward an equilibrium level of protection. The relief of protection seen in these two regions may be connected, or the results of this study may be resolving in more detail events that show the same slow

process of association between the bridge partners in this region. In either case the process of association is significantly slower at this bridge compared with the contacts made in H44.

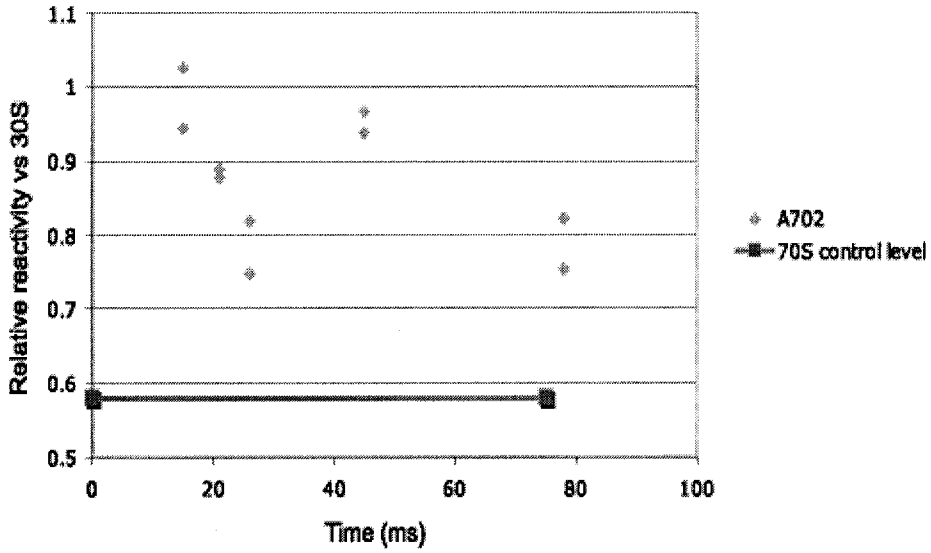

Figure 3-5 The protection of A702 appears to have two phases separated by almost complete deprotection around 50 ms.

In summary, the results of association without poly U show that association proceeds in a very different manner than with the mRNA prebound to the 30S subunit. Every class III site surveyed in this study showed the same pattern of reactivity. A790, A1413, A1483 and A909 are unchanged in reactivity and A1493 is becoming hyper-reactive. Yet at equilibrium after extended preincubation of subunits, control probing of 70S complexes showed these bases become protected. The lack of immediate signs of association in H27 is undoubtedly linked to the conformation that is represented by the class III protections. The base triplet interaction between A909 and A1413:G1487 is a likely participant in the conformational switch leading to the class III protections. This is supported by the lack of any significant short-term reactivity changes within H27 without mRNA. A lack of mRNA in the decoding site may disconnect the association of the

subunits from class III protections by not forcing interactions between the H27 and H44. The change in 30S conformation that would allow the immediate interaction is likely the removal of A1492 and A1493 from their internal loop that may allow both a tightening of the H44/H27 interaction and the intersubunit interactions at bridge B2a with H69 of the 50S subunit.

Poly U binding to the 30S subunit

The differences seen between the association of subunits with and without poly U as mRNA imply that its binding changes the structure of the decoding region of H44 and its interactions with H27. In fact, the binding of poly U to the 30S subunit rapidly alters the conformation of these regions with some bases becoming temporarily hyper-reactive or protected. At equilibrium with poly U, several bases in these regions establish positions that are significantly altered relative to the subunit alone.

In the decoding center at the top of H44 both A1408 and A1413 are immediately hyper-reactive and over the time course trend downward toward positions whose reactivity is greater than that of 30S subunits alone (Figure 3-6). The comparison of association with and without poly U showed changes to A1413 and A1408 to be severely delayed and significantly slower, respectively (Figure 3-2). The binding of poly U to the 30S subunit appears to reposition these bases in a conformation that is more solvent exposed than that of 30S alone.

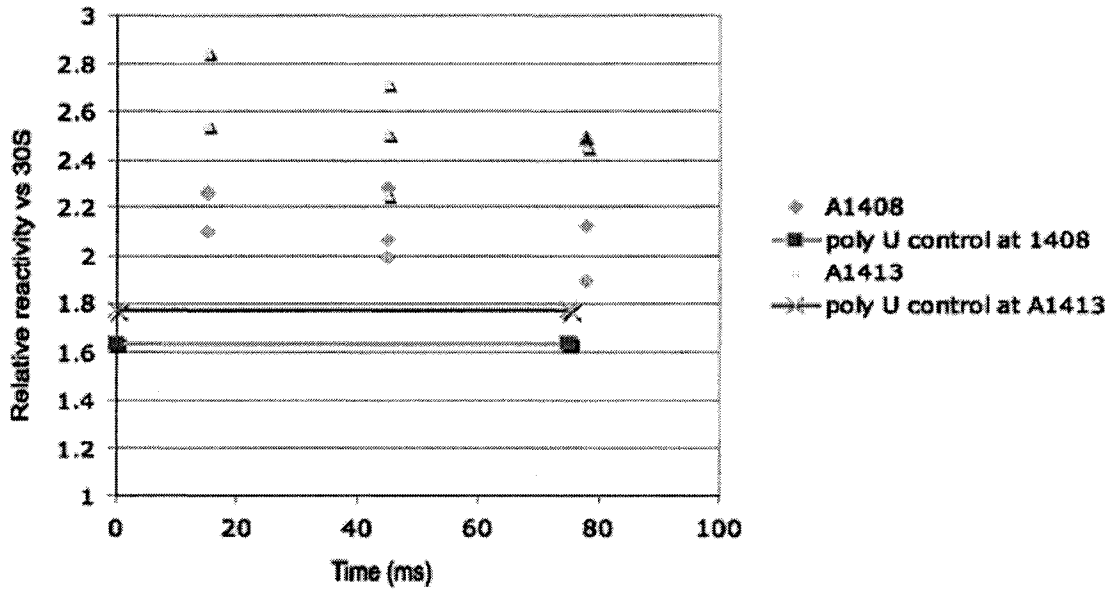

Figure 3-6 The addition of poly U to 30S subunits has a immediate and dramatic effect on the reactivity of bases in the A site and top of H44. Both A1413 and A1408 are hyper-reactive and proceed toward an equilibrium level of reactivity greater than that of the 30S alone.

The binding of poly U to the decoding center of H44 has both an immediate and long-term effect on the conformation of H27. While A1413 is immediately hyper-reactive, its interaction partner in H27, A909, and the other class III site, A790, are immediately protected from modification (Figure 3-7). As A1413 remains at a higher level of reactivity A909 continues as partially protected. A908 is rapidly protected by association of subunits containing poly U and is unchanged after association without poly U. Upon binding of poly U to the 30S A908 progresses toward a higher level of reactivity (Figure 3-7). In other words, the bases that slowly change reactivity in subunit association without poly U compared to with poly U, very rapidly change reactivity in response to the binding of poly U to the 30S subunit. Therefore, structural changes upon poly U binding seen in both H44 and H27 appear to establish a structure that is not only different from that of the free 30S subunit, but also one that is converted rapidly upon association to the form of a message-bound, translationally-competent 70S ribosome.

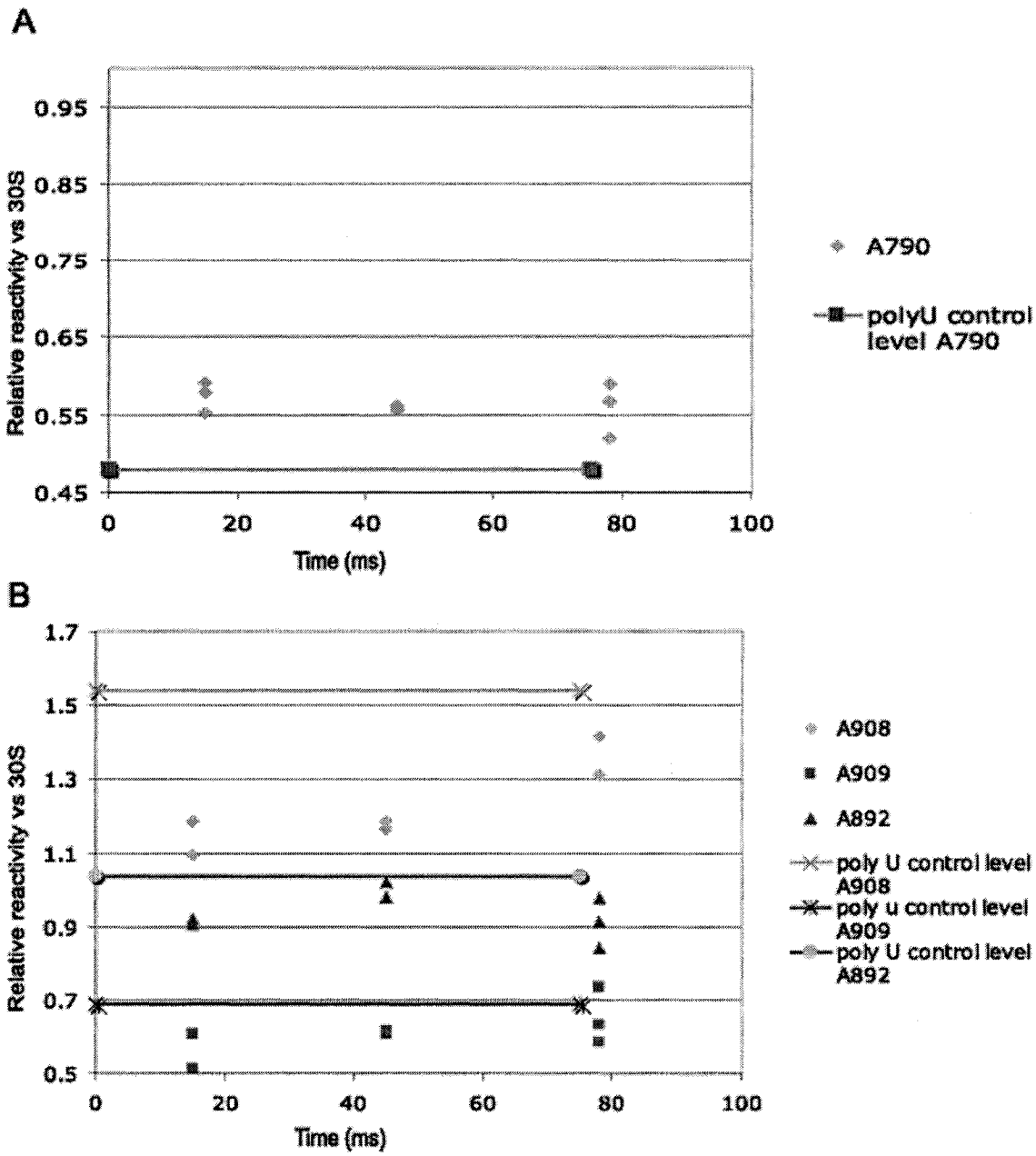

Figure 3-7. A909 in H27 and A790 in H24 are class III sites of protection that are immediately protected while the class III site in H44, A1413 becomes immediately hyper-reactive (see Figure 3-6). A892 becomes hyper-reactive in response to tRNA binding to the A site and temporarily hyper-reactive during association of subunits with mRNA, but is unchanged during and after the binding of poly U. A908 becomes protected during association with poly U but not without and, fittingly, becomes hyper-reactive upon the binding of poly U.

The A site discriminator bases A1492 and A1493 change reactivity in response to the binding of poly U. A1408, as mentioned, interacts across H44 with A1493. In the 30S structure model these bases are packed very tightly face to face in an internal loop and do

not appear to hydrogen bond. Upon binding of poly U, A1408 is forced immediately to a higher level of reactivity and diminishes smoothly toward 30S with poly U control reactivity. A1492 and A1493 on the other hand display 30S control levels of reactivity at the earliest time and proceed toward a higher level that matches the 30S with poly U control (Figure 3-8). This suggests that the rearrangements seen in H27 and H44 are driven by the strain placed on the interacting bases at and around A1408 and A1493. As will be discussed, the message-binding track is occupied by the phosphate backbone of A1492 and A1493 without mRNA. When mRNA binds, the bulged internal loop occupied by these bases must be rearranged. Full binding of message is accompanied by the displacement of A1492 and A1493 to levels of higher reactivity. This act may relieve some of the strain in the helix that caused the increased reactivity on the opposite side of the helix at A1413 and A1408.

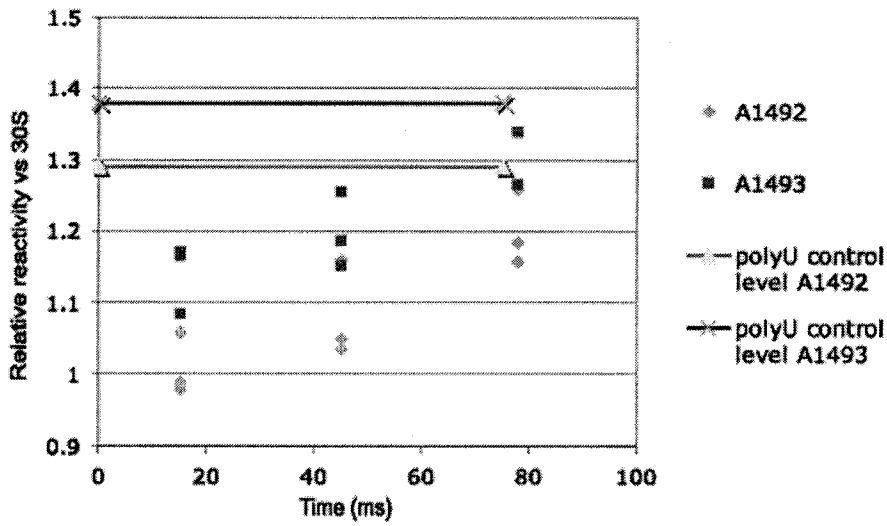

Figure 3-8. Both A1492 and A1493, which interact with the codon anticodon helix in the A site, become hyper-reactive as the A site is occupied by poly U. The increase in reactivity follows the very fast increase in reactivity of A1493's crosshelix interaction partner, A1408. This suggests poly U forces an increase in solvent exposure of A1408, A1413,and protection of A909 and A790 that may drive a rearrangement of A1492 and A1493.

The base A532 has been shown to crosslink to bound message (*10*) as well as being protected by tRNA in a poly U dependent manner (*158*). This research shows A532 is protected slightly by the binding of poly U. However in the presence of tRNA, Moazed and Noller showed an almost complete poly U dependent protection that is undoubtedly linked to the A site interaction of the third discriminator base G530 with the codon:anticodon helix (*158*). In the crystal structure of the 30S subunit, A532 can be seen to be pointing directly into the binding channel of mRNA close enough to interact directly with message. This makes the base an excellent indicator of the progress of binding for poly U as an mRNA to the 30S subunit. A532, in a manner exactly opposite to both A908 and A1492 -A1493, can be seen to become protected in a time dependent manner with control level protection achieved over the time period of the experiment (Figure 3-9). The progress of these bases is exactly what would be expected for a fast and orderly interaction of poly U with the 30S mRNA binding channel and shows no effects from the initial very fast changes seen in H27 and H44. This suggests that the initial very fast changes seen in these regions are due to interactions in the A and probably P sites that may induce changes leading to full binding of mRNA to the rest of the downstream channel.

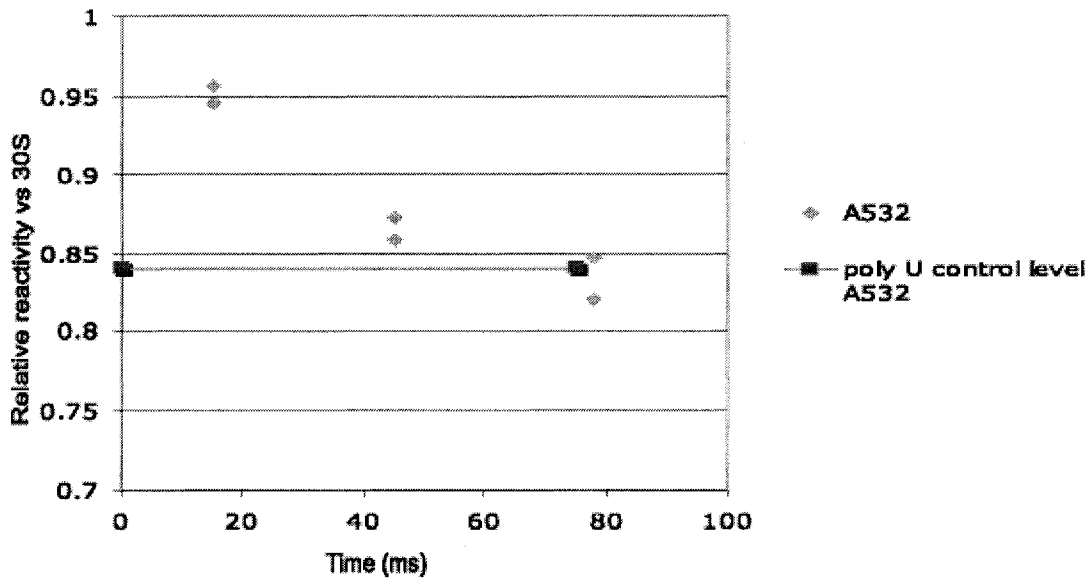

Figure 3-9. The placement of A532 in the mRNA binding channel and its history in crosslinking mRNA make its protection a very likely product of the full acceptance of mRNA onto the 30S subunit. As such, the initial interactions that cause hyperreactivity or protection of the A site and some class III sites respectively occur prior to the full binding of mRNA. However the rearrangement leading to the hyper-reactivity of A1492, A1493 and A908 seem to occur at the same rate as binding of mRNA.

Probing the 30S subunit as a natural mRNA binds

The experimental usefulness of poly U is its ability to bind to the ribosome and act as an mRNA in a simplified translation system with Phe-tRNA^{Phe} without the necessity to proceed through factor dependent initiation. This implies that it has an ability to insert itself fully into the 30S subunit or 70S ribosome. Poly U is not alone in this capacity, poly A with Lys-tRNA^{lys} is also competent for translation without initiation. Natural mRNAs containing a start codon and Shine-Dalgarno (SD) sequence are incapable of translation without initiation. Research has shown that the interaction of an SD with the anti-SD sequence can precede the initiation factors and initiator tRNA and may preclude the binding of the message fully to the 30S subunit. Instead, mRNA binds via its SD in a conformation known as the standby position (*10, 165, 173, 174*). This

work demonstrates time dependent changes in both the 30S subunit and message as the natural message 30S complex forms.

As with poly U, the protection of A532 is a good indicator of the progress toward full acceptance of message into the 30S subunit mRNA binding channel. With natural mRNA, A532 follows the same path toward protection, but unlike poly U the protection is not permanent and equilibrium binding controls with mRNA show reactivity is equivalent to 30S alone. This indicates that the binding of the mRNA is initially nonspecific but in the long-term binding in the standby position out-competes and precludes any observable interactions in this region.

The reactivity changes in H44 and H27 are unlike those of poly U binding to the 30S. For all of the bases surveyed, the progress during the delay times tend toward higher or lower reactivity. However like A532, they are mostly unrelated to the to final equilibrium state of the 30S with natural message. This suggests there may be an initial partial binding of the message to the 30S in the A and P sites. This binding seems to have an immediate (but short-lived) and small effect on the decoding center and H27. Both regions trend back toward 30S alone control levels of modification and after incubation find an equilibrium position that is different from that of poly U but still shows some familiar rearrangements in these two interacting regions. The permanent changes include a hyper-reactive A1408 and protection of A909. The sum of these results shows clearly that the structure is not easily related to that of the 30S subunit with poly U bound yet is different from that of the 30S alone (Figure 3-10). Furthermore there is an apparent removal of interactions in a message-bound form of the 30S suggesting a competition

between two different binding sites via a mechanism that is potentially allosteric rather than simply steric.

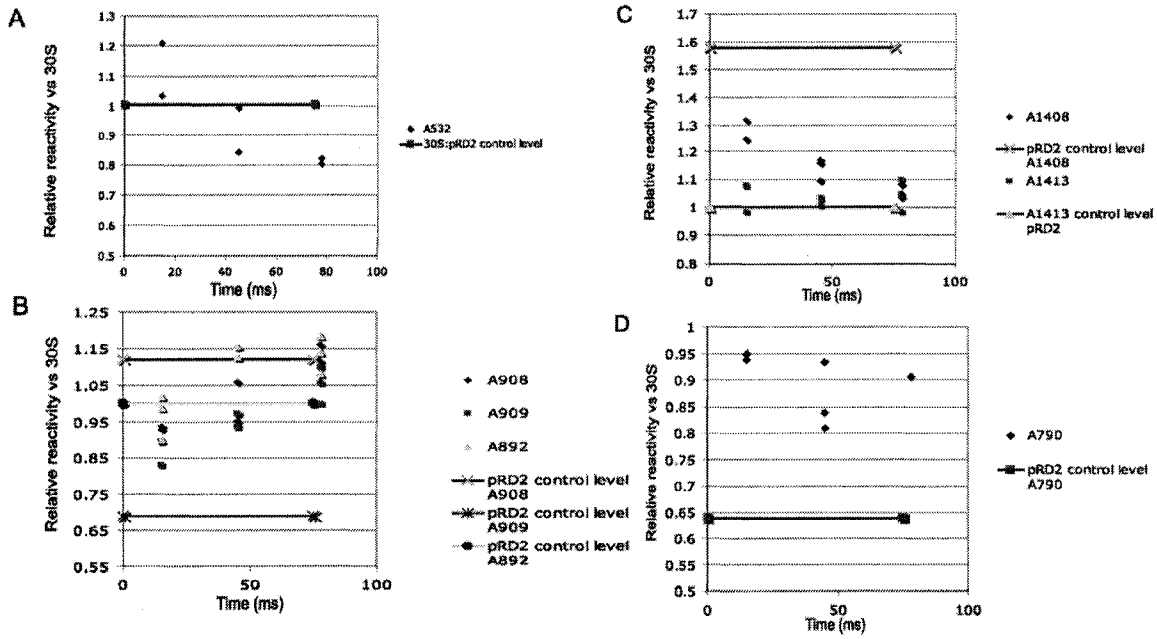

Figure 3-10. The results of probing the structure of the 30S subunit as mRNA (pRD2) binds. The trends in the time course are universally disconnected from the final equilibrium results, suggesting that there is more than one process in play as mRNA is accomodated (see text for discussion).

Probing the natural mRNA as it binds to 30S subunits

The probing of the natural message yielded a rather startling result. Messenger RNA that is bound to the 30S subunit without initiation factors, presumably to the standby position, becomes increasingly reactive at most of the bases susceptible to DMS as time of mixing prior to probing increases. The exception is in the SD region of the message, which remains at nearly the same level of reactivity. The implication of these results is that despite the fact that the message is not binding wholly to the mRNA binding track, it is still interacting with the subunit in a manner that partially unwinds the message and increases the exposure of the mRNA bases to modifier. This may be a required function of the 30S subunit prior to the insertion of message. Other groups have

shown that $tRNA_f^{Met}$ is capable of shifting message from standby to a P site decoding position (*3*). This implies that the message, while not fully seated in the mRNA binding track during standby, may be partially unwound with the start codon in a position near or in the P site and capable of interacting with the initiator tRNA. This may explain the differences seen in the structure of the 30S subunit upon natural mRNA binding. Full or partial occupation of the P site may influence the fine structure of the subunit. Efficient decoding in the P site may not occur when the A site is occupied by either message or the message and tRNA.

The shift of message from standby to P site decoding is catalyzed during the formation of a 30S initiation complex. A second more subtle shift may occur either after P site decoding or during the assembly of the 70S initiation complex that allow the occupation of the A site. This may also be catalyzed by the 50S subunit alone. While the addition of 30S subunits to natural messenger pRD2 elicits an overall increase in the reactivity of bases, the incubation of 30S and 50S subunits together yields a pattern of protection in the region that corresponds to the expected footprint by the 70S. There is especially good protection of bases that would occupy the A site and the next downstream codon (Figure 3-11). These protections are far greater than that of the A in the AUG start codon that is presumably in or near the P site while the SD interaction is present. This suggests a shift in the message to the downstream mRNA binding channel and supports the proposition that the message does not interact in the A site when the SD interaction is present.

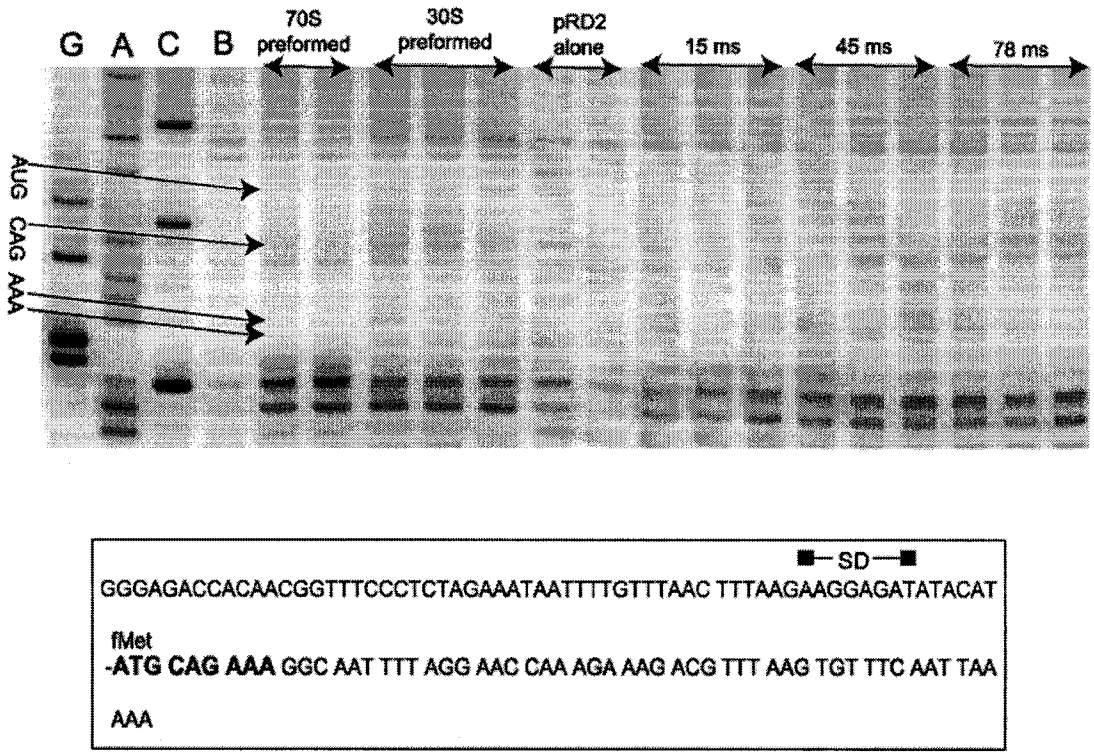

Figure 3-11. Image showing the primer extension results from a series of RNP experiments looking at natural messenger pRD2 as it binds to the 30S. The lanes include G, A, and C sequencing lanes and "B", an extension control lane of unmodified pRD2 mRNA followed by fast probing results from control shots with mRNA preincubated with 30S and 50S subunits then with only 30S subunits and no subunits. The last 9 lanes are three time points in triplicate. The delay times are noted above the lanes and include the modification delay plus the premodification delay. A single modification delay was used for all the experiments in this chapter, 8 ms. Note the lack of protection at the first codon and the protection of bases in the next two codons following the formation of the 70S. Below is the DNA sequence of the mRNA transcript; pRD2-PCR used in these experiments with the first three codons in bold. mRNA was 0.25 uM, and 30S was 1 uM, 50S was 2 uM.

Discussion

mRNA effects on subunit association

It is not immediately clear from the massive amount of structural data available whether the ribosome as a whole operates by organizing the movements of independently mobile regions or possesses the ability move through multiple states that represent a

continuum for a single motion. The former suggests that the ribosome has an almost unlimited number of conformer combinations while the latter would limit the possibilities to those allowed by the mechanism of the state to state path. Some regions of the ribosome appear to be extraordinarily and independently flexible, *e.g.* the L1 and L7/L12 stalks of the 50S subunit, yet while the L7/L12 stalk appears ill-defined under all conditions of analysis using cryo-EM the L1 stalk adopts specific positions dependent upon the ribosome's state. Aside from L7/L12, the conformations seen via direct techniques appear to involve rearrangements within an entire subunit or the 70S ribosome as a whole.

That the subunits or ribosome act as a whole with a limited number of potential states via a mechanism that is analogous to a molecular machine seems more likely for the sake of efficiency. This mechanical analogy is used widely in describing the function of the ribosome, however, for the relationship to prove accurate one or more central point(s) of reference need to be defined, against which other elements in the ribosome coordinate their positions. A likely candidate for a central position in conformational morphing of the 30S subunit is the decoding center and in particular its interaction with helix 27 of the small subunit. H27 and the decoding center at the top of H44 have arisen time and time again in the literature over the last three decades in relation to the importance of their proper structure for normal function. This region binds multiple antibiotics and harbors mutations that confer a broad range of phenotypes from antibiotic resistance to decoding accuracy and translocation. Also, H27 and H44 have been shown by chemical probing to change conformation in response to subunit association, as well as antibiotic, tRNA and factor binding. Recent cryo-EM analysis has shown that the axis

of rotation for the intersubunit movement during translocation can be drawn through the H27/H44 contact point (*68, 70*).

The conformational flexibility in H27 and its relation to function should not be a surprise considering its location in the 30S subunit. H27 lies at the junction between the three domains of the 16S rRNA making it an ideal center for the coordinated movement of the disparate parts of the subunit. The effector for one global rearrangement of the 30S subunit is the binding of tRNA to the A site. Crystallographic analysis of the 30S subunit with oligomeric uridine message and an anticodon stem loop analog have shown a conformational rearrangement of the entire 30S follows their interaction in the decoding center (*98*). Binding of a cognate tRNA analog to A site codon was demonstrated to radically alter the structure of the decoding site and allow closer contact between H44 and H27. The result of this change is characterized as a closure of the 30S subunit around the decoding center with distant elements of the subunit moving in a concerted manner. Binding of cognate tRNA promotes the flipping of A1492 and A1493 from an internal loop of H44 toward the codon:anticodon helix. These bases are induced to switch to this conformation by the correct geometry of the cognate codon:anticodon and allow the closer interaction of H44/H27 and ribosomal protein S12, driving the closing of the subunit around the decoding center and stabilizing and accelerating its acceptance into the A site.

When A1493 is within the internal loop it interacts directly across the helix with A1408. This interaction seems to result in increased reactivity of A1408 to DMS. Probing of the 30S subunit and 70S ribosome with tRNA bound to the A site shows that A1408 becomes slightly protected (*95, 158*). This protection is unlikely to be a direct result of

tRNA interactions. The crystal structure with A site tRNA analog shows tRNA interacts with the codon in the opened major groove on the A1492, A1493 side of the helix (*53, 98*). Therefore the protection of A1408 is most likely the result of the relief of strain on the helix by the flipping out of A1492 and A1493 allowing more room in the bulged pocket than in the A1408:A1493 helical interaction. This work shows that the strain may be increased by the binding of mRNA to the A site. When the 30S crystal structure with mRNA in the A site is aligned with the structure of the 30S without message, the mRNA overlaps the position of the phosphate backbone of A1492 and A1493 (Figure 3-12). This explains why the tRNA protection of A1408 was found to be poly U dependent and why the initial interaction of poly U with the 30S immediately increases the reactivity of A1408, after which reactivity decreases to the equilibrium level concomitant with increasing reactivity at A1492 and A1493.

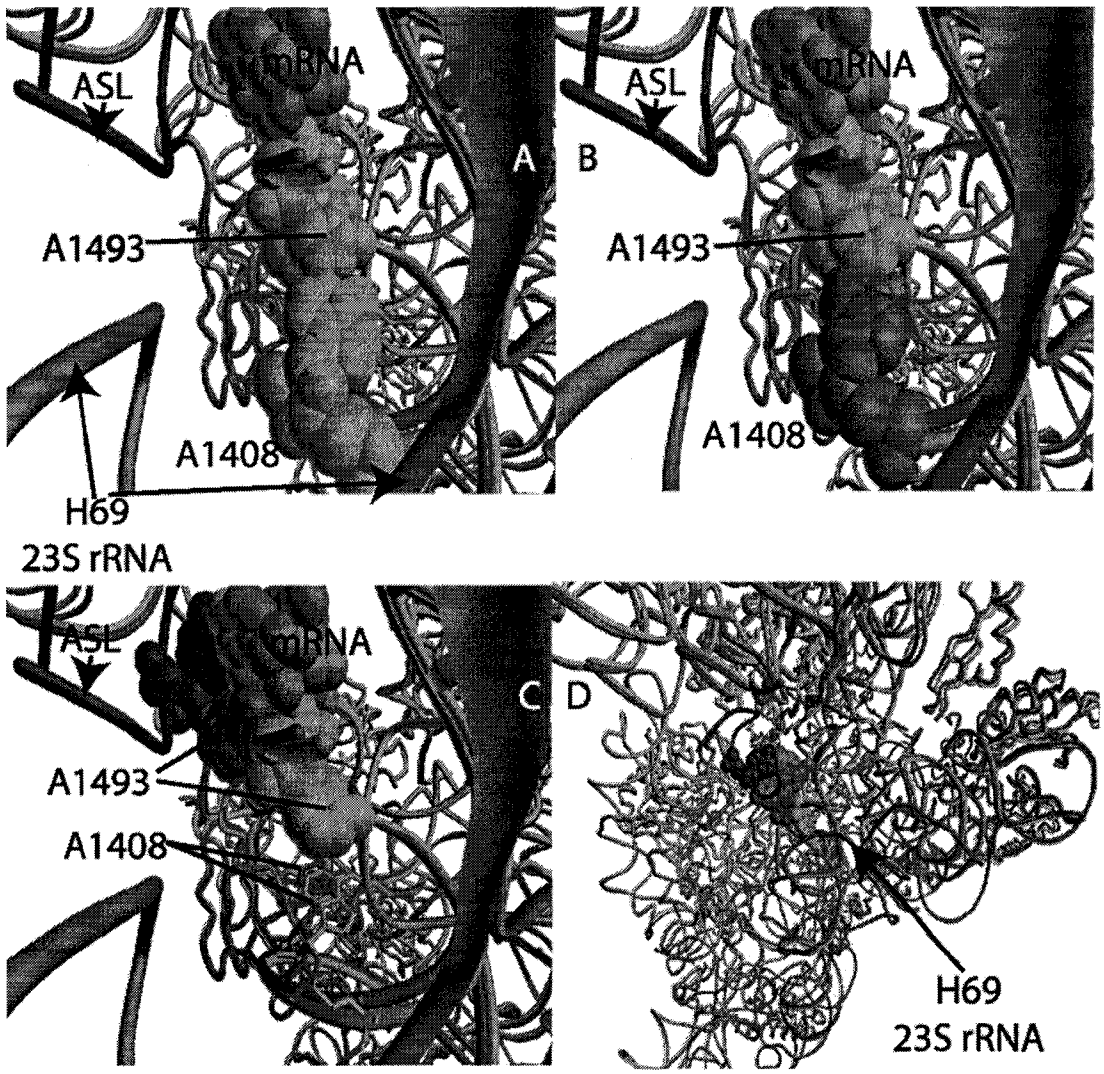

Figure 3-12. The effects of mRNA binding upon bases in the A site can be inferred by aligning structure models with A site mRNA and without. The structure of the 30S subunit alone (cyan, PDB accession # 1J5E) is aligned with a 30S structure model (red, PDB accession# 1IBM) containing an A site poly U mRNA (green) interacting with a tRNA anticodon stem loop analog (ASL, in blue). The position of 50S subunit H69 (PDB accession# 1GIY) as it interacts with the decoding center is shown in light blue. The structures were aligned using a pairwise helix alignment algorithm in the Ribosome Builder program (*175*). (A) A1493:A1408 interaction from 30S without mRNA are shown in spacefill as they interact with mRNA. The mRNA clashes with the backbone positions of A1493 and A1492 when the bases occupy the internal loop with crosshelix interaction (cyan). (B) When the position of A1408 (red) from the 30S with mRNA is shown interacting with A1493 from the 30S without mRNA (cyan) it is apparent the interaction has significant van der Waals radii overlap between A1408 and A1493. This suggests that even if A1493 in the structure with mRNA and ASL were not flipped out it would still not find enough space in the loop with A1408. (C) Showing movement of the base A1492 between structures with and without mRNA and ASL (red and cyan respectively). While mRNA and tRNA are known to cause A1492 and A1493 to flip and interact with the codon:anticodon helix it is equally likely that the interaction of mRNA with the backbone of these two bases changes the stability of the crosshelix interaction. (D) Showing the position of the decoding center on the 30S note the interaction between 50S H69 and the A site as well as the path of the mRNA as it passes through the major groove of H44. This interaction may be responsible for the slow rearrangement of the decoding site in the absence of mRNA after association.

The conversion of A1492 and A1493 from cross-helical interactions to the flipped out conformation is closely linked to the geometry of the codon:anticodon interaction. This interaction is an induced fit of tRNA, with the fit signaled by the stabilizing interaction of A1492, A1493 and G530 leading to a conversion in the structure of the entire 30S subunit. Disturbing the thermodynamic balance of this interaction, as antibiotics like paromomycin do, allow these bases to flip out and stabilize even noncognate tRNAs. One effect of mRNA binding to the A site may be to establish the proper interaction of mRNA with the backbone positions of A1492 and A1493.

This proposal may also explain why the rate of protection for A1408 was significantly slower in the association-dependent protection without poly U as compared to with poly U. The formation of intersubunit bridges with H27 and H44 may further stabilize the decoding site by relieving strain within the internal loop containing A1408. The likely bridges responsible for this effect are B2a and B3. This study found that bridge B3 interactions next to the G1487:A1413 interaction are likely responsible for the fast orderly protection of A1413 when poly U is present. This is evident by the protection of A1483 and A1413 that, while on the opposite sides of H44, have the exact same reactivity profile and become protected only after association. A1483 interacts directly with the 50S subunit in bridge B3. The rearrangement necessary without message proposed here is initiated by interactions with the 50S subunit and may be facilitated through interactions in bridge B2a. H69 of the 50S subunit forms B2a by interacting with bases on either side of H44 including 1408-1410 and 1494-1495 (Figure 3-1, Figure 3-12). This interaction has been shown to be important for the stability of the 70S ribosome. In fact, a single modification of a base in H69 has been shown to disrupt

association (*38*). This may be due to a defect in the ability of this interaction to facilitate the rearrangement these studies have shown to be modulated by the presence of an A site bound mRNA. This would prevent not only the formation of this bridge but also interactions at bridge B3 and bridge B2c with H27. Without this array of interactions the 70S ribosome would surely lack stability.

Proposed in the previous chapter is that the pattern of base reactivity seen during association may reflect an intermediate in association that is both catalyzed by IF1 and aids in the formation of the A site for translation. This research demonstrates that this process is expedited by the presence of message. These data also raise the possibility that the association process without message bypasses the necessity to rearrange the A site and this intermediate conformation. Instead the formation of vacant ribosomes may follow a more direct path that is prohibited normally by interactions triggered by the presence of mRNA in the 30S A and possibly P sites.

The role of IF1 is murky, yet crystallographic analysis of 30S subunits bound with IF1 reveals that the factor distorts the A site dramatically including the flipping out of A1492 and A1493 into custom-made pockets on the factor (*31*) (Figure 3-13). This very specific activity allows the top of H44 to open and perhaps facilitates mRNA placement in the A site after association or at completion of decoding in the P site. Other effects of IF1 on 30S structure include the deformation of H44 over a ~70 Å distance and subtle repositioning of various distant regions.

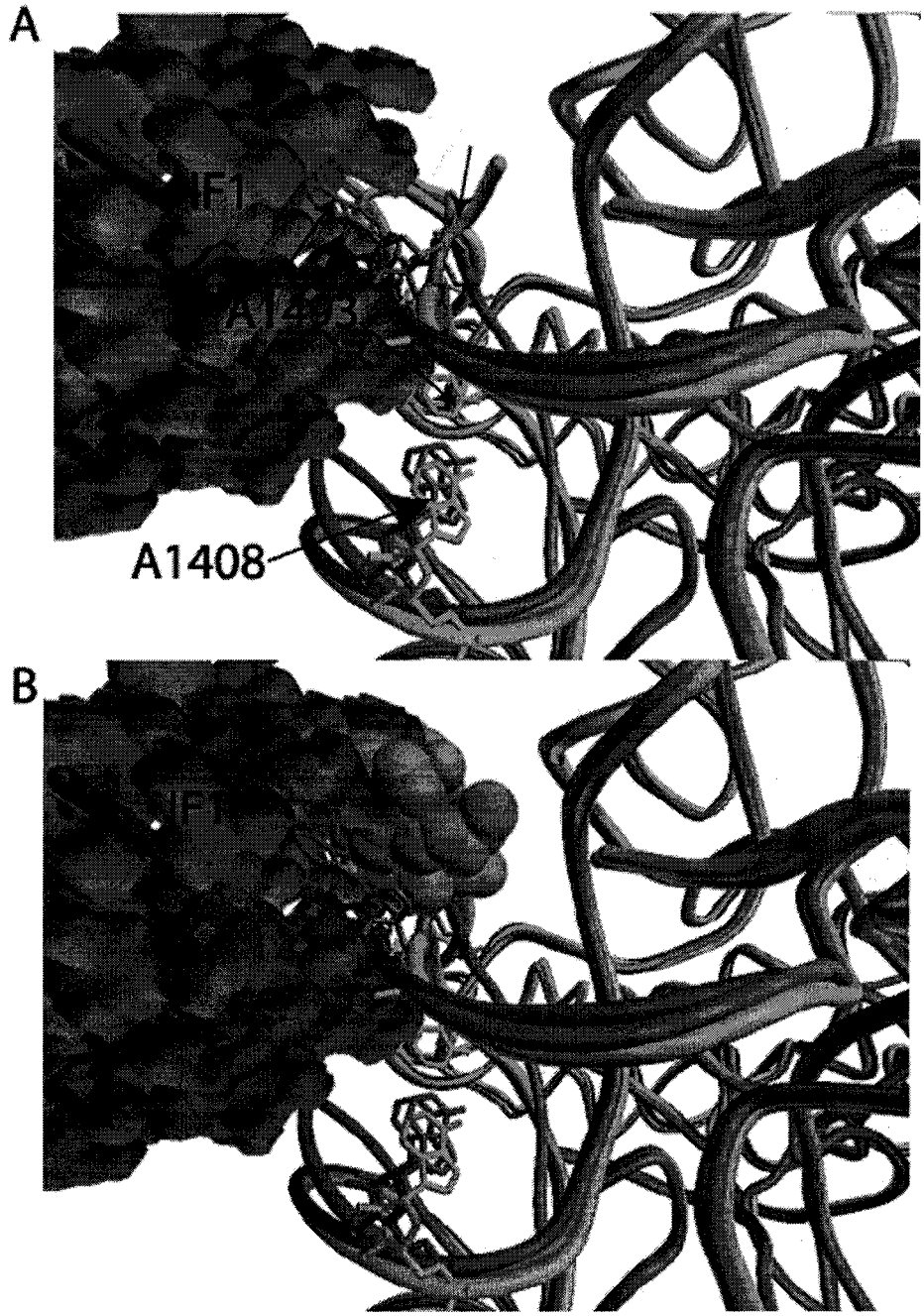

Figure 3-13. Three crystallographic models were aligned to show the effect IF1 has on the structure of the decoding center. The structures were the 30S alone (PDB accession # 1J5E) (*52*) in cyan, the 30S with A site mRNA and ASL (PDB accession # 1IBM) (*53*) in blue and a 30S with IF1 bound (PDB accession # 1HRO) (*31*) in red. (A) IF1 flips A1492 and A1493 into pockets on its surface and radically distorts the A site. The action of IF1 narrows the major groove of H44 pushing the backbone position at A1492 and A1493 into the path of mRNA in the A site. (B) IF1 not only narrows the A site, but also occupies the space that an mRNA would, making the binding of mRNA in the A site in its presence highly unlikely.

As mentioned previously, IF1 accelerates association and dissociation of the 70S without changing the equilibrium point, presumably by lowering the activation energy of transition state. Lending credence to the translocation intermediate for association, many of the 30S structural changes seen with IF1 in the crystal structure are also associated with the translocation intermediate (*31, 71, 176*). This includes cryo-EM/modeling results that show the decoding site is relocated toward the P site by up to 12 Å during the switch between the translocation intermediate with intersubunit rotation, and the post-translocation state prior to the dissociation of EF-G:GDP. This conformation distorts the A site significantly as well as displacing H44 over a distance, very similar to IF1's effect (Figure 3-14). Furthermore, the pretranslocation state of the 30S subunit is a state with the bases A1492 and A1493 flipped out from their helix in response to a A site codon:anticodon interaction. Our results show that the path to association is very different with and without mRNA present in the A site. Placement of mRNA obviously rearranges the A site including increasing the exposure of bases in the internal loop but also effecting the exposure of several bases distant from but associated with the functional rearrangement of the A site.

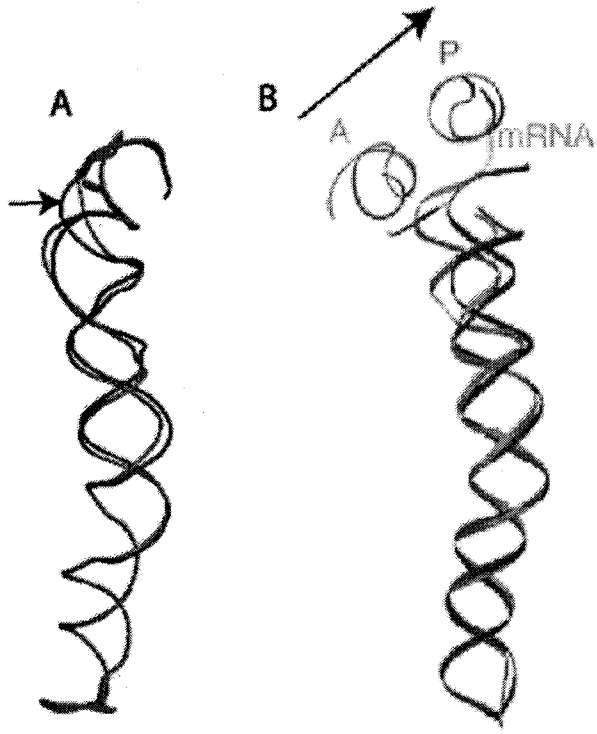

Figure 3-14. Comaprison of the structure of the decoding region of H44 from cryo-EM/modeling data from VanLoock *et al.* showing the movement in response to translocation (*176*) and crytallographic data with and without IF1 bound. (A) H44 was aligned from the 30S with A site mRNA and ASL (blue) and the 30S with IF1 (red). The decoding site at the top of H44 is distorted and shifted toward the P site when IF1 is present. (B) Movement of the top of H44 from the pre (blue) and post translocation state before EF-G release (red). Evident is a similar localized displacement of the decoding center toward the P site. The original image of (B) is from VanLoock *et al.* (*176*).

One of the major differences in H44 in the presence and absence of mRNA was the reactivity of A1413. This base became temporarily hyper-reactive and then protected only after association was complete in what can only be described as a secondary rearrangement. A1413 and its interaction partner A909 in H27 and A790 are sites of class III protections, meaning they are protected by tRNA, some antibiotics and the 50S subunit (*172*). All of these bases followed the same path without mRNA present during association, *i.e.* there was no protection during the actual association. Only after extended incubation was protection seen via what must be a structural conversion that is catalyzed slowly by the 50S subunit interactions without mRNA. These experiments have also

shown that rearrangements associated with poly U binding to the 30S lead directly to partial Class III protections at A790 and A909 through interactions in the A site that cause major changes in the decoding site including an increase in reactivity of A1408, A1413, A1492 and A1493. These may result from interactions between H27 and H44 around the A1413:G1487:A909 base triplet. All three of these bases are class III sites and both the hyper-reactivity of A1413 and the protection of A909 and A790 are very rapid upon introduction of poly U, which are driven by the change in position of the region of H44 containing A1413. This pattern of protection is obviously not the same as that seen with the binding of tRNA, antibiotic or 50S subunit. However, the rearrangements seem to be setting up the 30S subunit for the fast conversion of its structure toward a structure in the 70S that does contains full class III protections.

Both tRNA binding and neomycin type aminoglycoside antibiotics are known to have the effect of either flipping out A1492 and A1493 (A site tRNA) or lowering the threshold for the flipping out (antibiotic), and understandably both of these allow class III type protections. But the 50S subunit accomplishes the same Class III protections. These results have shown that it does so quickly with message and hesitantly without. These data also support a proposition that this may be via bridging interactions in H27 and H44 that reform the A site after subunit association without mRNA. However, differences in the fine structure of the vacant 70S in H27 (protection of A908 is not apparent without mRNA) show the structure is not exactly the same as that of a 70S with mRNA. The binding of poly U has the effect of converting A908 to a higher level of reactivity and perhaps this confers a structure that can then be protected by the 50S. Experiments with pre-formed 30S structures with message prior to association the show that interactions

between the 50S and H27 precede those in the A site of H44. Another proposition in the previous chapter is that this indicates H27 may move independently of H44. Now the results show this is related directly to the presence of mRNA. Message appears therefore to force the subunit to interact through bridge B2c at the tip of H27. Without message the interaction is very similar in the long term but is not equivalent.

The function of H27 interactions with the 50S subunit may be to position the local structure of the 30S subunit so that movement of the decoding site with respect to this point will confer a structural change on the entire subunit and/or allow it to move with respect to the rest of the subunit. These movements occur in the case of A site acceptance of tRNA and to a greater extent with both translocation and IF1 interactions. Interestingly, the main bridging interaction with the H44 portion of decoding site is the mobile helix 69 of the 23S rRNA. H69 is flexible and only becomes organized in the 70S ribosome while making contacts with H44 and the A and P site tRNAs (*1, 159*). In contrast, H27 interactions with the 50S are to structures with little or no prospect for independent motion. With mRNA the interactions between H27 or the H27/H44 decoding site unit may force interactions between the subunit that allow it to act as a pivot point for the intersubunit motions associated with both tRNA acceptance and translocation by separating the subunits by a small but important distance. Without mRNA the structure may be collapsed and not be required for either association or available as a center of rotation. This would explain our results as well as all the previously mentioned examples of differences in gross ribosomal structure in the presence and absence of mRNA.

Natural message interactions with the 30S subunit

The proposition that the message interacts with the 30S subunit in two different positions is widely accepted. One interaction is mediated primarily via the SD:ASD helix and the other with the message shifted to the mRNA binding track. The shift of mRNA has been demonstrated to be the result of the interactions with initiator tRNA and initiation factors, to a lesser and greater extent respectively (*3, 173, 174*). The nature of the two mRNA binding sites and the contribution of each initiation factor to the process of switching the mRNA position remain unclear. For instance, studies of competition between an octameric DNA oligomer complementary to the 16S rRNA ASD sequence and mRNA with and without SD sequences showed competition between mRNA with and without SD sequences for binding of the 30S subunit. This competition was not present when initiation factors were included. This suggests that with IFs, both the SD oligomer and the mRNA find a happy home on the 30S subunit. The addition of initiator tRNA changes the outcome to the exclusion of the SD oligomer in favor of mRNA. This in turn suggests that there are two processes at work. First, the binding of the SD sequence precludes interactions in the binding site of the 30S that include the P and/or A sites. Second, the inclusion of initiation factors allow the partial stabilization of mRNA while maintaining the SD interaction. However the addition of initiator tRNA brings about a reversal of the specificity of the 30S subunit to the exclusion of the SD oligomer in favor of a natural messenger.

Recent crystallographic models of the 70S ribosome demonstrate a SD oligomer would not occupy any portion of the A or P sites (*36, 177*). This reinforces a proposition that the mRNA binding to the 30S subunit alone could bind to either the downstream

binding track or the SD sequence. The fact that this does not occur except in the presence of IFs is indicative of their function in overcoming an allostery between these sites by opening the binding track in preparation for the decoding of initiator tRNA in the P site. Furthermore, binding of an ASD complementary sequence to the ribosome likely changes the structure of the 30S subunit to a structure amenable to P site decoding at the expense of A site interactions. This would explain other results showing that with leaderless messages the P site AUG start codon is discriminated against by the action of initiation factors, particularly IF3 (*7, 8*). The implication is that the mRNA without the SD interaction is bound to the full message binding track and the structure of the initiating ribosome discriminates against these as it would with initiation from an internal methionine codon. This further suggests that one function of the SD:ASD interaction is to preclude interactions in the A site that may interfere with P site decoding. This is supported by crosslinking data following the acceptance of mRNA into the 30S in response to IFs and fMet-tRNA$_f^{Met}$ (*3*). These experiments demonstrate that while the inclusion of IFs effect the positioning of mRNA full, acceptance of the mRNA into the mRNA binding channel of the 30S, as determined by crosslinks to A532, do not form until after the start has been decoded by fMet-tRNA$_f^{Met}$.

The research cited indicate dual binding sites on the ribosome that may be allosteric between SD interactions and A site binding. These results support this proposal and also show for the first time that message binding to the ribosome confers a distinct reactivity profile when the message contains a SD sequence. The binding of natural message does not elicit the same short term or permanent structural alterations on the 30S subunit as poly U. While some of the trends in protection are similar in the time course to

those of poly U, none of the trajectories coincide with permanent equilibrium levels of reactivity. And while some partial class III protections (A790 and A909) are similar to those found with poly U, they do not seem to result from changes in the decoding A site. A possible explanation is that while there is binding initially to the full mRNA binding track it is only a partial binding that is competing with structures formed by interactions at the ASD:SD that exclude the A site and may include interaction in or near the P site.

The complete lack of coincidence between the time course of probing and the final equilibrium levels of protection make interpretation of the results challenging. This is probably due to the initial competition in binding site selection that could be resolved by a more complete time course. This is supported by initial protection followed by deprotection in equilibrium binding controls at A532, which is a good indication of binding to the downstream binding channel. The equilibrium protection pattern of other regions are assumed to represent an interaction of the mRNA to a site that, at the very least, includes the ASD sequence demonstrating that the structure forms only when a natural mRNA containing the SD sequence binds to the 30S subunit.

Experiments performed to look at the reactivity of bases in the mRNA afforded by increasing time of incubation with the 30S show that binding to the 30S increases the reactivity of all bases in the portion of the mRNA that should be footprinted by the 30S, with the exception of the SD portion and the extreme 5' UTR. While the helicase activity of the subunit necessary to present bases in the A and P sites can be expected to have this effect, the totality was surprising. Furthermore the equilibrium controls with both subunits show that protection is afforded to mRNA bases in the 70S ribosome, especially the A site and the third coding triplet. These protections are necessarily a product of the

message binding track that is exclusively on the 30S subunit. This includes a very specific protection of a C that is the 5' base of the A site codon while the A of the P site AUG is maintained at the same level of reactivity (Figure 3-11). Therefore, the binding site is seemingly shifted subtly and specifically to include the A site and downstream codons. The ability of the 50S to facilitate the shift of message from standby is known (*178, 179*). What is novel here is that the P site may be occupied by the mRNA preferentially and exclusively when the SD sequence is present.

The results from both the 30S structure binding to mRNA and the structure of mRNA as it interacts with the 30S subunit and 70S ribosome are consistent with the hypothesis that natural mRNAs interact through the SD in a manner different from that of an A site decodable message. This study demonstrates that natural message does not effect the A site in the same manner as poly U and that the fine structure of the 30S is different with natural mRNA. This prompts a proposal that this structure precludes interactions in the A site and may instead be the structure required for the P site to engage in the activity of decoding a start codon. In fact, the kink in message that is required for the simultaneous binding of mRNA to both the A and P sites may interfere with the use of this site in decoding. This view is reinforced by experiments performed looking at the affinity of tRNA toward the A and P sites (*180*). These experiments indicate that there is an inverse relationship between affinity of A and P sites. Higher affinity in one site is correlated to a decreases the affinity of the other. In fact the use of antibiotic now known to induce conformations in the A site destabilizing A1492 and A1493 lower the affinity of the P site.

We suggest that the mRNA occupancy of the A site is potentially inhibitory for decoding in the P site and is therefore discriminated against prior to P site decoding. Further experiments will be needed to delineate at what point the A site does accept mRNA. As mentioned, IF1 occupies the A site and will undoubtedly preclude tRNA binding. Whether mRNA can occupy the A site in the presence of IF1 is unknown. The position of IF1 in the crystal structure of the 30S subunit would seem to preclude this possibility (Figure 3-13). The independently proposed function of IF1 in association that we have extended to mRNA may add further functional implications to IF1's placement and effect on ribosome structure. If the A site were occupied by mRNA and association does proceed through a translocation intermediate, the lack of mRNA binding to the A site may allow the formation of a 70S initiation complex without the danger of partial mRNA translocation that would destroy the reading frame. In this light, the function of IF1 can be seen as not only deforming the A site to lower the activation energy of the association process, but also aid in the establishment of an empty A site that can be occupied by message only after association is complete. This might help to explain why IF1 has been shown to be synergistic in promoting the activities of all the initiation factors. It may also explain why P site bound fMet-tRNA in the absence of initiation factors is not puromycin reactive (*3*). Together these results suggest the association of the 30S with 50S subunits without the stabilizing interactions of factors results in the improper placement of the tRNA on the 50S subunit. The proposal that association proceeds through a translocation intermediate is also supported by structural homology between IF1 and IF2 to domains of EF-G suggesting an evolutionary and functional connection (*181, 182*).

Materials and methods

Preparation of mRNAs

The natural mRNA pRD2-PCR was prepared by PCR amplification of the N terminal region of the nucleocapsid (NC) protein from HIV. The region amplified contained the T7 RNA polymerase promoter and 5'UTR from the pET-3a plasmid as well as a portion of the coding region of NC. The primers were designed to introduce a UAA stop codon at amino acid 18. The mRNA was transcribed from a PCR product obtained using these primers via an Epicentre T7 transcription kit. 30 pmoles of the PCR amplified template were used per reaction. Following transcription the reactions were treated with RNAse free DNase I and preciptitated by addition of 1 volume of 5 M ammonium acetate and centrifugation. Concentration was determined using 1 A_{260} unit equals 1.23 μM. Reactions typically yielded 100 pmoles of product per pmole of template. Binding of the natural messenger pRD2-PCR to 30S subunits was analyzed using nitrocellulose filtration of α^{32}P-UTP labeled trancripts on 30S subunits. Time and concentration titration were used to establish parameters for the RNP probing of the complexes. The potassium salt of poly uridylic acid was obtained from Sigma Aldrich. Poly U was diluted in ultrapure H_2O at 5 mg/ml and stored at –86° C until use.

Modification to the RNP protocol

Fast probing experiments of 30S:mRNA and 30S:50S association were done similar to those outlined in the previous chapter with some modifications. All of the

following probing experiments were performed using a single "continuous flow" fast mixing protocol on the Bio-Logic SFM-400. The design allows for variation of the delay times prior to exposure to DMS while maintaining the same modification delay times. The main advantage of this protocol is an increased consistency of results. This is due to the larger volume of material used per probing experiment and the use of a single flow rate and DMS modification time for all. Delay lines of various lengths were used to vary the delay time of the mixed components while the second delay line for modification remained the same. The disadvantage is that the experiment's mixing times for the constituents of the probed complexes are limited to the delay lines available. In these experiments 500 μl of each of the two constituents are mixed and proceed through the first delay line to the second mixer where the flow combines with 85 μl of 1:1 DMS:EtOH and following the second delay line with 2000 μl of quench (10 M β-mercaptoethanol, 0.5 M NH_4oAc and 25% isopropyl alcohol). 80 % of the total flow is allowed to exit to waste from the fast mixing apparatus and the final 20% is diverted to collection. The early volume allows the delay lines to be purged of any unwanted volume and the hydrostatic pressure to equalize. All subunits were activated by preincubation in NB10 buffer at 42° C for 15 minutes prior to loading into the quench flow apparatus thermostatted at 20° C.

30S:mRNA probing

The binding of natural messenger and poly uridylic acid to 30S subunits was analyzed using RNP. The first experiments were designed to analyze the mRNA as it bound to the 30S subunit. pRD2-PCR mRNA was made 0.5 μM in 1X NB10 buffer and pushed against 2 μM 30S subunits for a mixed concentration of 0.25 μM and 1 μM

respectively. The following experiments were made super stoichometric in mRNA and poly U for the analysis of the effects of message on the structure of the 30S subunit. In the poly U reactions 0.5 μM 30S subunits were pushed against 4 μM poly U. Since poly U is of an undefined length, molartiy is calculated from the mass assuming all poly U was 60 nucleotides in length (the approximate footprint of the 30S on message). For experiments of 30S versus pRD2-PCR mRNA the 30S starting concentration is 0.5 μM and the messenger is set at 2 μM. Control shots were made with the preformed complexes and with the target alone without either 30S subunits or mRNA. The concentration for the control shots was made the same as that of the mixed components in the mixing experiments.

Three pre-modification delay times were used, 7 ms, 37 ms and 70 ms with a modification delay time of 8 ms. A total volume of 600 μl of reaction was collected for each shot and the delay lines were then rinsed via a fifth syringe before the shot was repeated. Three shots were taken for every control reaction and fast mixing time point. Reactions were then precipitated by the addition of 1 volume of isopropyl alcohol and resuspended in extraction buffer followed by three phenol, two 1:1 phenol:chloroform and two chloroform extractions. The samples were then precipitated by addition of 2.5 volumes of ethanol and centrifugation. After resuspension the samples were quantified and the concentration normalized. The samples were then analysed by primer extention using primer against either the 30S subunit or the pRD2-PCR mRNA depending on the experiment. Differences were quantified between reactions using a Fuji FLA-3000G phosphorimager and Fuji Image Guage software. Profiles of the bands in a given lane were generated and the area in integration of all peaks representing bands was done

carefully to avoid contamination from neighboring bands. Intensity was normalized by selecting a common, preferably DMS reactive, band from all lanes that displayed no noticeable trend in reactivity. The intensity from this band was used to normalize the intensity for all bands in that lane.

The association of subunits without message

Subunits were followed through the association process without the addition of a natural mRNA or poly U. These experiments used the same parameters as those above except 5 pre-modification delay times were used: 7 ms, 13 ms, 18 ms, 37 ms and 70 ms. The premixing concentration of the subunits was 0.5 and 1 μM for the 30S and 50S subunits respectively.

Chapter 4

Summary, conclusions and future work.

The goal of the experiments presented in this dissertation was the development and use of a technique to probe the transitions of rRNA conformation that occur as the ribosome functions. The combination of fast-mixing quenched-flow and chemical modification has proved to be capable of resolving conformational changes on the time scale of tens of milliseconds to seconds.

Using this technique aspects of long studied processes that have never been seen before have been revealed, including the multiple steps involved in subunits association as well as the contributions of A site bound mRNA to the structure of the 30S subunit. The binding of message to the A site was seen to favor a structure of the 30S subunit that can be found in the 70S ribosome and in doing so mRNA changes the conformational pathway for association. This ensemble of studies also found that interaction of a natural mRNA with the 30S subunit, presumably via the SD sequence, favors a structure that bars full interaction of the mRNA with the A site.

The rapid nonequilibrium probing (RNP) technique used in these studies has the potential to provide information on many more aspects of translation. RNP not only provides data on transitory structural alterations but also allows the resolution of fine structural alterations that have not been seen before. This is undoubtedly due to the control available for the modification reaction. Traditional chemical modification experiments with DMS use small concentrations of modifier over periods of a few

minutes to an hour, this is adequate when looking for altered structures that are extremely stable. In fact some of the keystone experiments on ribosome structure and interactions were carried out at 20 mM or greater Mg^{++} concentrations, which undoubtedly stabilized the structure and allowed for clear protections and activations (*46, 158, 183, 184*). RNP in combination with a phosphorimager is able to analyze differences in reactivity that could never be seen directly on film. Analysis of traditional chemical probing experiments relied heavily on a very stable structure giving simple reactive or protected results. Instead, There is also information present in a significant average down or average up reactivity in a population in near physiologic conditions.

Future work.

Continuation of this work has the potential to resolve many aspects of not only translational mechanisms, but also other processes involving nucleic acids. Future work in the investigation of translational mechanisms will involve most aspects of ribosome function. However, some specific questions present themselves as bearing immediate significance based on the research presented here. First, is the relationship between ASD and A site an allosteric interaction mediated via the 30S subunit conformation or is it a function of mRNA structure as it interacts with the 30S IC? The former would imply that A site occupation is not possible on the 30S subunit due to a conformation catalyzed via the SD:ASD interaction, while the latter would mean that SD interactions preclude A site occupation simply as a result of prohibitions of mRNA conformation as it interacts with the 30S subunit. Both hypotheses require that during formation of a 70S IC a conformational rearrangement of the 30S subunit occurs that either allows for the simultaneous interaction at both sites or forces the mRNA to adopt a conformation by

which it can then occupy both. Further probing with RNP can delineate all the structural alterations in the 30S as mRNA binds to the subunit and then as the 70S forms. Following the pattern of protection in the mRNA in the same experiments will verify and clarify the results. This could be done with different mRNAs with and without a SD sequence as well as with a SD oligomer comprising the full 9 bp SD:ASD complement. Further work using IFs and initiator tRNA will help define the timing of A site occupation of mRNA during initiation.

Another important question is how does the ribosome recruit mRNA in a prokaryotic organism? The high resolution crystal structure of the 30S subunit shows the exit tunnel for mRNA is a closed loop. Assuming this ring can not be opened easily by mRNA makes threading of the message through the opening a requirement. If it is opened, how and when is it opened? And does this represent a mechanism by which 30S IC formation is promoted usually from the 5' of the mRNA? If so, then assembly on internal mRNA SD sequences may be impossible or unusual. This question can be answered by generating mRNAs with SD sequences spaced at varying distances from the 5' terminus and measuring the rate at which the ribosome forms interactions on these sequences. This can also be studied using quench flow assays of fMet reaction with puromycin with these constructs. The position of IF3 on the 30S complex as determined recently by Cryo-EM of the 70S IC places it in the vicinity of the probable site of opening (*185*). As such, the careful analysis of the contributions of IFs and specifically IF3 to the recruitment and positioning of mRNA in the 30S subunit may help to shed light on how SD position within an mRNA may be handled during initiation.

Three of the four GTP hydrolyzing translation factors; IF2, EF-G and RF3 have now been shown to require an unlocked ribosome for activity. The nature of the conformation of the 50S subunit in binding these proteins while unlocked is of great interest. This is especially true for IF2 and EF-G considering that both have been demonstrated to cause the ratchet-like conformational change between the subunits as they bind. The effects on both the 30S and 50S fine structure as this occurs is of great interest and is a prime target for this technique in the study of ribosomal dynamics.

Finally, and without any sarcasm, the entirety of ribosome interactions and processes should be carefully analyzed with RNP. In the short time this technique has been used many interesting things have been found using very simple systems. It is apparent from these early studies that the technique has great potential for uncovering the small details of ribosome function that allow for the proposition of models at atomic resolution for all steps in the translation cycle.

1. Yusupov, M. M., Yusupova, G. Z., Baucom, A., Lieberman, K., Earnest, T. N., Cate, J. H., and Noller, H. F. (2001) *Science 292*, 883-96.
2. Laursen, B. S., Sorensen, H. P., Mortensen, K. K., and Sperling-Petersen, H. U. (2005) *Microbiol Mol Biol Rev 69*, 101-23.
3. La Teana, A., Gualerzi, C. O., and Brimacombe, R. (1995) *RNA 1*, 772-82.
4. Ma, J., Campbell, A., and Karlin, S. (2002) *J Bacteriol 184*, 5733-45.
5. Tedin, K., Resch, A., and Blasi, U. (1997) *Mol Microbiol 25*, 189-99.
6. Komarova, A. V., Tchufistova, L. S., Supina, E. V., and Boni, I. V. (2002) *RNA 8*, 1137-47.
7. Moll, I., Resch, A., and Blasi, U. (1998) *FEBS Lett 436*, 213-7.
8. Tedin, K., Moll, I., Grill, S., Resch, A., Graschopf, A., Gualerzi, C. O., and Blasi, U. (1999) *Mol Microbiol 31*, 67-77.
9. Chen, H., Bjerknes, M., Kumar, R., and Jay, E. (1994) *Nucleic Acids Res 22*, 4953-7.
10. Canonaco, M. A., Gualerzi, C. O., and Pon, C. L. (1989) *Eur J Biochem 182*, 501-6.
11. Yusupova, G. Z., Yusupov, M. M., Cate, J. H., and Noller, H. F. (2001) *Cell 106*, 233-41.
12. Culver, G. M. (2001) *Structure (Camb) 9*, 751-8.
13. Tomsic, J., Vitali, L. A., Daviter, T., Savelsbergh, A., Spurio, R., Striebeck, P., Wintermeyer, W., Rodnina, M. V., and Gualerzi, C. O. (2000) *EMBO J 19*, 2127-36.
14. Roll-Mecak, A., Cao, C., Dever, T. E., and Burley, S. K. (2000) *Cell 103*, 781-92.
15. La Teana, A., Gualerzi, C. O., and Dahlberg, A. E. (2001) *RNA 7*, 1173-9.
16. Antoun, A., Pavlov, M. Y., Andersson, K., Tenson, T., and Ehrenberg, M. (2003) *EMBO J 22*, 5593-601.
17. Guenneugues, M., Caserta, E., Brandi, L., Spurio, R., Meunier, S., Pon, C. L., Boelens, R., and Gualerzi, C. O. (2000) *EMBO J 19*, 5233-40.
18. Schmitt, E., Panvert, M., Blanquet, S., and Mechulam, Y. (1998) *EMBO J 17*, 6819-26.
19. O'Connor, M., Gregory, S. T., Rajbhandary, U. L., and Dahlberg, A. E. (2001) *RNA 7*, 969-78.
20. Schweisguth, D. C., and Moore, P. B. (1997) *J Mol Biol 267*, 505-19.
21. RajBhandary, U. L. (1994) *J Bacteriol 176*, 547-52.
22. Gualerzi, C. O., and Pon, C. L. (1990) *Biochemistry 29*, 5881-9.
23. Canonaco, M. A., Calogero, R. A., and Gualerzi, C. O. (1986) *FEBS Lett 207*, 198-204.
24. Wu, X. Q., and RajBhandary, U. L. (1997) *J Biol Chem 272*, 1891-5.
25. Meunier, S., Spurio, R., Czisch, M., Wechselberger, R., Guenneugues, M., Gualerzi, C. O., and Boelens, R. (2000) *EMBO J 19*, 1918-26.
26. Laursen, B. S., Mortensen, K. K., Sperling-Petersen, H. U., and Hoffman, D. W. (2003) *J Biol Chem 278*, 16320-8.
27. Giuliodori, A. M., Brandi, A., Gualerzi, C. O., and Pon, C. L. (2004) *RNA 10*, 265-76.

28. Boileau, G., Butler, P., Hershey, J. W., and Traut, R. R. (1983) *Biochemistry 22*, 3162-70.
29. Marzi, S., Knight, W., Brandi, L., Caserta, E., Soboleva, N., Hill, W. E., Gualerzi, C. O., and Lodmell, J. S. (2003) *RNA 9*, 958-69.
30. Zavialov, A. V., and Ehrenberg, M. (2003) *Cell 114*, 113-22.
31. Carter, A. P., Clemons, W. M., Jr., Brodersen, D. E., Morgan-Warren, R. J., Hartsch, T., Wimberly, B. T., and Ramakrishnan, V. (2001) *Science 291*, 498-501.
32. Petrelli, D., Garofalo, C., Lammi, M., Spurio, R., Pon, C. L., Gualerzi, C. O., and La Teana, A. (2003) *J Mol Biol 331*, 541-56.
33. Petrelli, D., LaTeana, A., Garofalo, C., Spurio, R., Pon, C. L., and Gualerzi, C. O. (2001) *EMBO J 20*, 4560-9.
34. Sacerdot, C., de Cock, E., Engst, K., Graffe, M., Dardel, F., and Springer, M. (1999) *J Mol Biol 288*, 803-10.
35. Shapkina, T. G., Dolan, M. A., Babin, P., and Wollenzien, P. (2000) *J Mol Biol 299*, 615-28.
36. Noller, H. F., Yusupov, M. M., Yusupova, G. Z., Baucom, A., Lieberman, K., Lancaster, L., Dallas, A., Fredrick, K., Earnest, T. N., and Cate, J. H. (2001) *Cold Spring Harb Symp Quant Biol 66*, 57-66.
37. Dallas, A., and Noller, H. F. (2001) *Mol Cell 8*, 855-64.
38. Maivali, U., and Remme, J. (2004) *Rna 10*, 600-4.
39. Karimi, R., Pavlov, M. Y., Buckingham, R. H., and Ehrenberg, M. (1999) *Mol Cell 3*, 601-9.
40. Antoun, A., Pavlov, M. Y., Tenson, T., and Ehrenberg, M. M. (2004) *Biol Proced Online 6*, 35-54.
41. Moreau, M., de Cock, E., Fortier, P. L., Garcia, C., Albaret, C., Blanquet, S., Lallemand, J. Y., and Dardel, F. (1997) *J Mol Biol 266*, 15-22.
42. Biou, V., Shu, F., and Ramakrishnan, V. (1995) *EMBO J 14*, 4056-64.
43. Sette, M., Spurio, R., van Tilborg, P., Gualerzi, C. O., and Boelens, R. (1999) *RNA 5*, 82-92.
44. Heimark, R. L., Kahan, L., Johnston, K., Hershey, J. W., and Traut, R. R. (1976) *J Mol Biol 105*, 219-30.
45. Stoffler, G., and Stoffler-Meilicke, M. (1984) *Annu Rev Biophys Bioeng 13*, 303-30.
46. Moazed, D., Samaha, R. R., Gualerzi, C., and Noller, H. F. (1995) *J Mol Biol 248*, 207-10.
47. Muralikrishna, P., and Wickstrom, E. (1989) *Biochemistry 28*, 7505-10.
48. McCutcheon, J. P., Agrawal, R. K., Philips, S. M., Grassucci, R. A., Gerchman, S. E., Clemons, W. M., Jr., Ramakrishnan, V., and Frank, J. (1999) *Proc Natl Acad Sci U S A 96*, 4301-6.
49. Blaha, G., Burkhardt, N., and Nierhaus, K. H. (2002) *Biophys Chem 96*, 153-61.
50. Hennelly, S. P., Antoun, A., Ehrenberg, M., Gualerzi, C. O., Knight, W., Lodmell, J. S., and Hill, W. E. (2005) *J Mol Biol 346*, 1243-58.
51. Noller, H. F., and Baucom, A. (2002) *Biochem Soc Trans 30*, 1159-61.

52. Wimberly, B. T., Brodersen, D. E., Clemons, W. M., Jr., Morgan-Warren, R. J., Carter, A. P., Vonrhein, C., Hartsch, T., and Ramakrishnan, V. (2000) *Nature 407*, 327-39.
53. Ogle, J. M., Brodersen, D. E., Clemons, W. M., Jr., Tarry, M. J., Carter, A. P., and Ramakrishnan, V. (2001) *Science 292*, 897-902.
54. Pon, C. L., and Gualerzi, C. O. (1986) *FEBS Lett 195*, 215-9.
55. Moazed, D., and Noller, H. F. (1989) *Nature 342*, 142-8.
56. Rheinberger, H. J., Sternbach, H., and Nierhaus, K. H. (1981) *Proc Natl Acad Sci U S A 78*, 5310-4.
57. Noller, H. F., Yusupov, M. M., Yusupova, G. Z., Baucom, A., and Cate, J. H. (2002) *FEBS Lett 514*, 11-6.
58. Wilson, D. N., and Nierhaus, K. H. (2003) *Angew Chem Int Ed Engl 42*, 3464-86.
59. Frank, J., and Agrawal, R. K. (1998) *Biophys J 74*, 589-94.
60. Stark, H., Orlova, E. V., Rinke-Appel, J., Junke, N., Mueller, F., Rodnina, M., Wintermeyer, W., Brimacombe, R., and van Heel, M. (1997) *Cell 88*, 19-28.
61. Schmeing, T. M., Seila, A. C., Hansen, J. L., Freeborn, B., Soukup, J. K., Scaringe, S. A., Strobel, S. A., Moore, P. B., and Steitz, T. A. (2002) *Nat Struct Biol 9*, 225-30.
62. Valle, M., Sengupta, J., Swami, N. K., Grassucci, R. A., Burkhardt, N., Nierhaus, K. H., Agrawal, R. K., and Frank, J. (2002) *EMBO J 21*, 3557-67.
63. Valle, M., Zavialov, A., Li, W., Stagg, S. M., Sengupta, J., Nielsen, R. C., Nissen, P., Harvey, S. C., Ehrenberg, M., and Frank, J. (2003) *Nat Struct Biol 10*, 899-906.
64. Wilson, D. N., Blaha, G., Connell, S. R., Ivanov, P. V., Jenke, H., Stelzl, U., Teraoka, Y., and Nierhaus, K. H. (2002) *Curr Protein Pept Sci 3*, 1-53.
65. Wower, J., Kirillov, S. V., Wower, I. K., Guven, S., Hixson, S. S., and Zimmermann, R. A. (2000) *J Biol Chem 275*, 37887-94.
66. Fredrick, K., and Noller, H. F. (2002) *Mol Cell 9*, 1125-31.
67. Spirin, A. S. (1985) *Prog Nucleic Acid Res Mol Biol 32*, 75-114.
68. Valle, M., Zavialov, A., Sengupta, J., Rawat, U., Ehrenberg, M., and Frank, J. (2003) *Cell 114*, 123-34.
69. Frank, J., and Agrawal, R. K. (2001) *Cold Spring Harb Symp Quant Biol 66*, 67-75.
70. Frank, J., and Agrawal, R. K. (2000) *Nature 406*, 318-22.
71. Stark, H., Rodnina, M. V., Wieden, H. J., van Heel, M., and Wintermeyer, W. (2000) *Cell 100*, 301-9.
72. Joseph, S., and Noller, H. F. (1998) *EMBO J 17*, 3478-83.
73. Belitsina, N. V., Tnalina, G. Z., and Spirin, A. S. (1981) *FEBS Lett 131*, 289-92.
74. Borowski, C., Rodnina, M. V., and Wintermeyer, W. (1996) *Proc Natl Acad Sci U S A 93*, 4202-6.
75. Rodnina, M. V., Savelsbergh, A., Katunin, V. I., and Wintermeyer, W. (1997) *Nature 385*, 37-41.
76. Czworkowski, J., and Moore, P. B. (1997) *Biochemistry 36*, 10327-34.
77. Lodmell, J. S., and Hennelly, S. P. (2002) in *Translational Mechanisms.* (Brakier-Gingras, L., Lapointe, J.,, Ed.), Landes Bioscience, Austin, TX.

78. Harms, J., Schluenzen, F., Zarivach, R., Bashan, A., Gat, S., Agmon, I., Bartels, H., Franceschi, F., and Yonath, A. (2001) *Cell 107*, 679-88.
79. Liljas, A., A, A. E., al-Karadaghi, S., Garber, M., Zheltonosova, J., and Brazhnikov, E. (1995) *Biochem Cell Biol 73*, 1209-16.
80. Czworkowski, J., Wang, J., Steitz, T. A., and Moore, P. B. (1994) *EMBO J 13*, 3661-8.
81. Nissen, P., Kjeldgaard, M., Thirup, S., Polekhina, G., Reshetnikova, L., Clark, B. F., and Nyborg, J. (1995) *Science 270*, 1464-72.
82. Nyborg, J., Nissen, P., Kjeldgaard, M., Thirup, S., Polekhina, G., and Clark, B. F. (1996) *Trends Biochem Sci 21*, 81-2.
83. Kim, K. K., Min, K., and Suh, S. W. (2000) *EMBO J 19*, 2362-70.
84. Selmer, M., Al-Karadaghi, S., Hirokawa, G., Kaji, A., and Liljas, A. (1999) *Science 286*, 2349-52.
85. Toyoda, T., Tin, O. F., Ito, K., Fujiwara, T., Kumasaka, T., Yamamoto, M., Garber, M. B., and Nakamura, Y. (2000) *RNA 6*, 1432-44.
86. Vestergaard, B., Van, L. B., Andersen, G. R., Nyborg, J., Buckingham, R. H., and Kjeldgaard, M. (2001) *Mol Cell 8*, 1375-82.
87. Song, H., Mugnier, P., Das, A. K., Webb, H. M., Evans, D. R., Tuite, M. F., Hemmings, B. A., and Barford, D. (2000) *Cell 100*, 311-21.
88. Nakamura, Y., and Ito, K. (2003) *Trends Biochem Sci 28*, 99-105.
89. Gao, H., Valle, M., Ehrenberg, M., and Frank, J. (2004) *J Struct Biol 147*, 283-90.
90. Pape, T., Wintermeyer, W., and Rodnina, M. V. (1998) *EMBO J 17*, 7490-7.
91. Rodnina, M. V., Pape, T., Fricke, R., Kuhn, L., and Wintermeyer, W. (1996) *J Biol Chem 271*, 646-52.
92. Rodnina, M. V., Pape, T., Fricke, R., and Wintermeyer, W. (1995) *Biochem Cell Biol 73*, 1221-7.
93. Rodnina, M. V., Daviter, T., Gromadski, K., and Wintermeyer, W. (2002) *Biochimie 84*, 745-54.
94. Rodnina, M. V., and Wintermeyer, W. (2001) *Annu Rev Biochem 70*, 415-35.
95. Moazed, D., and Noller, H. F. (1990) *J Mol Biol 211*, 135-45.
96. Pape, T., Wintermeyer, W., and Rodnina, M. (1999) *EMBO J 18*, 3800-7.
97. Piepenburg, O., Pape, T., Pleiss, J. A., Wintermeyer, W., Uhlenbeck, O. C., and Rodnina, M. V. (2000) *Biochemistry 39*, 1734-8.
98. Ogle, J. M., Murphy, F. V., Tarry, M. J., and Ramakrishnan, V. (2002) *Cell 111*, 721-32.
99. Berchtold, H., Reshetnikova, L., Reiser, C. O., Schirmer, N. K., Sprinzl, M., and Hilgenfeld, R. (1993) *Nature 365*, 126-32.
100. Frank, J., Sengupta, J., Gao, H., Li, W., Valle, M., Zavialov, A., and Ehrenberg, M. (2005) *FEBS Lett 579*, 959-62.
101. Hansen, J. L., Schmeing, T. M., Moore, P. B., and Steitz, T. A. (2002) *Proc Natl Acad Sci U S A 99*, 11670-5.
102. Ban, N., Freeborn, B., Nissen, P., Penczek, P., Grassucci, R. A., Sweet, R., Frank, J., Moore, P. B., and Steitz, T. A. (1998) *Cell 93*, 1105-15.
103. Katunin, V. I., Muth, G. W., Strobel, S. A., Wintermeyer, W., and Rodnina, M. V. (2002) *Mol Cell 10*, 339-46.

104. Muth, G. W., Ortoleva-Donnelly, L., and Strobel, S. A. (2000) *Science 289*, 947-50.
105. Thompson, J., Kim, D. F., O'Connor, M., Lieberman, K. R., Bayfield, M. A., Gregory, S. T., Green, R., Noller, H. F., and Dahlberg, A. E. (2001) *Proc Natl Acad Sci U S A 98*, 9002-7.
106. Polacek, N., Gaynor, M., Yassin, A., and Mankin, A. S. (2001) *Nature 411*, 498-501.
107. Robertus, J. D., Ladner, J. E., Finch, J. T., Rhodes, D., Brown, R. S., Clark, B. F., and Klug, A. (1974) *Nature 250*, 546-51.
108. Ban, N., Nissen, P., Hansen, J., Capel, M., Moore, P. B., and Steitz, T. A. (1999) *Nature 400*, 841-7.
109. Tate, W., Greuer, B., and Brimacombe, R. (1990) *Nucleic Acids Res 18*, 6537-44.
110. Poole, E. S., Brimacombe, R., and Tate, W. P. (1997) *RNA 3*, 974-82.
111. Nakamura, Y., and Ito, K. (2002) *FEBS Lett 514*, 30-3.
112. Inagaki, Y., and Doolittle, W. F. (2001) *Nucleic Acids Res 29*, 921-7.
113. Lozupone, C. A., Knight, R. D., and Landweber, L. F. (2001) *Curr Biol 11*, 65-74.
114. Kisselev, L., Ehrenberg, M., and Frolova, L. (2003) *EMBO J 22*, 175-82.
115. Dincbas-Renqvist, V., Engstrom, A., Mora, L., Heurgue-Hamard, V., Buckingham, R., and Ehrenberg, M. (2000) *EMBO J 19*, 6900-7.
116. Wilson, K. S., Ito, K., Noller, H. F., and Nakamura, Y. (2000) *Nat Struct Biol 7*, 866-70.
117. Moffat, J. G., and Tate, W. P. (1994) *J Biol Chem 269*, 18899-903.
118. Freistroffer, D. V., Pavlov, M. Y., MacDougall, J., Buckingham, R. H., and Ehrenberg, M. (1997) *EMBO J 16*, 4126-33.
119. Zavialov, A. V., Buckingham, R. H., and Ehrenberg, M. (2001) *Cell 107*, 115-24.
120. Zavialov, A. V., Mora, L., Buckingham, R. H., and Ehrenberg, M. (2002) *Mol Cell 10*, 789-98.
121. Nakamura, Y. (2001) *J Mol Evol 53*, 282-9.
122. Pavlov, M. Y., Freistroffer, D. V., MacDougall, J., Buckingham, R. H., and Ehrenberg, M. (1997) *EMBO J 16*, 4134-41.
123. Fujiwara, T., Ito, K., Yamami, T., and Nakamura, Y. (2004) *Mol Microbiol 53*, 517-28.
124. Ishino, T., Atarashi, K., Uchiyama, S., Yamami, T., Saihara, Y., Yoshida, T., Hara, H., Yokose, K., Kobayashi, Y., and Nakamura, Y. (2000) *Genes Cells 5*, 953-63.
125. Herr, W., Chapman, N. M., and Noller, H. F. (1979) *J Mol Biol 130*, 433-49.
126. Chapman, N. M., and Noller, H. F. (1977) *J Mol Biol 109*, 131-49.
127. Merryman, C., Moazed, D., Daubresse, G., and Noller, H. F. (1999) *J Mol Biol 285*, 107-13.
128. Merryman, C., Moazed, D., McWhirter, J., and Noller, H. F. (1999) *J Mol Biol 285*, 97-105.
129. Mitchell, P., Osswald, M., and Brimacombe, R. (1992) *Biochemistry 31*, 3004-11.
130. Frank, J., Verschoor, A., Li, Y., Zhu, J., Lata, R. K., Radermacher, M., Penczek, P., Grassucci, R., Agrawal, R. K., and Srivastava, S. (1995) *Biochem Cell Biol 73*, 757-65.

131. Frank, J., Zhu, J., Penczek, P., Li, Y., Srivastava, S., Verschoor, A., Radermacher, M., Grassucci, R., Lata, R. K., and Agrawal, R. K. (1995) *Nature 376*, 441-4.
132. Cate, J. H., Yusupov, M. M., Yusupova, G. Z., Earnest, T. N., and Noller, H. F. (1999) *Science 285*, 2095-104.
133. Gao, H., Sengupta, J., Valle, M., Korostelev, A., Eswar, N., Stagg, S. M., Van Roey, P., Agrawal, R. K., Harvey, S. C., Sali, A., Chapman, M. S., and Frank, J. (2003) *Cell 113*, 789-801.
134. Gabashvili, I. S., Agrawal, R. K., Spahn, C. M., Grassucci, R. A., Svergun, D. I., Frank, J., and Penczek, P. (2000) *Cell 100*, 537-49.
135. Spahn, C. M., Beckmann, R., Eswar, N., Penczek, P. A., Sali, A., Blobel, G., and Frank, J. (2001) *Cell 107*, 373-86.
136. Wishnia, A., and Boussert, A. S. (1977) *J Mol Biol 116*, 577-91.
137. Wishnia, A., Boussert, A., Graffe, M., Dessen, P. H., and Grunberg-Manago, M. (1975) *J Mol Biol 93*, 499-15.
138. Hapke, B., and Noll, H. (1976) *J Mol Biol 105*, 97-109.
139. Antoun A, P. M., Tenson T, Ehrenberg M Ma. (2004) *Biol Proced Online 2004*, 35-54.
140. Gabashvili, I. S., Whirl-Carrillo, M., Bada, M., Banatao, D. R., and Altman, R. B. (2003) *RNA 9*, 1301-7.
141. de Smit, M. H., and van Duin, J. (2003) *J Mol Biol 331*, 737-43.
142. Moore, P. B., and Steitz, T. A. (2003) *Annu Rev Biochem 72*, 813-50.
143. Wilson, K. S., and Noller, H. F. (1998) *Cell 92*, 337-49.
144. Polacek, N., Patzke, S., Nierhaus, K. H., and Barta, A. (2000) *Mol Cell 6*, 159-71.
145. Savelsbergh, A., Katunin, V. I., Mohr, D., Peske, F., Rodnina, M. V., and Wintermeyer, W. (2003) *Mol Cell 11*, 1517-23.
146. Ehrenberg, M., Bilgin, N. and Kurland, C. (1990) in *In Ribosomes and Protein Synthesis. A practical Approach.* pp 101-128, Oxford University Press,, Oxford,.
147. Herr, W., and Noller, H. F. (1979) *J Mol Biol 130*, 421-32.
148. Lodmell, J. S., and Dahlberg, A. E. (1997) *Science 277*, 1262-7.
149. Rodriguez-Correa, D., and Dahlberg, A. E. (2004) *Rna 10*, 28-33.
150. Belanger, F., Leger, M., Saraiya, A. A., Cunningham, P. R., and Brakier-Gingras, L. (2002) *J Mol Biol 320*, 979-89.
151. Belanger, F., Gagnon, M. G., Steinberg, S. V., Cunningham, P. R., and Brakier-Gingras, L. (2004) *J Mol Biol 338*, 683-93.
152. Tama, F., Valle, M., Frank, J., and Brooks, C. L., 3rd. (2003) *Proc Natl Acad Sci U S A 100*, 9319-23.
153. Velichutina, I. V., Dresios, J., Hong, J. Y., Li, C., Mankin, A., Synetos, D., and Liebman, S. W. (2000) *RNA 6*, 1174-84.
154. Gabashvili, I. S., Agrawal, R. K., Grassucci, R., Squires, C. L., Dahlberg, A. E., and Frank, J. (1999) *Embo J 18*, 6501-7.
155. Carter, A. P., Clemons, W. M., Brodersen, D. E., Morgan-Warren, R. J., Wimberly, B. T., and Ramakrishnan, V. (2000) *Nature 407*, 340-8.
156. Schluenzen, F., Tocilj, A., Zarivach, R., Harms, J., Gluehmann, M., Janell, D., Bashan, A., Bartels, H., Agmon, I., Franceschi, F., and Yonath, A. (2000) *Cell 102*, 615-23.

157. Vassilenko, S. K., Carbon, P., Ebel, J. P., and Ehresmann, C. (1981) *J Mol Biol 152*, 699-721.
158. Moazed, D., and Noller, H. F. (1986) *Cell 47*, 985-94.
159. Ban, N., Nissen, P., Hansen, J., Moore, P. B., and Steitz, T. A. (2000) *Science 289*, 905-20.
160. Dahlquist, K. D., and Puglisi, J. D. (2000) *J Mol Biol 299*, 1-15.
161. Moazed, D., and Noller, H. F. (1987) *Nature 327*, 389-94.
162. Brakier-Gingras, L., Pinard, R., and Dragon, F. (1995) *Biochem Cell Biol 73*, 907-13.
163. Pinard, R., Cote, M., Payant, C., and Brakier-Gingras, L. (1994) *Nucleic Acids Res 22*, 619-24.
164. Grunberg-Manago, M., Dessen, P., Pantaloni, D., Godefroy-Colburn, T., Wolfe, A. D., and Dondon, J. (1975) *J Mol Biol 94*, 461-78.
165. Calogero, R. A., Pon, C. L., Canonaco, M. A., and Gualerzi, C. O. (1988) *Proc Natl Acad Sci U S A 85*, 6427-31.
166. Schreier, M. H., and Noll, H. (1971) *Proc Natl Acad Sci U S A 68*, 805-9.
167. Noll, M., Hapke, B., Schreier, M. H., and Noll, H. (1973) *J Mol Biol 75*, 281-94.
168. Burma, D. P., Srivastava, A. K., Srivastava, S., and Dash, D. (1985) *J Biol Chem 260*, 10517-25.
169. Agrawal, R. K., and Burma, D. P. (1996) *J Biol Chem 271*, 21285-91.
170. Tapprich, W. E., Goss, D. J., and Dahlberg, A. E. (1989) *Proc Natl Acad Sci U S A 86*, 4927-31.
171. Tapprich, W. E., and Hill, W. E. (1986) *Proc Natl Acad Sci U S A 83*, 556-60.
172. Noller, H. F., Moazed, D., Stern, S., Powers, T., Allen, P.N., Robertson, J.M., Weiser, B. Triman, K. (1990) in *The Ribosome* (Walter E. Hill, A. D., Roger A. Garrett, peter B. Moore, David Schlessinger, and Jonathan R. Warner, Ed.) pp 73-92, American Society for Microbiology, Washington, D.C.
173. Brandt, R., and Gualerzi, C. O. (1991) *Biochimie 73*, 1543-9.
174. Brandt, R., and Gualerzi, C. O. (1992) *FEBS Lett 311*, 199-202.
175. Knight, W., Hill, W., and Lodmell, J. S. (2005) *Comput Biol Chem 29*, 163-74.
176. VanLoock, M. S., Agrawal, R. K., Gabashvili, I. S., Qi, L., Frank, J., and Harvey, S. C. (2000) *J Mol Biol 304*, 507-15.
177. Jenner, L., Romby, P., Rees, B., Schulze-Briese, C., Springer, M., Ehresmann, C., Ehresmann, B., Moras, D., Yusupova, G., and Yusupov, M. (2005) *Science 308*, 120-3.
178. Rinke-Appel, J., Junke, N., Brimacombe, R., Lavrik, I., Dokudovskaya, S., Dontsova, O., and Bogdanov, A. (1994) *Nucleic Acids Res 22*, 3018-25.
179. Rinke-Appel, J., Junke, N., Stade, K., and Brimacombe, R. (1991) *Embo J 10*, 2195-202.
180. Karimi, R., and Ehrenberg, M. (1996) *Embo J 15*, 1149-54.
181. Choi, S. K., Olsen, D. S., Roll-Mecak, A., Martung, A., Remo, K. L., Burley, S. K., Hinnebusch, A. G., and Dever, T. E. (2000) *Mol Cell Biol 20*, 7183-91.
182. Brock, S., Szkaradkiewicz, K., and Sprinzl, M. (1998) *Mol Microbiol 29*, 409-17.
183. Moazed, D., and Noller, H. F. (1991) *Proc Natl Acad Sci U S A 88*, 3725-8.
184. Woodcock, J., Moazed, D., Cannon, M., Davies, J., and Noller, H. F. (1991) *EMBO J 10*, 3099-103.

185. Allen, G. S., Zavialov, A., Gursky, R., Ehrenberg, M., and Frank, J. (2005) *Cell 121*, 703-12.